α,ω-Di(vinylene carbonate) telechelic polyolefins: Synthesis by metathesis reactions and studies as potential precursors toward hydroxy-oxazolidone-based polyolefin NIPUs

Cyril Chauveau, Stéphane Fouquay, Guillaume Michaud, Frédéric Simon, Jean-François Carpentier, Sophie M. Guillaume

α,ω-Di(vinylene carbonate) telechelic polyolefins: Synthesis by metathesis reactions and studies as potential precursors toward hydroxy-oxazolidone-based polyolefin NIPUs

Cyril Chauveau,[a] Stéphane Fouquay,[b] Guillaume Michaud,[c] Frédéric Simon,[c] Jean-François Carpentier (ORCID: 0000-0002-9160-7662),[a,*] and Sophie M. Guillaume (ORCID: 0000-0003-2917-8657) [a,*]

[a] Univ Rennes, CNRS, ISCR (Institut des Sciences Chimiques de Rennes) – UMR 6226, F-35000 Rennes, France

[b] BOSTIK S.A., 420 rue d'Estienne d'Orves, F-92705 Colombes Cedex, France

[c] BOSTIK, ZAC du Bois de Plaisance, 101, Rue du Champ Cailloux, F-60280 Venette, France

[*] Corresponding authors: jean-francois.carpentier@univ-rennes1; sophie.guillaume@univ-rennes1.fr

Graphical abstract

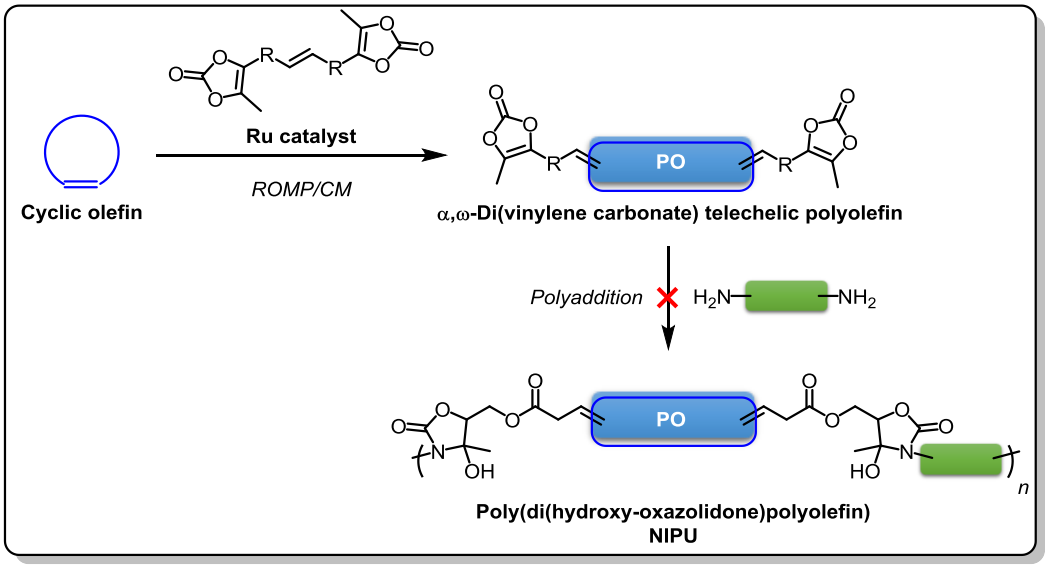

Abstract

Current polyurethane (PU) industrial and academic research aims at developing non-isocyanate PUs, referred to as NIPUs. Within this context, we report herein the synthesis of original vinylene carbonate (VC) compounds, subsequently used as chain-transfer agents (CTAs) towards the preparation of α,ω-di(VC) telechelic (co)polyolefins from the tandem ring-opening metathesis polymerization (ROMP)/cross-metathesis (CM) of cyclic olefins. Thus, (5-methyl-2-oxo-1,3-dioxol-4-yl)methyl acrylate (**VC1**), bis((5-methyl-2-oxo-1,3-dioxol-4-yl)methyl) fumarate (**VC2**), and bis((5-methyl-2-oxo-1,3-dioxol-4-yl)methyl) (*E*)-hex-3-enedioate (**VC3**) were synthesized from 4-(hydroxymethyl)-5-methyl-1,3-dioxol-2-one (DMDO-OH). Among these, only **VC3** successfully and selectively afforded well-defined α,ω-di(vinylene carbonate) telechelic polyolefins, namely di(**VC3**)-PCOE and di(**VC3**)-P(NB-*co*-CDT), from the ROMP/CM of COE, and norbonene (NB)/*trans*,*trans*,*cis*-1,5,9-cyclododecatriene (CDT), respectively, using Grubbs' 2nd-generation ruthenium catalyst (**G2**) under mild operating conditions (CH_2Cl_2, 40 °C, 3 h). Preliminary investigations on the reactivity of a model VC, namely 4,5-dimethyl-1,3-dioxol-2-one (DMDO), towards nucleophiles such as a primary or secondary amine, promisingly showed the formation of hydroxy-oxazolidone compounds **1** and **2**, and oxo-urethane **3** species, respectively. Yet, the ultimate reaction of di(**VC3**)-PCOE with 2,2′-(ethylenedioxy)bis(ethylamine) (EDR-148) did not give the expected poly(di(hydroxy-oxazolidone)polyolefin) polyaddition type of NIPUs; competing amidation and/or dehydration or urea formation reactions evidenced by detailed NMR, FTIR and MS analyses, were proposed to account for this inefficiency.

Keywords: telechelic polyolefin, metathesis, oxazolidone, vinylene carbonate, non-isocyanate polyurethane (NIPU)

Introduction

Polyurethanes (PUs), as one of the most important plastic families, are commonly marketed as both commodity and specialty thermoplastics or thermosets for many types of application such as foams, coatings, adhesives, sealants and elastomers.[1,2,3,4] PUs are typically straightforwardly prepared from the catalyzed polyaddition reaction of diols (or polyols) with diisocyanates (or polyisocyanates). However, in light of the toxicity issues raised by phosgene- and amine-derived isocyanates, greener alternative strategies have been increasingly investigated towards the design of non-isocyanate polyurethanes (NIPUs).[5,6,7,8,9,10,11,12] Among various routes, the transurethanization polycondensation of a biscarbamate and a diol, and the polyaddition of cyclic carbonates with amines, are the most encouraging ones. While PUs obtained by transurethanization display comparable properties to classical PUs made from diisocyanates and diols, harsh operating conditions (reduced pressure and/or high temperatures) and the required removal of alcohol by-product precluded thus far industrial outcomes.[7] The preparation of polyhydroxyurethanes (PHUs) from the ring-opening aminolysis of multicyclic carbonates with aliphatic amines is nowadays the most investigated and industrially promising approach toward NIPUs (Scheme 1).[5,6,8,10,13,14,15,16,17,18] Although PHUs exhibit somewhat different properties than common PUs due to the hydroxyl functions (both primary and secondary alcohols; ratio ca. 35:65)[5–10,13–18] flanked on the polymer backbone, there are still to date, the best NIPU-compromise to comply with safety regulations. Five-, six-, seven- and eight-membered ring cyclic carbonates successfully undergo polyaddition with amines with an efficiency and a selectivity depending on the size of the cyclic carbonate, its substituent(s), the nature of the diamine, the catalyst and the operating conditions. The molar mass of the resulting PHUs most often remains limited by impeding side-reactions dependent on all these parameters (e.g. amidation or dehydration leading to the formation of ureas, or oxazolidinones, respectively), and by the hydrogen

bonding network arising from the numerous urethane functions throughout the macromolecules.[5-8,13,19,20,21,22,23,24,25,26] In spite of their relatively high stability, five-membered cyclic carbonates remain the most investigated precursors to NIPUs since they are synthetically more readily available, in particular by carboxylation of epoxides.[21,22,27,28,29,30,31]The objectives are thus to establish a room temperature, ideally catalyst-free and solvent-free, efficient aminolysis of such five-membered ring cyclic carbonates towards NIPUs/PHUs.

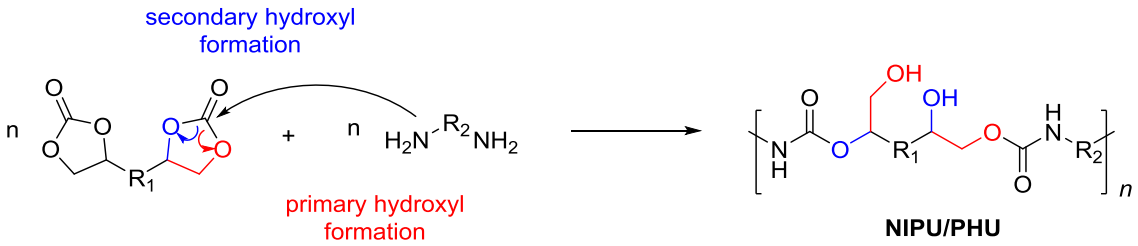

Scheme 1. Illustration of the synthesis of NIPUs/PHUs by the polyaddition of a biscyclocarbonate and a diamine depicting the formation of primary and secondary hydroxyl groups.

Related five-membered cyclic thiocarbonates have revealed higher reactivity than peroxygenated carbonates towards the formation of poly(thiourethane)s in a catalyst-free room temperature polyaddition.[32,33,34,35,36,37,38] However, Endo *et al.* demonstrated that poly(thiourethane)s are thermally less stable than similar PHUs, probably due to the lower stability of thiourethane moieties.[35] Moreover, the synthesis of the thiocarbonates requires the use of toxic and volatile CS_2, thiophosgene, or isocyanates, which do not address the environmental and health concerns.[32,36,37] Further efforts to promote the reactivity of five-membered cyclic carbonates has been recently claimed by BASF[39,40,41,42] and reported by the group of Detrembleur[43] upon destabilizing the cyclic ring via the use of α-alkylidene cyclocarbonates.[44] The room-temperature polyaddition of bis(α-alkylidene cyclocarbonate)s

with dinucleophiles, such as primary or secondary diamines, or diols gave a poly(oxo-urethane) that ultimately cyclized into poly(hydroxy-oxazolidone), or poly(oxo-urethane) or poly(oxo-carbonate), respectively (Scheme 2).[43]

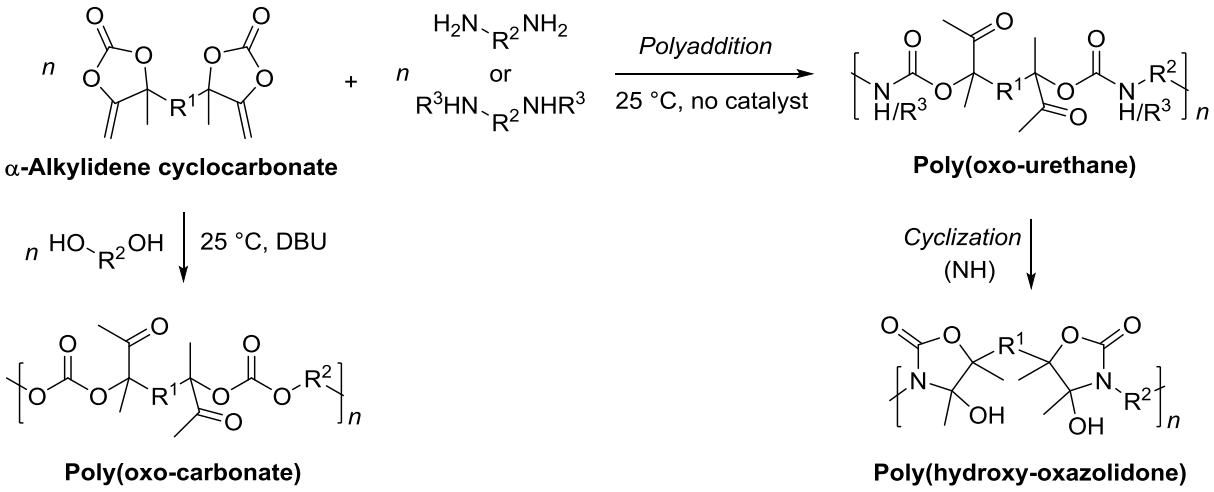

Scheme 2. Synthesis of poly(hydroxy-oxazolidone), poly(oxo-urethane) and poly(oxo-carbonate) from the polyaddition of a bis(α-alkylidene cyclocarbonate) with a primary, secondary diamine, or a diol, respectively.[43]

We hypothesized that an endocyclic olefinic group onto a five-membered ring cyclic vinylene carbonate (VC) may sufficiently promote the nucleophilic amine ring opening at room temperature. To the best of our knowledge, such a VC functional group, which was only described in pharmaceutics,[45] could serve as a new synthon towards the preparation of NIPUs.

Our objective is to develop original polyolefin-based NIPUs in order to provide greener alternatives to current PUs. Indeed, commercially available hydroxyl-terminated PUs such as dihydroxy telechelic polybutadiene or polyisoprene are commonly reacted with di- and polyisocyanate curing agents to provide general-purpose PU elastomers for housing, construction, automotive, sealing and coating materials or electrical insulation

applications.[46,47] Our ongoing strategy to develop NIPUs is based on the post-polymerization polyaddition of α,ω-telechelic polyolefins with a di- or multi-functional amine to generate the urethane moieties along the polyolefinic backbone. The polyolefin is first prepared from the ring-opening metathesis polymerization (ROMP)/cross metathesis (CM) approach of cyclic olefins in the presence of the corresponding functional chain-transfer agent (CTA).[32,48,49,50,51,52,53,54,55,56] While various prepolymer end-capping functional groups have been studied, more reactive chain-ends are desirable to improve the overall efficiency of the NIPUs synthesis. Along this line, we then investigate in the present work, first the preparation of original di(vinylene carbonate) telechelic polyolefins (di(VC)-PO) via metathesis, and subsequently, its polyaddition reaction with a diamine. Ultimately, the formation of poly(di(hydroxy-oxazolidone)polyolefin)s (PHOPOs) type of NIPUs is targeted (Scheme 3).

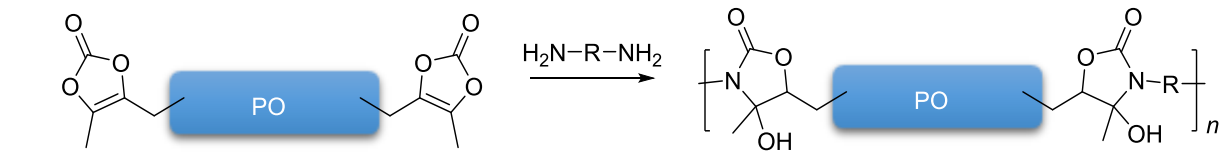

α,ω-Di(vinylene carbonate) telechelic polyolefin
di(VC)-PO

Poly(di(hydroxy-oxazolidone)polyolefin)
PHOPO NIPU

Scheme 3. Anticipated polyaddition of an α,ω-di(vinylene carbonate) telechelic polyolefin (di(VC)-PO) with a diamine into the corresponding poly(di(hydroxy-oxazolidone)polyolefin) (PHOPO) NIPU.

We thus first report herein: (i) the model reaction of the 4,5-dimethyl-1,3-dioxol-2-one (DMDO) with nucleophiles, namely a primary or secondary monoamine, or a primary diamine (Scheme 4); (ii) the Ru-catalyzed ROMP/CM of cyclooctene (COE) in the presence of original VC CTAs, either (5-methyl-2-oxo-1,3-dioxol-4-yl)methyl acrylate (**VC1**), bis((5-methyl-2-oxo-1,3-dioxol-4-yl)methyl) fumarate (**VC2**), or bis((5-methyl-2-oxo-1,3-dioxol-4-

yl)methyl) (*E*)-hex-3-enedioate (**VC3**) (Schemes 5 and 6); and (iii) attempts to perform the subsequent polyaddition of di(**VC3**)-PCOE with isopropylamine or 2,2′-(ethylenedioxy)bis(ethylamine) (EDR-148) (Scheme 8).

Experimental section

Materials. All syntheses and manipulations of air- and moisture-sensitive compounds and all catalytic metathesis experiments were performed under argon atmosphere using standard Schlenk line and glove box techniques. CH_2Cl_2 (stabilized with amylene, Sigma-Aldrich) was purified on a MBraun system over activated 3 Å molecular sieves. Cyclooctene (COE, ACROS) was dried and distilled over CaH_2 before use. 4-(Hydroxymethyl)-5-methyl-1,3-dioxol-2-one (DMDO-OH; Fluorochem) was distilled under vacuum and kept under argon over molecular sieves. *N*-methylpropan-2-amine (Fischer), EDR-148 (2,2'-(ethane-1,2-diylbis(oxy))bis(ethan-1-amine) (Huntsman), 4,5-dimethyl-1,3-dioxol-2-one (DMDO), (*E*)-hex-3-enedioic acid (TCI), Grubbs' 2nd-generation catalyst ([$(IMesH_2)(Cy_3P)RuCl_2$(=CHPh)], **G2**, Aldrich), and all other reagents (Aldrich or ACROS) were used as received.

Instrumentation and measurements. ^{1}H (400 MHz) and J-MOD $^{13}C\{^1H\}$ (100 MHz) NMR spectra were recorded on a Bruker Avance AM 400 spectrometer at 23 °C in $CDCl_3$. Chemical shifts (δ) are reported in ppm and were referenced internally relative to tetramethylsilane (δ 0 ppm) using the residual ^{1}H and ^{13}C solvent resonances of the deuterated solvent.

Monomer conversions were determined from ^{1}H NMR spectra of the crude polymer sample, from the integration (Int.) ratio $Int._{polymer}/[Int._{polymer} + Int._{monomer}]$, using the methine hydrogens (–C*H*=C*H*–: δ (ppm) 5.30, 5.66 (PCOE, COE); 5.44, 5.09 (PCDT, CDT); 5.31, 6.04 (PNB, NB)). CTA conversions were determined from ^{1}H NMR spectra of the crude

polymer samples, from the integration (Int.) ratio $Int._{polymer}/[Int._{polymer} + Int._{CTA}]$, using –O(C=O)$(CH_2)_{0–1}$CH=C*H*– (δ (ppm) 6.46, 7.06 (**VC1**, di(**VC1**)-PCOE); 6.90, 7.06 (**VC2**, di(**VC2**)-PCOE); 5.74, 5.60 (**VC3**, di(**VC3**)-PCOE)).

The molar mass values of PCOE samples were determined by ^{1}H NMR analysis in $CDCl_3$ ($M_{n,NMR}$) from the integral value ratio of the signals of VC end-groups' hydrogens (typically δ_{Hc} ca. 3.09 ppm) to internal olefin hydrogens (δ_{HA} ca. 5.40 ppm) (e.g. Figure 1 for **VC1**).

The average molar mass ($M_{n,SEC}$) and dispersity ($Đ_M = M_w/M_n$) values of the polymers were determined on freshly prepared samples by size exclusion chromatography (SEC) in THF at 30 °C (flow rate = 1.0 mL.min^{-1}) on a Polymer Laboratories PL50 apparatus equipped with a refractive index detector and a set of two ResiPore PLgel 3 µm MIXED-E 300 × 7.5 mm columns. The polymer samples were dissolved in THF (2 mg.mL^{-1}). All elution curves were calibrated with 12 monodisperse polystyrene standards (M_n range = 580–380,000 g.mol^{-1}). $M_{n,SEC}$ values of polymers were uncorrected for their possible difference in hydrodynamic volume in THF vs. polystyrene. The SEC traces of the polymers all exhibited a monomodal and symmetric peak.

ESI (ElectroSpray Ionization) mass spectra were recorded at CRMPO-Scanmat (Univ Rennes) on an orbitrap type Thermo Fisher Scientific Q-Exactive instrument with an ESI source in positive or negative mode using solutions prepared in CH_2Cl_2 at 10 µg.mL^{-1}.

MALDI-ToF mass spectra of polymers were recorded at the CRMPO Scanmat (Rennes, France) on a Bruker Ultraflex III that was equipped with a pulsed N_2 laser source (337 nm, 4 ns pulse width) and a time-delayed extracted ion source. Spectra were recorded in the positive-ion mode using the reflectron mode and with an accelerating voltage of 20 kV. A freshly prepared solution of the polymer sample in THF (HPLC grade, 10 mg·mL^{-1}) and a

saturated solution of *trans*-2-[3-(4-*tert*-butylphenyl)-2-methyl-2-propenylidene]-malononitrile (10 mg, DCTB) in THF (1 mL, HPLC grade) were prepared. A MeOH solution of the cationizing agent (NaI or AgOTf, 10 mg.mL^{-1}; Na^+ ions interact with the polymer's heteroatoms enabling the observation of functional PCOE, while Ag^+ ions interact with all C=C containing products enabling also the observation of heteroatom-free polymers such as cyclic nonfunctional PCOE) was also prepared. The solutions were combined in a 10:1:1 *v/v/v* of matrix-to-sample-to-cationizing agent. The resulting solution (1−2 g/L) was deposited onto the sample target and vacuum-dried.

FTIR spectra of the polymers were acquired (16 scans) with a resolution of 4 cm^{-1} on a Shimadzu IRAffinity-1 equipped with an ATR module.

4-Hydroxy-3-isopropyl-4,5-dimethyloxazolidin-2-one (1). DMDO (100 mg, 0.88 mmol) and isopropylamine (52 mg, 0.88 mmol, 1.0 equiv.) were mixed in a glass vial and stirred for 2 h at room temperature (Scheme 4a). The resulting compound **1** was isolated as colorless crystals after recrystallization from pentane at –40 °C (119 mg, 78%, mixture of two diastereoisomers in a ca. 3:2 ratio). ^{1}H NMR: δ 4.39, 4.24 (2 q, *J* = 7 Hz, 1H, C*H*(CH$_3$)O), 3.70, 3.64 (2 q, *J* = 7 Hz, 1H, N(C*H*(CH$_3$)$_2$)), 1.43 (d, *J* = 7 Hz, 3H, C(OH)(C*H*$_3$)), 1.40−1.35 (m, 9H, N(CH(C*H*$_3$)$_2$ and C*H*$_3$CH) (Figure S1). ^{13}C NMR (mixture of two diastereoisomers): δ 156.1, 155.3 (O*C*(O)N), 89.9, 88.6 (N*C*(OH)(CH$_3$)), 81.2, 79.5 (O*C*H(CH$_3$)), 44.3, 43.7 (N(*C*H(CH$_3$)$_2$)), 23.9 (NC(OH)(*C*H$_3$)), 21.1, 20.9, 20.7, 20.5, 20.5 (NC(OH)(*C*H$_3$), N(CH(*C*H$_3$)$_2$), OCH(*C*H$_3$)), 16.1 (N(CH(*C*H$_3$)$_2$)), 13.0 (OCH(*C*H$_3$)) (Figure S1). COSY, HSQC and HMBC (Figures S2−S4). FT-IR ν (cm^{-1}): 3410 (vs, br, O−H), 3000 (m, =C−H), 2950 (w, =C−H), 1710 (vs, C=O), 1350 (s, C−O), 1220 (s, C−N) (Figure S5). Single-crystal X-ray diffraction (Figure S6, Table S1). ESI-MS [M.Na$^+$]: major species-($C_8H_{15}NO_3Na$): m/z_{calcd} = 196.09441, m/z_{exp} = 196.0943 for z = 1 (Figure S7).

3,3'-((Ethane-1,2-diylbis(oxy))bis(ethane-2,1-diyl))bis(4-hydroxy-4,5-dimethyloxazolidin-2-one) (2). DMDO (100 mg, 0.88 mmol) and EDR-148 (65 mg, 0.44 mmol, 0.5 equiv.) were mixed in a glass vial and stirred for 2 h at room temperature (Scheme 4b). Full conversion in EDR-148 was reached within 1 h, as assessed by ^{1}H NMR analysis. Compound **2** was isolated without further purification as a colorless liquid by removal of volatiles under vacuum (164 mg, 99%). ^{1}H NMR (mixture of stereoisomers): δ 5.27, 5.15, 5.12, 4.97, 4.85, 4.75, 4.71, 4.65 (s, 2H, C(O*H*)), 4.40 and 4.25 (2 m, 2H, OC*H*(CH_3)C), 3.8−3.5 and 3.35−3.15, (m, 12H, C*H*$_2$OC*H*$_2$C*H*$_2$N), 1.46−1.38 and 1.3−1.2 (2 m, 12H, OC*H*(C*H*$_3$)C and NC(C*H*$_3$)(OH)CH) (Figure S8). ^{13}C NMR (mixture of stereoisomers): δ 156.4 (O*C*(O)N), 88.0, 86.1 (N*C*(OH)(CH_3)), 81.4, 80.2 (O*C*H(CH_3)), 73.4, 70.2, 69.8, 68.9 (*C*H$_2$OCH$_2$CH$_2$N), 40.2 (CH$_2$OCH$_2$*C*H$_2$N), 23.3, 20.3 (NC(OH)(*C*H$_3$)), 16.3, 13.0 (OCH(*C*H$_3$)C) (Figure S8). COSY, HSQC, HMBC NMR spectra (Figures S9−S11). FT-IR ν (cm^{-1}): 3450 (vs, br, O−H), 3000 (w, =C−H), 2950 (m, C−H), 2900 (m, C−H), 1710 (vs, C=O), 1350 (s, C−O), 1220 (m, C−N), 1110 (s, C−O) (Figure S12). ESI-M [M.Na^{+}] major species-(C$_{16}$H$_{28}$N$_2$O$_8$Na): m/z_{calcd} = 399.1738, m/z_{exp} = 399.1741 for z = 1 (Figure S13).

3-Oxobutan-2-yl isopropyl(methyl)carbamate (3). DMDO (229 mg, 2.0 mmol), *N*-methyl-propan-2-amine (147 mg, 2.0 mmol, 1.0 equiv.) and DBU (3.0 mg, 0.02 mmol, 0.01 equiv.)[43] were mixed in a glass vial and stirred for 3 h at room temperature (Scheme 4c). Compound **3** was quantitatively isolated without further purification upon removal of volatiles under vacuum as a colorless liquid (373 mg, 98%). ^{1}H NMR: δ 4.98 (bs, 1H, C(O)C*H*(CH_3)O), 4.35 (bs, 1H, NC*H*(CH_3)$_2$), 2.77 (s, 3H, N(C*H*$_3$)), 2.13 (s, 3H, (C*H*$_3$)C(O)), 1.36 (d, J = 7 Hz, 3H, CH(C*H*$_3$)O), 1.13 (d, J = 7 Hz, 6H, NCH(C*H*$_3$)$_2$) (Figure S14). ^{13}C NMR: δ 207.0 ((CH_3)*C*(O)CH), 155.2 (O*C*(O)N), 75.4 (C(O)*C*H(CH_3)O), 46.7 (N(*C*H(CH_3)$_2$)), 27.0 (N(*C*H$_3$)), 25.4 ((*C*H$_3$)(O)), 19.4 (C(O)CH(*C*H$_3$)O), 16.2 (N(CH(*C*H$_3$)$_2$)) (Figure S14). COSY, HSQC, HMBC NMR spectra (Figures S15−S17). FT-IR ν (cm^{-1}): 3000 (s, br, =C−H),

2950 (w, C−H), 2900 (w, C−H), 1690 (vs, C=O), 1350 (s, C−O), 1120 (vs, C−N), 1070 (vs, C−O) (Figure S18). ESI-MS [M.Na^+] ($C_9H_{17}NO_3Na$): m/z_{calcd} = 210.1106, m/z_{exp} = 210.1096 for z = 1 (Figure S19).

(5-Methyl-2-oxo-1,3-dioxol-4-yl)methyl acrylate (VC1). DMDO-OH (130 mg, 1.00 mmol) and triethylamine (0.18 mL, 1.35 mmol, 1.35 equiv) were added into CH_2Cl_2 (10 mL) precooled at 0 °C in a round-bottom flask. Acryloyl chloride (0.08 mL, 1.05 mmol, 1.05 equiv) was then added dropwise under stirring. The reaction mixture was then slowly warmed to room temperature and stirred for 2 h. The reaction was monitored by TLC (pentane/ethyl acetate 7:3 *v/v*, Rf = 0.8). After completion, the black reaction mixture was washed first with concentrated aqueous $NaHCO_3$ (20 mL), then distilled water (2 × 20 mL), and finally concentrated under vacuum. The resulting oily residue was purified by flash chromatography (pentane/ethyl acetate 9:1 *v/v*) to give analytically pure **VC1** as a yellowish oil (50 mg, 27%). ^{1}H NMR: δ 6.49 (dd, J_{trans} = 17 Hz, J_{gem} = 1 Hz, 1H, C(O)CHCH*H*), 6.15 (dd, J_{trans} = 17 Hz, J_{cis} = 11 Hz, 1H, C(O)C*H*CH_2), 5.94 (dd, J_{cis} = 11 Hz, J_{gem} = 1 Hz, 1H, C(O)CHCH*H*), 4.94 (s, 2H, CC*H*$_2$OC(O)), 2.22 (s, 3H, CC*H*$_3$) (Figure S20). ^{13}C NMR: δ 165.5 (O*C*(O)CH), 152.1 (O*C*(O)O), 140.2 (s, O*C*(CH_3)C), 133.5 (*C*(CH_2O)O), 132.4 (OC(O)*C*HCH_2), 127.4 (OC(O)CH*C*H_2), 53.8 (C*C*H_2OC(O)), 9.4 (C(*C*H_3)) (Figure S20). FT-IR ν (cm^{-1}): 1810 (vs, C=O, carbonate), 1720 (vs, C=O, acrylate), 1630 (m, C=C), 1400 (m, =C–H), 1300 (m, C–O), 1230 (C–O), 1160 (vs, C–O), 1040 (s, C–O) (Figure S21). ESI-MS [MNa^+] ($C_8H_8O_5Na$): m/z_{calcd} = 207.0264, m/z_{exp} = 207.0266 for z = 1 (Figure S22).

Bis((5-methyl-2-oxo-1,3-dioxol-4-yl)methyl) fumarate (VC2). DMDO-OH (500 mg, 3.85 mmol) and triethylamine (0.78 mL, 5.77 mmol, 1.5 equiv) were added into CH_2Cl_2 (20 mL) pre-cooled at 0 °C in a round-bottom flask under argon atmosphere. A solution of fumaroyl chloride (0.25 mL, 2.31 mmol, 0.45 equiv) in CH_2Cl_2 (5 mL) was then added dropwise under

stirring. The reaction mixture was slowly warmed to room temperature and stirred under a weak stream of argon for 2 h. The reaction mixture was then washed with concentrated aqueous $NaHCO_3$ (2 × 20 mL), distilled water (2 × 20 mL), and concentrated under vacuum. The resulting black oily residue was purified by flash chromatography (pentane/ethyl acetate 7:3 *v/v*) to give a colorless oil. This oil was dissolved in MeOH (2 mL) and kept at –40 °C for 48 h to afford analytically pure **VC2** as colorless crystals (120 mg, 10%). ^{1}H NMR: δ 6.90 (s, 2H, C(O)C*H*C*H*C(O)), 4.97 (s, 4H, OCH_2C), 2.20 (s, 6H, C(CH_3)) (Figure S23). ^{13}C NMR: δ 163.9 (CH*C*(O)O), 151.8 (O*C*(O)O), 140.6 (C*C*(CH_3)O), 133.6 (C(O)*C*H*C*HC(O)), 132.8 (OCH_2*C*(O)(C)), 54.6 (C(O)O*C*H_2(C)), 9.4 (C(*C*H_3)(O)) (Figure S23). FT-IR ν (cm^{-1}): 1810 (vs, C=O, carbonate), 1720 (vs, C=O, ester), 1630 (s, C=C), 1380 (s, =C–H), 1290 (s, C–O), 1230 (m, C–O), 1160 (vs, C–O), 1040 (s, C–O) (Figure S24). ESI-MS [M.Na^+] ($C_{14}H_{12}O_{10}Na$): m/z_{calcd} = 363.0323, m/z_{exp} = 363.0325. X-Ray structure (Figure S25, Table S2).

Bis((5-methyl-2-oxo-1,3-dioxol-4-yl)methyl) (*E*)-hex-3-enedioate (VC3). A solution of (*E*)-hex-3-enedioic acid (3.1 g, 27.0 mmol) and thionyl chloride (26.2 g, 0.22 mol) was refluxed overnight. The reaction mixture was then cooled to room temperature. After 1 h, excess thionyl chloride was distilled out under vacuum and DMDO-OH (7.4 g, 57.0 mmol) was added. The reaction mixture was cooled down to −40 °C and triethylamine (8.2 g, 81.0 mmol, 1.45 equiv) was added dropwise. The reaction mixture was warmed to room temperature over 4 h, then washed with a concentrated aqueous $NaHCO_2$ solution (4 × 200 mL) and brine (200 mL), and then purified by column chromatography (CH_2Cl_2) to give analytically pure **VC3** as a pale yellowish oil (1.32 g, 13%). ^{1}H NMR: δ 5.67 (t, *J* = 4 Hz, 2H, CH_2C*H*=C*H*CH_2), 4.82 (s, 4H, CCH_2OC(O)), 3.12 (d, *J* = 4 Hz, 2H, CHCH_2C(O)O), 2.15 (s, 6H, C(CH_3)) (Figure S26). ^{13}C NMR: δ (ppm) 170.8 (O*C*(O)CH_2), 152.1 (O*C*(O)O), 140.1

(O*C*(CH_3)C), 132.8 (O*C*CH_2), 125.9 (CH_2*C*H=*C*HCH_2), 53.9 (C(O)O*C*H_2), 37.2 (CHC*H*$_2$C(O)), 9.4 (C(*C*H_3)) (Figure S26). FT-IR ν (cm^{-1}): 1810 (vs, C=O, carbonate), 1740 (vs, C=O, ester), 1400 (w, =C–H), 1300 (m, C–O), 1220 (m, C–O), 1160 (s, C–O), 1040 (m, C–O) (Figure S27). ESI-MS [M.Na^+] ($C_{14}H_{12}O_{10}Na$): m/z_{calcd} = 391.0636, m/z_{exp} = 391.0640 (Figure S28).

General procedure for the ROMP/CM of COE with VC1–VC3 CTAs. All polymerizations were performed according to the following typical procedure (Scheme 6, Table S3, entry 1). The only differences lie in the nature of the solvent, catalyst loading ([**G2**]$_0$), nature of CTA and its initial concentration ([CTA]$_0$). Under an argon atmosphere, a Schlenk flask equipped with a magnetic stir bar was charged sequentially with dry CH_2Cl_2 (5.0 mL), COE (1.53 mL, 1.29 g, 11.7 mmol) and **VC1** (27 mg, 0.15 mmol). The initial concentration of COE was kept at 1.5 mol.L^{-1}. The resulting solution was heated at 40 °C and the polymerization was started upon addition, *via* a cannula, of a freshly prepared CH_2Cl_2 solution (2.0 mL) of **G2** (9.9 mg, 11.7 μmol). The reaction mixture turned highly viscous within 2 min. The viscosity then slowly decreased over the following 10 min. After the desired reaction time (typically 3 h; reaction time was not necessarily optimized), volatiles (solvent and ethylene) were removed under vacuum. The polymers were all recovered as brownish and brittle solids, which were readily soluble in $CHCl_3$ and THF, and insoluble in MeOH (Schemes 6,S2,S3, Tables 1,S2,S3). All experiments were at least duplicated (Tables 1,S3,S4). The isolated polymers were characterized by NMR and FT-IR spectroscopies, SEC and MS analyses (Figures 1–3, S29–40). CNF could not be quantified[32,52-54,52] because not enough sample was recovered.

General procedure for the copolymerization of NB and CDT. In a typical experiment (Scheme 7), the reaction was performed as described above using $(CH_2Cl)_2$ (10.0 mL), NB

(0.66 g, 7.01 mmol), CDT (1.40 mL, 1.13 g, 7.01 mmol), CTA **VC3** (258 mg, 0.70 mmol) and a freshly prepared CH_2Cl_2 solution (4.0 mL) of **G2** (5.9 mg, 7.0 μmol). The copolymer di(**VC3**)-P(NB-*co*-CDT) was recovered without further purification, as a brownish viscous liquid at 25 °C, which is readily soluble in $CHCl_3$ and THF, and insoluble in MeOH. The copolymers were characterized by NMR and FT-IR spectroscopies, and SEC analyses (Figures 4, S41–S46). The experimental molar mass $M_{n,NMR}$ = 3300 g.mol^{-1} was determined with the following formula: $M_{n,theo}$ = {(M_{NB} × [NB]$_0$ × conv.$_{NB}$) + (M_{CDT} × [CDT]$_0$ × conv.$_{CDT}$) / [**VC3**]$_0$ × conv.$_{\mathbf{VC3}}$)} + $M_{\mathbf{VC3}}$.

Determination of the VC content in di(VC3)-PCOE or in di(VC3)-P(NB-*co*-CDT). The **VC3** content in VC-end capped (co)polymers was determined using 4-bromobenzonitrile (BBN) as an internal NMR standard, from the characteristic resonances of BBN ($\delta_{Hd,e}$ 7.75, 7.69 ppm) and VC (δ_{Ha} 2.10 ppm) (Figure S45). The concentration in **VC3** function was calculated by the following equation: $C_{VC3}(mmol.g^{-1}) = \frac{\frac{\int H_{VC3}}{\int H_{BBN}} \times n_{BBN}}{m_{PCOE}}$, where $\int H_x$ is the integration value for one hydrogen of compound x, with x = **VC3** or BBN.

Reaction of di(VC3)-PCOE or di(VC3)-P(NB-*co*-CDT) with primary amines. In a typical experiment, di(**VC3**)-PCOE was dissolved in dry CH_2Cl_2 (0.5 mL) at 35 °C under argon and a freshly prepared solution of EDR-148 (0.5 mL of a 0.05 M solution, 1.0 equiv) in dry CH_2Cl_2 was added. The resulting crude reaction polymer was then analyzed by NMR spectroscopy and SEC analysis (Figures 5, S46–S55; Schemes 8,S2).

X-ray diffraction crystallography. X-ray diffraction data for compounds **1** and **VC2** were collected at 150 K using a Bruker APEX CCD diffractometer with graphite-monochromated Mo Kα radiation (λ = 0.71073 Å). A combination ω and Φ scans was carried out to obtain at least a unique data set. The crystal structures were solved by direct methods, and remaining atoms were located from difference Fourier synthesis followed by full-matrix least-squares

based on F^2 (programs SIR97 and SHELXL-97).[57] The hydrogen atom contributions were calculated, but not refined. All non-hydrogen atoms were refined with anisotropic displacement parameters. The locations of the largest peaks in the final difference Fourier map calculation as well as the magnitude of the residual electron densities were of no chemical significance. A summary of crystallographic data for **1** (CCDC # 1897222) and **VC2** (CCDC # 1897221) is collected in Tables S1 and S2, respectively.

Results and Discussion

Model reaction of 4,5-dimethyl-1,3-dioxol-2-one (DMDO) with nucleophiles. To assess the possibility of synthesizing poly(di(hydroxy-oxazolidone)polyolefin)s NIPUs from the polyaddition of α,ω-di(vinylene carbonate) telechelic polyolefins with diamines, the model reaction between the commercially available VC DMDO and a nucleophile such as amines was first investigated (Scheme 4).

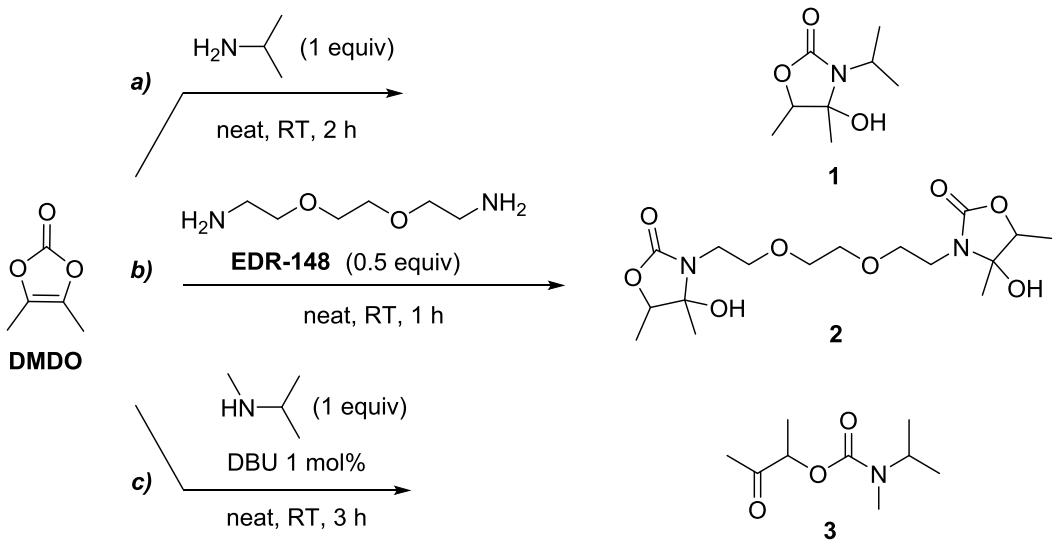

Scheme 4. Reactivity of DMDO: a-b) Synthesis of hydroxy-oxazolidone compounds **1** and **2** from the aminolysis of DMDO; and synthesis of c) oxo-urethane **3** from the reaction of DMDO with *N*-isopropylmethylamine.

The neat room temperature reaction of DMDO with isopropylamine smoothly afforded the hydroxy-oxazolidone compound **1** as colorless crystals (Scheme 4a), as evidenced by NMR, FTIR, ESI-MS and also by an X-Ray diffraction analysis (Figures S1–S7, Table S1). Of note, in the ^{1}H NMR spectrum, hydrogens H^{a-e} displayed two sets of distinct signals (3:2 ratio) as the signature of the two diastereomers; the same splitting was correspondingly observed in the ^{13}C NMR spectrum (Figures S1–S4). Furthermore, ESI-MS analyses of the isolated crystals revealed, besides compound **1**, the presence of several impurities (Figure S7). These latter were identified as compound **1a** resulting from the dehydration of **1** – as predicted by Shi *et al.* (Scheme S1)–,[58] as well as the urea derivatives **1b** and **1c**. Such urea species were not surprising, as they had already been reported as side-products during the synthesis of PHUs from cyclocarbonates.[19,28] These **1a–1c** trace compounds, which could not be quantified by MS and yet which were not observed by NMR spectroscopy (possibly arising from the MS analysis itself), probably remained minor DMDO aminolysis side-species, thus most likely not impeding the envisioned ensuing synthesis of poly(hydroxy-oxazolidone) species therefrom.

Similarly, the neat room temperature aminolysis of DMDO by a primary diamine, namely EDR-148, afforded compound **2** as a colorless viscous liquid (Scheme 4b), as supported by 1D and 2D NMR spectroscopy, FTIR and MS analyses (Figures S8–S13). Interestingly, the ^{1}H NMR resonance of the hydroxyl group (H^{c}) appeared as a set of eight resolved sharp singlets, a hyperfine structure possibly resulting from strong intra- and/or inter-molecular hydrogen bonds. Diasteromers of **2** were, similarly to **1**, observed in the ^{1}H and ^{13}C NMR spectra as two distinct sets of signals. ESI-MS analysis of the isolated sample further evidenced the formation of the expected major hydroxyl-oxazolidone species **2**, along with its corresponding dehydration compound **2a**, the mono-adduct **2'**, and the corresponding

urea compound **2b** (Figure S13). Note that, again, the latter three species were not detected by NMR analysis.

The potential synthesis of a poly(oxo-urethane)/polyolefin from the polyaddition of an α,ω-di(vinylene carbonate) telechelic polyolefin (di(VC)-PO) and a secondary diamine,[43] was next assessed upon reacting DMDO with *N*-isopropylmethylamine (Scheme 4c). The oxo-urethane (Figures S14–19) compound **3** was thus isolated (almost quantitatively; no detected impurities), as evidenced by NMR, FT-IR and ESI-MS analyses.

At this stage, the reactivity of DMDO towards amines highlighted that: i) the reactivity of VC compounds towards nucleophiles, as reported herein for the first time, gives similar compounds as those prepared from the related α-alkylidene cyclic carbonates;[39,43] ii) the synthesis of (hydroxy-oxazolidone) species from bis(VC) compounds and diamines is indeed feasible; iii) the formation of urea side-compounds[59] as hinted by ESI-MS analyses may occur – apparently to a minor extent – during the synthesis of poly(hydroxy-oxazolidone) derivatives; and iv) symmetric VC compounds may potentially afford, at room temperature, NIPUs or poly(carbonate)s upon addition to a diamine or a diol, respectively.[43]

ROMP/CM of olefins in the presence of a vinylene carbonate chain-transfer agent. *Synthesis of vinylene carbonate VC1–VC3 CTAs.* The VC compounds to be ultimately used as chain-transfer agents in metathesis reactions towards the preparation of poly(di(hydroxy-oxazolidone)polyolefin) (PHOPO) NIPUs were first synthesized from 4-(hydroxymethyl)-5-methyl-1,3-dioxol-2-one (DMDO-OH) (Scheme 5). The simplest asymmetric acrylate-type CTA, namely (5-methyl-2-oxo-1,3-dioxol-4-yl)methyl acrylate (**VC1**) was initially considered, even though such mono-acrylate CTAs are known to be effective yet not selective for the metathesis preparation of the targeted PHOPOs.[49–51] **VC1** was obtained from DMDO-

OH and acryloyl chloride with trimethylamine, as a yellowish oil (Scheme 5), and unequivocally characterized by NMR, FT-IR and ESI-MS analyses (Figures S20–S22). Symmetric fumarate- and hex-3-endioate-type CTAs, already established as successfully enabling the selective synthesis of telechelic polyolefins by metathesis,[32,50,52] were next considered. Bis((5-methyl-2-oxo-1,3-dioxol-4-yl)methyl) (*E*)-hex-3-enedioate (**VC2**) was isolated as colorless crystals from the reaction of DMDO-OH, fumaroyl chloride and triethylamine (Scheme 5), as evidenced by NMR, FT-IR, ESI-MS and X-ray analysis (Figures S23–S25, Table S2). Bis((5-methyl-2-oxo-1,3-dioxol-4-yl)methyl) (*E*)-hex-3-enedioate (**VC3**) was similarly obtained as a colorless oil from DMDO-OH and (*E*)-hex-3-ene-1,6-dioyl dichloride (Scheme 5), and spectroscopically and spectrometrically characterized (Figures S26–S28).

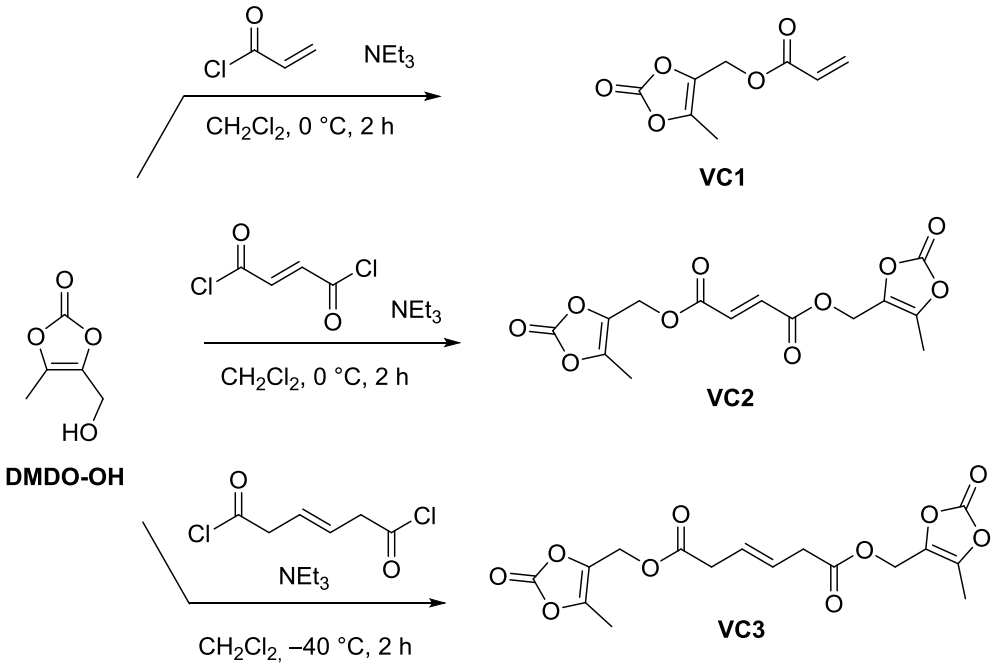

Scheme 5. Synthesis of vinylene carbonate chain-transfer agents **VC1–VC3** from 4-(hydroxymethyl)-5-methyl-1,3-dioxol-2-one (DMDO-OH).

Synthesis of α,ω-di(vinylene carbonate) telechelic polyolefins from the tandem ROMP/CM of cyclic olefin(s) catalyzed by G2 in the presence of VC1–VC3 CTAs. Compounds **VC1–VC3** were next used as CTAs in the tandem ROMP/CM of cyclooctene (COE) with Grubbs' 2nd-generation catalyst (**G2**) under the standard conditions previously established ([COE]$_0$/[**VC1**]$_0$/[BZQ]$_0$/[**G2**]$_0$ = 2000:100:100:1; 40 °C, CH_2Cl_2, argon atmosphere).[48–55] The ROMP/CM of COE performed in the presence of the asymmetric monofunctional acrylate-type CTA **VC1** and 1,4-benzoquinone (BZQ; a hydrogen acceptor known to successfully inhibit undesirable C=C isomerization process in various olefin metathesis reactions),[51,52,60,61,62] afforded a polyolefin referred to as **VC1**-PCOE (Scheme 6). The metathesis was found to proceed with quantitative conversion of both the monomer and the CTA, along with a good control of the PCOE molar mass and dispersity values (Table S3). As expected,[32,50–53] a statistical distribution of **VC1** end-capped PCOEs, including α-monofunctional (MF) and/or α,ω-difunctional (DF), linear, and/or cyclic non-functional (LNF, CNF, respectively) PCOEs (Scheme 6), was obtained. Indeed, ^{1}H and J-MOD NMR analyses of the recovered **VC1**-PCOE evidenced the presence of characteristic functionalized (MF and DF PCOEs; H$^{a–d}$, C$^{a–h}$) and non-functionalized (LNF, CNF PCOEs; H$^{i–k}$, C$^{i–k}$) chain-end groups' hydrogens and carbon atoms, as well as of the PCOE backbone (H$^{A–D}$, C$^{A–D}$) (Figure S29). As anticipated, no isomerization of the terminal C=C bonds was observed as it was inhibited by benzoquinone. These observations were further supported by COSY, HSQC, and HMBC 2D NMRs, FT-IR and ESI-MS (either using NaI as ionization salt to confirm the presence of DF and MF PCOEs, or using AgTFA as ionization salt to selectively evidence the presence of LNF and CNF along with DF PCOEs) analyses (Figures S29–S35). The formation of a mixture of MF and/or DF, LNF, CNF PCOEs prompted us to favor the use of symmetric VC-alkene CTAs, namely **VC2** and **VC3**, towards the targeted PHOPO NIPUs.

The symmetric fumarate **VC2** was evaluated in a typical ROMP/CM of COE catalyzed by **G2** ($[COE]_0/[\mathbf{VC2}]_0/[\mathbf{G2}]_0$ = 2000:20:1) (Scheme 6; Table S4, entries 1–2). Benzoquinone was not required since isomerization is impossible with this CTA. However, the reaction did not proceed efficiently under standard conditions (40 °C, CH_2Cl_2, argon atmosphere) with less than 5% of **VC2** being consumed in 24 h. Addition of 3 more equiv of **G2** raised the **VC2** conversion up to 83%, thus suggesting that the CTA (and/or some impurities within the sample; see thereafter) is deleterious to the catalysis. ^{1}H NMR analysis of the resulting polymer, referred to as di(**VC2**)-PCOE, revealed the presence of **VC2**-functional groups ($H^{a–d}$) and of a PCOE backbone ($H^{A–D}$), but also of phenyl chain-ends ($H^{e–g}$) arising from the large amount of catalyst used (G2 features a Ru–benzylidene initiating moiety at the origin of this phenyl end-capping group;[63,64,65] Figure S36). As expected, no MF or LNF PCOEs (both of which would be revealed by the presence of vinyl end-groups) were observed. To verify whether **VC2** was poisoning the **G2** catalyst or whether it was only intrinsically unreactive, it was used in the ROMP/CM of COE concomitantly with a CTA of a known moderate reactivity in the alike metathesis of COE, namely bis(oxiran-2-ylmethyl) maleate (**(*Z*)-GA$_2$**)[32] (Table S4). The ROMP/CM of COE with **VC2** (Table S4, entries 1,2), or with **VC2** and **(*Z*)-GA$_2$** (Table S4, entry 4), systematically displayed a lower CTA conversion than the ROMP/CM of COE performed with only **(*Z*)**-GA_2 alone (Table S4, entry 3) (< 5–35% vs 78%, respectively). This supported the inhibition of **G2** by **VC2** during the metathesis, or by unknown impurities contained therein (unlikely since **VC2** was recrystallized; refer to the Experimental Section); yet, the exact origin of the inhibition remains unclear. Nevertheless, **VC2** appeared unsuitable for the synthesis of di(VC)-telechelic polyolefins.

The tandem ROMP/CM of COE in the presence of the symmetric hex-3-ene-1,6-dioate-type CTA **VC3** afforded, under the standard operating conditions

([COE]$_0$/[**VC3**]$_0$/[**G2**]$_0$ = 2000:100:1; 40 °C, CH_2Cl_2, argon atmosphere), a mixture of **VC3**-end functional DF and CNF PCOEs, referred to as **VC3**-PCOE (Scheme 6, Table 1). The resulting polymer was isolated after 3 h by evaporation of volatiles as a brownish and brittle solid. All reactions were at least duplicated and showed a quite good reproducibility of the conversion and macromolecular data (±10%). Representative results are summarized in Table 1.

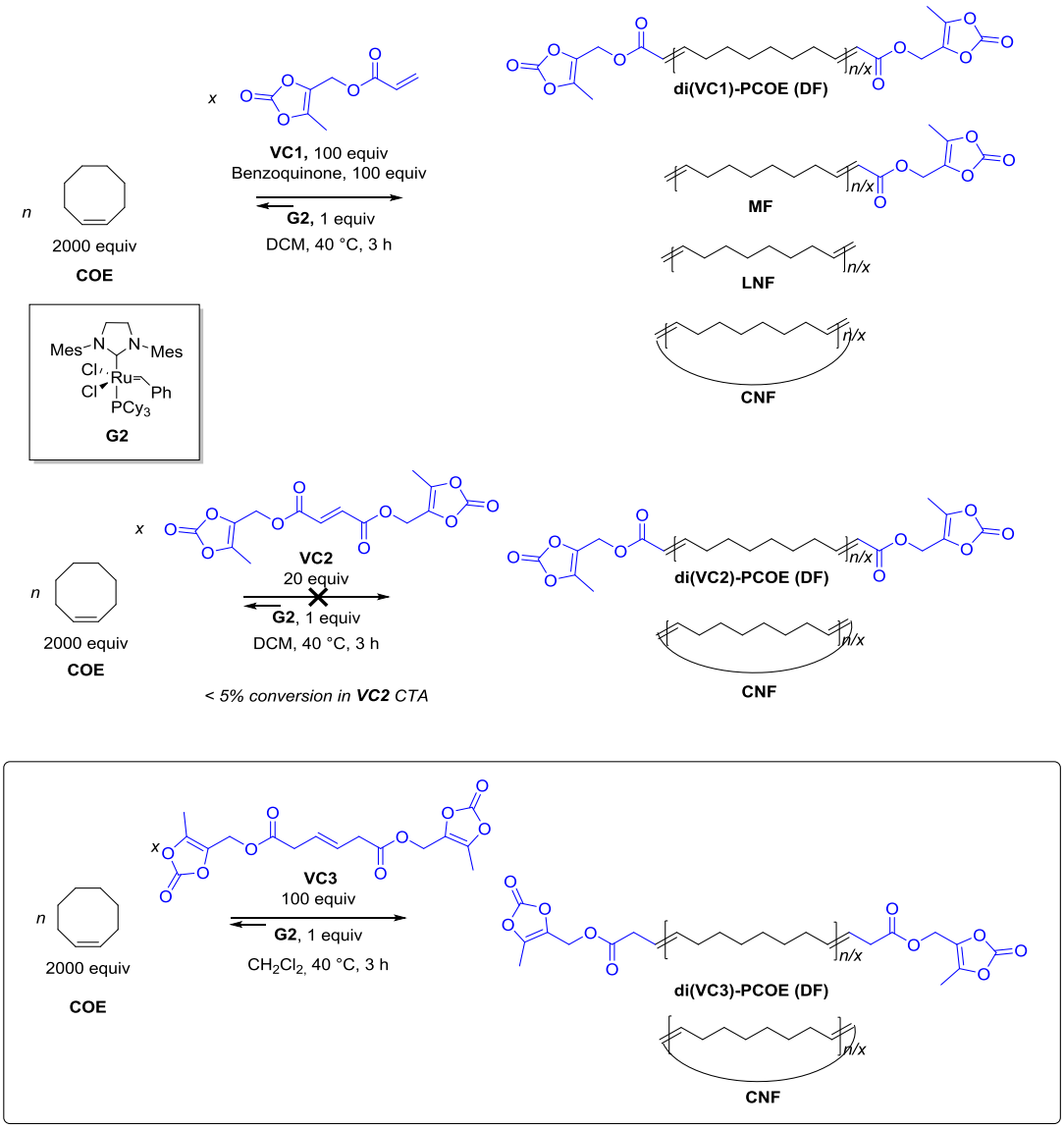

Scheme 6. Tandem ROMP/CM of COE catalyzed by Grubbs' catalyst **G2** in the presence of top: **VC1** as CTA and 1,4-benzoquinone; middle: **VC2** as CTA; and bottom: **VC3** as CTA,

showing the possible polymers (MF: α-monofunctional PCOE, LNF: linear non-functional PCOE, CNF: cyclic non-functional PCOE, and DF: α,ω-difunctional PCOE).

Table 1. ROMP/CM of COE catalyzed by **G2** in the presence of CTA **VC3** (Scheme 6).[a]

Entry	$[COE]_0/[\mathbf{VC3}]_0/[\mathbf{G2}]_0$	**VC3** Conv.[b] (%)	$M_{n,theo}$[c] ($g.mol^{-1}$)	$M_{n,NMR}$[d] ($g.mol^{-1}$)	$M_{n,SEC}$[e] ($g.mol^{-1}$)	$Đ_M$[e]
1	2000:20:1	100	11 400	18 500	34 000	1.9
2	2000:50:1	99	4800	6600	9000	2.3
3	2000:100:1	100	2600	2500	7000	1.7
4	10000:250:1	100	4800	6400	15 000	2.2
5	50000:1250:1	71	6600	8100	27 700	1.7
6	50000:1250:1	66	7000	9900	36 000	1.5

[a] General operating conditions: reactions performed in CH_2Cl_2 at 40 °C for 3 h; Catalyst = 11.7 µmol, $[COE]_0$ = 1.5 $mol.L^{-1}$; COE and NB conversion = 100% as determined by ^1H NMR analysis. [b] Conversion in CTA as determined by ^1H NMR analysis (refer to the Experimental Section). [c] Theoretical molar mass value calculated from $M_{n,theo} = \{M_{COE} \times ([COE]_0 \times Conv._{COE}) / ([\mathbf{VC3}]_0 \times Conv._{\mathbf{VC3}})\} + M_{\mathbf{VC3}}$, with M_{COE}= 110 $g.mol^{-1}$ and $M_{\mathbf{VC3}}$ = 368 $g.mol^{-1}$, on the basis of the formation of only DF (i.e. without taking into account any CNF PCOEs). [d] Experimental molar mass value determined by ^1H NMR analysis (refer to the Experimental Section). [e] Number-average molar mass ($M_{n,SEC}$) and dispersity ($Đ_M = M_w/M_n$) values determined by SEC vs polystyrene standards (uncorrected M_n values) in THF at 30 °C.

The catalyst loading was varied to compare the efficiency of the ROMP and CM steps. Quantitative conversion of the monomer and the CTA was observed at initial contents up to 10 000 and 250 equiv, respectively (Table 1, entries 1–4). Increasing the COE and CTA **VC3** loadings up to 50 000 and 1250 equiv, respectively, highlighted a high productivity of the ruthenium catalyst with effective turnover numbers (TONs) up to 50 000 $mol_{COE}\ mol_{(Ru)}^{-1}$ in the ROMP process, and 887 $mol_{\mathbf{VC3}}\ mol_{(Ru)}^{-1}$ in the CM step (Table 1, entry 5). Under similar operating conditions, different monomer-to-CTA and monomer-to-catalyst ratios induced, as anticipated, lower molar mass values when higher CTA loadings were used (Table 1, entries

1–3). The molar mass values of di(**VC3**)-PCOE as evaluated by ^{1}H NMR analyses ($M_{n,NMR}$) remained in fair agreement with the calculated ones determined from the consumption of the COE and CTA ($M_{n,theo}$), highlighting the fair control of the polymerization. The dispersities as determined by SEC were all monomodal, moderately narrow, and within the typical range for metathesis polyolefins prepared in the presence of a CTA ($Đ_M$ = 1.5–2.3).[66,67,68,69,70,71,72] The difference between $M_{n,SEC}$ values with $M_{n,NMR}$ and $M_{n,theo}$ data most likely results from the difference between the hydrodynamic radius of PCOE and of polystyrene standards used for the calibration.[48–55] Noteworthy, the $M_{n,SEC}$ values proportionally increased with the consumption of COE.

The di(**VC3**)-PCOE samples isolated exhibited the expected vinylene carbonate chain end-function(s) as evidenced by NMR, FT-IR and MS analyses (Figures 1,S37–S40). The ^{1}H and J-MOD NMR spectra showed the presence of VC functional groups ($H^{a–e}$, $C^{a–i}$) and PCOE backbone ($H^{A–D}$, $C^{A–D}$) (Figure 1) as further supported by COSY, HSQC and HMBC experiments (Figures S37–S39). ESI-MS analysis confirmed the presence of α,ω-di(**VC3**)-PCOE (NaI ionizing salt: major DF population observed with a repeating unit of 110 g.mol^{-1}, with e.g., m/z_{exp} = 1051.7210 g.mol^{-1} vs. m/z_{calcd} = 1051.7209 g.mol^{-1} for n =7; Figure 2), while MALDI-ToF MS analysis confirmed the presence of CNF (AgTFA ionizing salt; with a repeating unit of 110 g.mol^{-1}; Figure 3).

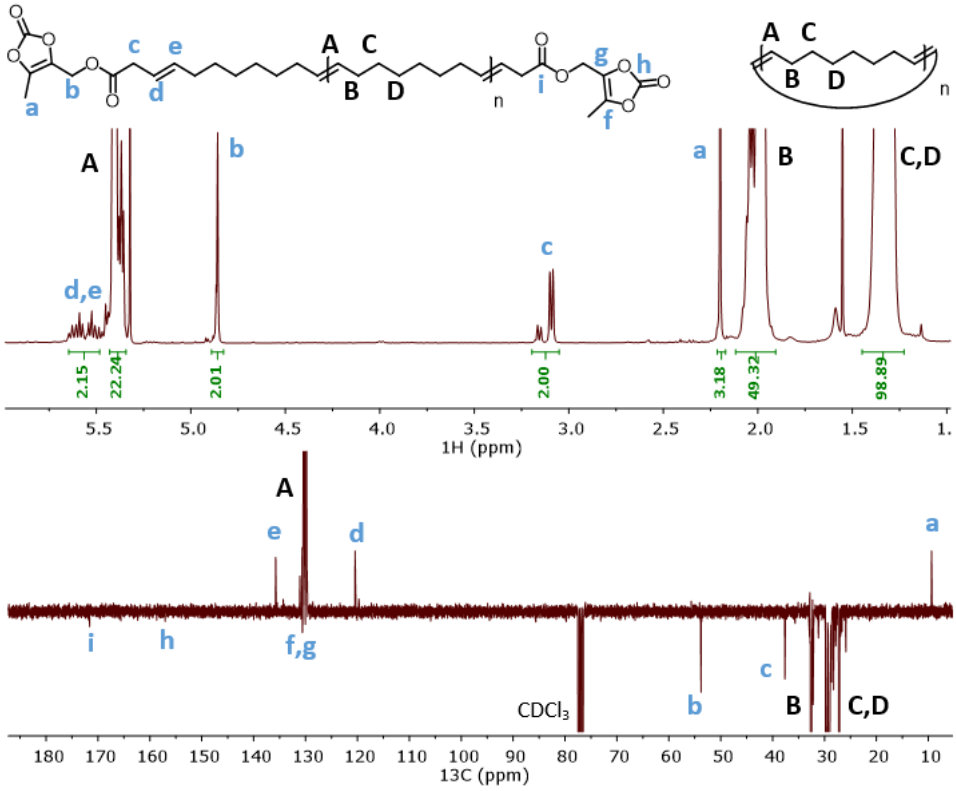

Figure 1. ^{1}H and J-MOD NMR spectra (400 and 100 MHz, $CDCl_3$, 25 °C) of a α,ω-di(**VC3**) telechelic PCOE sample prepared by ROMP/CM of COE in the presence of **G2** and **VC3** in CH_2Cl_2 (Table 1, entry 3).

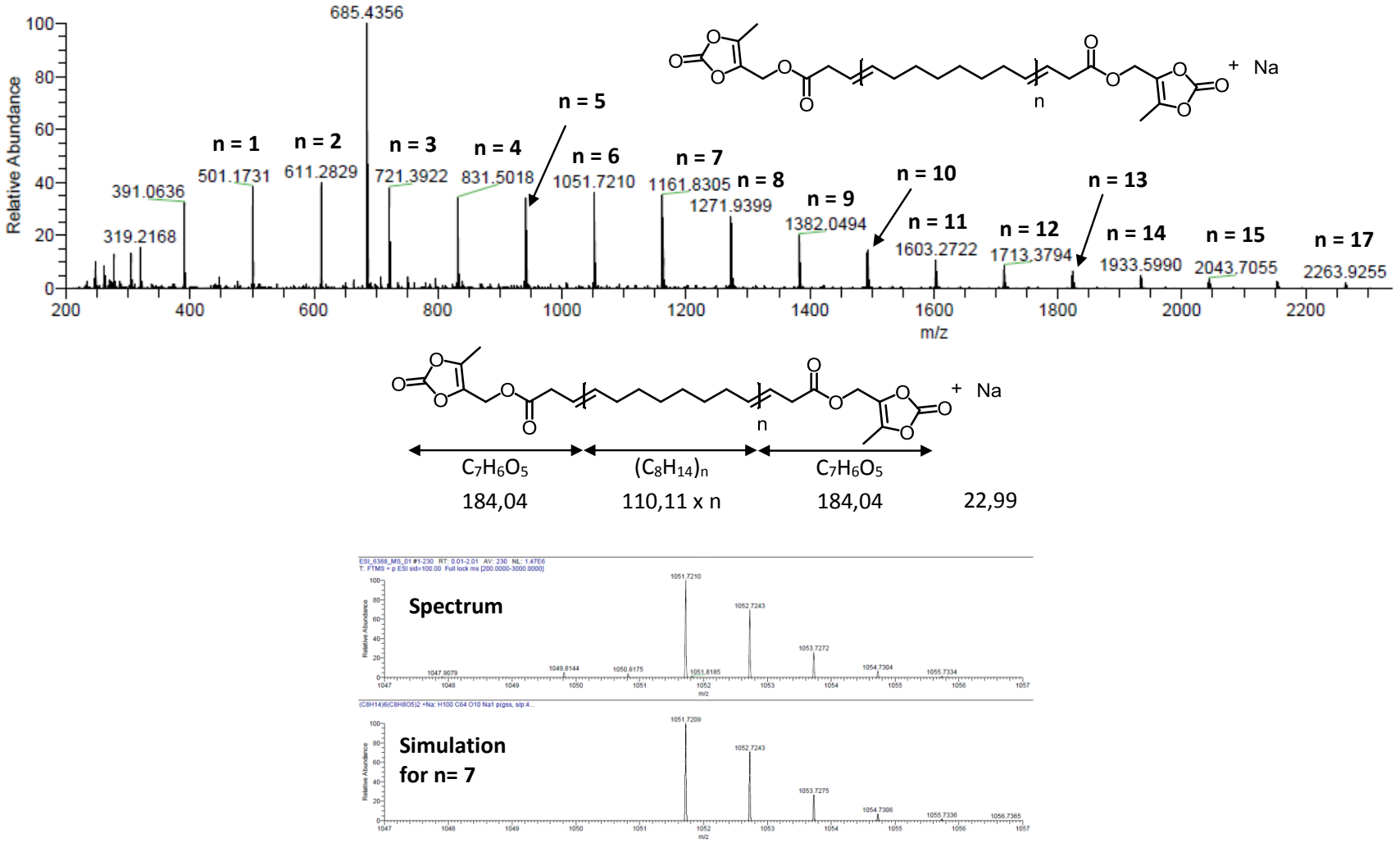

Figure 2. Top: ESI-mass spectrum (DCTB matrix, NaI ionizing salt) of an α,ω-di(**VC3**) telechelic PCOE sample prepared by ROMP/CM of COE using **G2** and **VC3** (Table 1, entry 3); bottom: zoomed spectrum and simulation of an α,ω-di(**VC3**)-PCOE for *n* = 7.

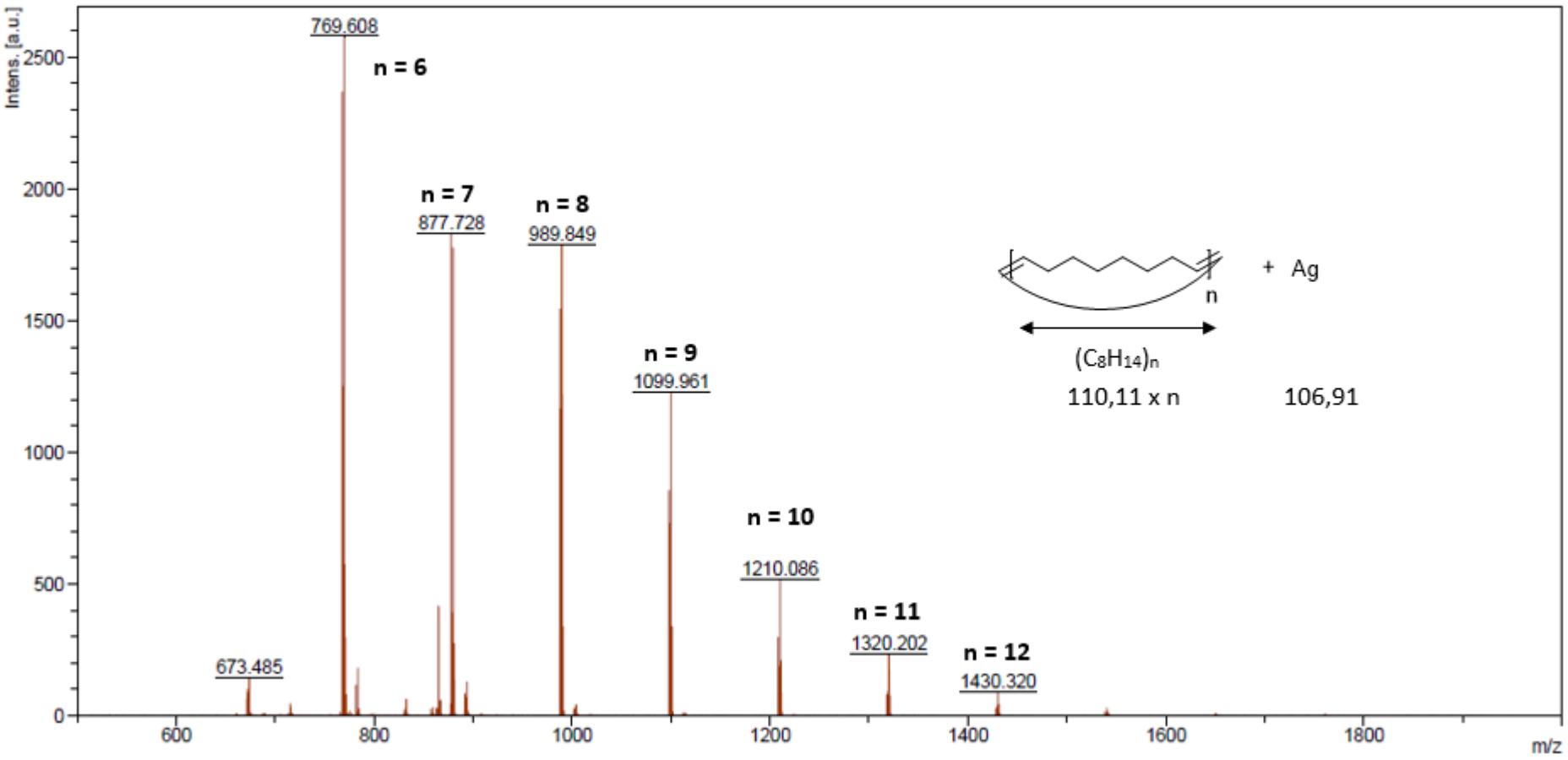

Figure 3. MALDI-ToF mass spectrum (DCTB matrix, AgTFA ionizing salt) of a α,ω-di(**VC3**) telechelic PCOE sample prepared by ROMP/CM of COE using **G2** and **VC3** showing CNF PCOE (Table 1, entry 3).

Telechelic di(**VC3**)-PCOE of different molar masses were thus successfully obtained from the ROMP/CM of COE from the catalytic system **G2**/**VC3**. Due to the symmetric nature of **VC3** CTA, the recovered polyolefin was only composed of DF and CNF PCOEs. The absence of mono-functional macromolecules enabled to reasonably foresee the use of di(**VC3**)-PCOEs as prepolymers in a polyaddition reaction with a diamine (NB: CNF PCOEs do not take part in the polyaddition; see thereafter).

ROMP/CM of norbonene (NB) and cyclododecatriene (CDT) in the presence of VC3 as CTA. In order to expend the library of VC telechelic polyolefins, the one-pot simultaneous copolymerization of an equimolar mixture of norbonene (NB) and cyclododecatriene (CDT) was performed under similar conditions ($[NB]_0$=$[CDT]_0$/$[\mathbf{VC3}]_0$/[**G2**] = 1000:1000:100:1; 40 °C, 3 h, CH_2Cl_2) (Scheme 7). Telechelic P(NB-*co*-CDT)s have already been previously reported as low viscosity liquid polyolefins, which facilitate their subsequent use in polyaddition reactions.[53–56] Thus, after reacting for 3 h under argon, volatiles were distilled out under vacuum to give a mixture of DF and CNF copolymers as a pale brownish liquid, thereafter referred to as di(**VC3**)-P(NB-*co*-CDT). No evidence of residual **VC3** or of monomers was observed by NMR analyses (see below), thus demonstrating their quantitative consumption, and therefore, the effective ROMP and CM processes. A theoretical molar mass of $M_{n,theo}$ = 2900 g.mol^{-1} was calculated from the initial monomers-to-**VC3** ratio. The experimental molar mass $M_{n,NMR}$ = 3300 g.mol^{-1}, determined by comparing the integration of the characteristic methylene hydrogens (δ_{Hc} 3.10 ppm) signal of the VC chain-ends, to the typical hydrogens' resonance of NB and CDT (δ_{HB} 2.81 ppm, $\delta_{HE,G}$ 5.23 ppm) from the polymer backbone (Figure 4), closely matched the $M_{n,theo}$ one. SEC analysis in THF gave $M_{n,SEC}$ = 9600 g.mol^{-1} and a dispersity $Đ_M$ = 1.5 values. The ^{1}H and ^{13}C J-MOD NMR spectra

of di(**VC3**)-P(NB-*co*-CDT) displayed distinct signals for the VC chain ends' hydrogens (H^{a-e}) and carbon atoms (C^{a-i}) along with the resonances of the NB and CDT segments (H^{B} and $H^{E,G}$), thereby evidencing unambiguously the presence of the expected **VC3** functional chain-end groups on the copolymer backbone (Figure 4). 2D COSY, HSQC and HMBC NMR spectra, as well as the FT-IR signature further supported the chemical structure of the telechelic copolyolefin (Scheme 7, Figures S41–S44).

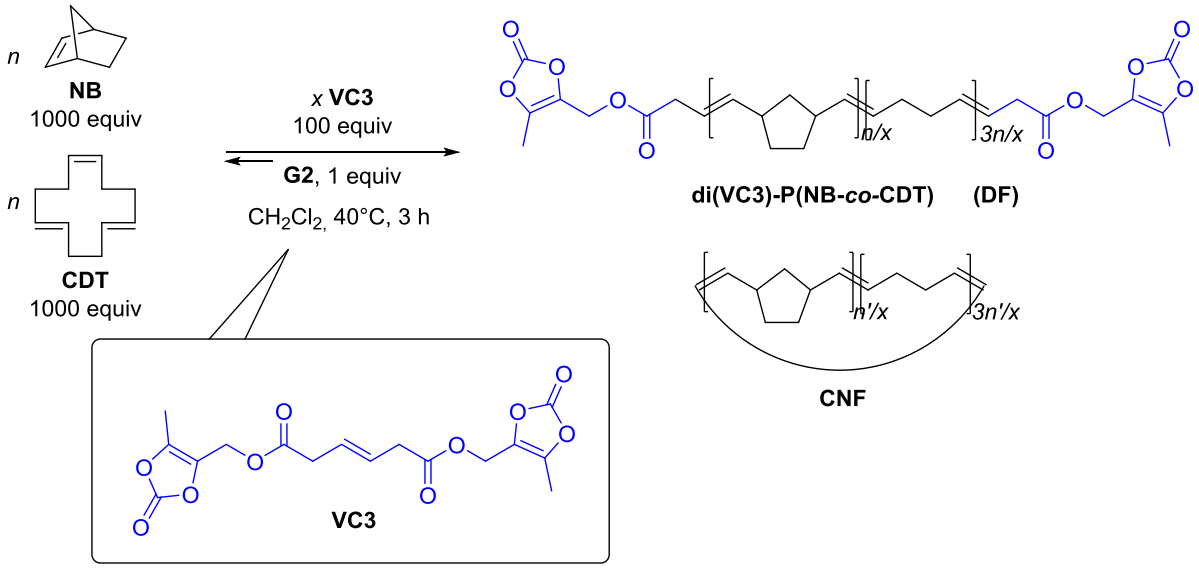

Scheme 7. Tandem ROMP/CM of NB and CDT (equimolar mixture) catalyzed by **G2** in the presence of **VC3** as CTA, showing the possible polymers (DF: α,ω-di(**VC3**) telechelic P(NB-*co*-CDT); CNF: cyclic non-functional P(NB-*co*-CDT)).

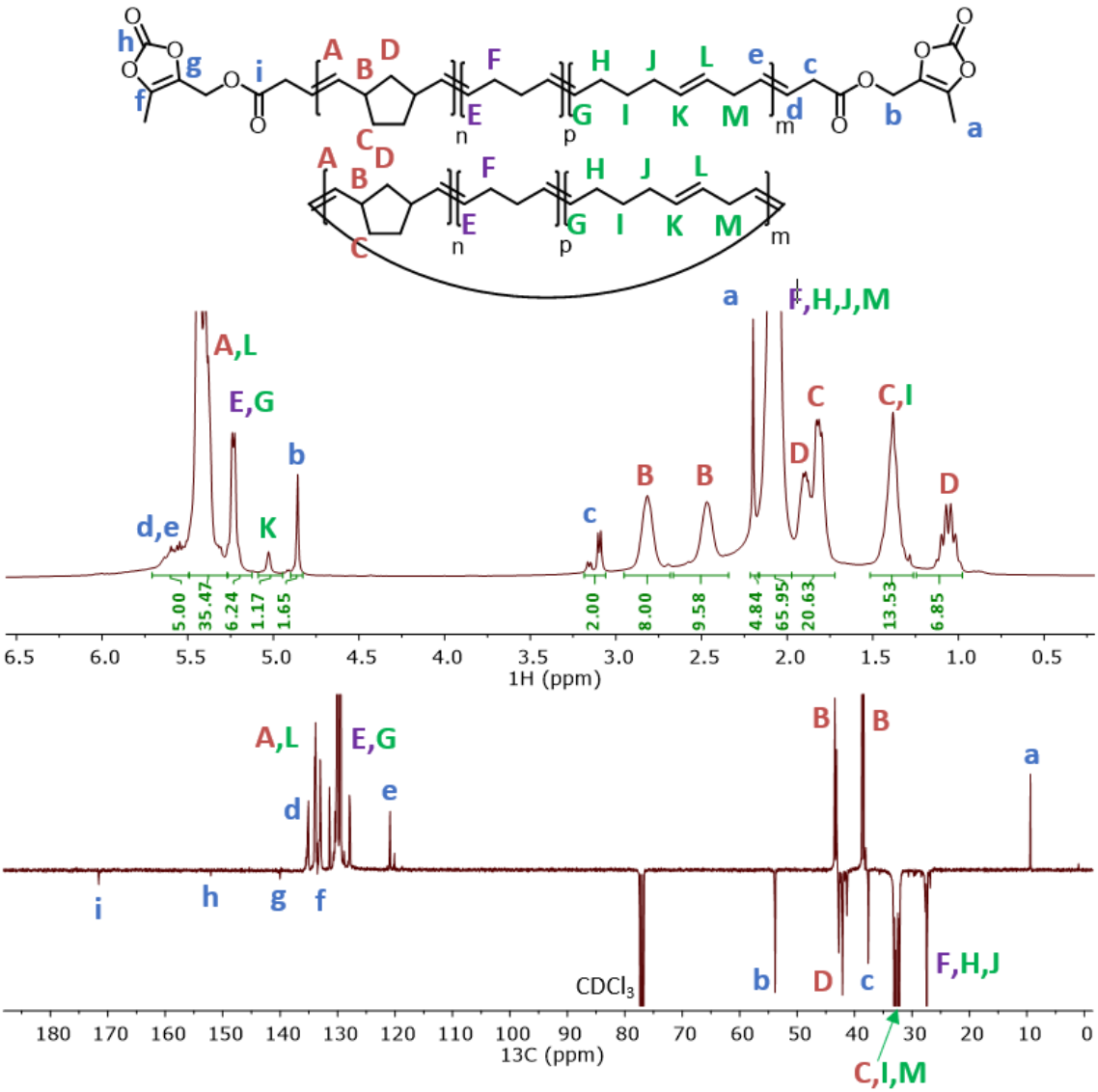

Figure 4. ^{1}H and J-MOD NMR spectra (400 and 100 MHz, $CDCl_3$, 25 °C) of a α,ω-di(**VC3**) telechelic P(NB-*co*-CDT) sample prepared by ROMP/CM of NB/CDT in the presence of **G2** and CTA **VC3**.

Attempted synthesis of poly(di(hydroxy-oxazolidone)polyolefin) NIPUs from the polyaddition of α,ω-di(VC3) telechelic polyolefins with a diamine. With the objective to synthesize a poly(di(hydroxy-oxazolidone)polyolefin) (PHOPO) NIPUs (Scheme 3), di(**VC3**)-PCOE and di(**VC3**)-P(NB-*co*-CDT) were reacted with a primary diamine, namely EDR-148,[32,54] in an equimolar mixture (Scheme 8). In order to precisely control the

stoichiometry of the reaction, the exact amount of chain-ends in the VC-end capped prepolymers was determined by ^{1}H NMR spectroscopy, using 4-bromobenzonitrile as an internal reference (refer to the Experimental section; Figure S45).

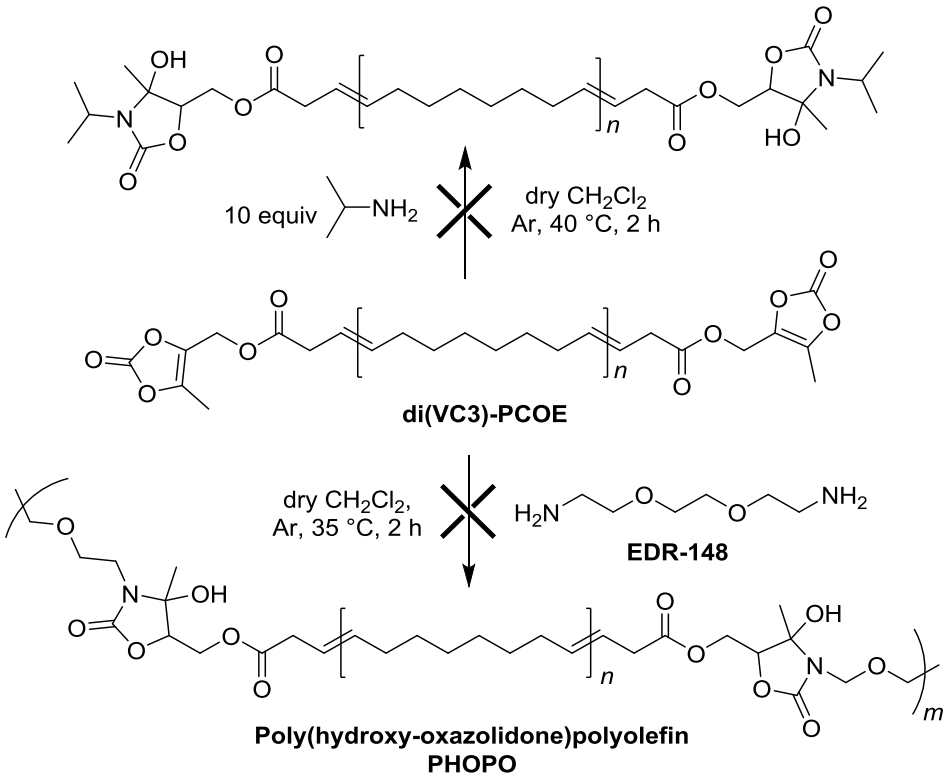

Scheme 8. Attempted reaction of di(**VC3**)-PCOE with EDR-148 or isopropylamine depicting the expected PHOPO compounds.

The resulting product from the equimolar reaction of di(**VC3**)-PCOE with EDR-148 (CH_2Cl_2, 35 °C, 2 h) was analyzed by NMR. The ^{1}H NMR spectrum showed a 46% consumption of **VC3** functions as monitored using the methyl H^{e} signal (Figure 5). Attempts to reach a higher-to-quantitative **VC3** consumption upon addition of DBU as catalyst,[43] or by prolonging the reaction time, all remained unsuccessful. The ^{1}H NMR spectrum of the recovered polymer also revealed broad and numerous signals at δ 3.0–4.0 ppm, hinting for a variety of species. The sharp resonances observed at δ ca.1.5 ppm suggested the presence of several methyl groups, and the multiplets recorded at δ ca. 4.7 ppm were reminiscent of

methylene hydrogens located in between the ester function and the hydroxy-oxazolidone group (C(O)OC*H*$_2$C(O)(C(OH)(CH$_3$)N)) (Figure 5). Further careful analyses of J-MOD, COSY, HSQC and HMBC NMR spectra proved uninformative to support a plausible structure (Figures S46–S49).[73] SEC analysis of the recovered polymers revealed molar mass values identical to those of the initial di(**VC3**)-PCOE, respectively. Altogether, these observations suggested that the polyaddition reaction did not occur as anticipated. Performing the polyaddition of di(**VC3**)-P(NB-*co*-CDT) with EDR-148 under the same operating conditions did not reveal more successful nor informative (Scheme 8, Figures S50−S53).

The reactivity of di(**VC3**)-PCOE$_2$ and di(**VC3**)-P(NB-*co*-CDT) towards the EDR-148 diamine appears in sharp contrast to that of DMDO (Scheme 4) or of α-alkylidene cyclocarbonates (Scheme 2).[43] Side-reactions such as the formation of urea or dehydration derivatives, evidenced with DMDO model reactions (*vide supra*), may be taking place to a larger extent during the polyaddition reaction involving VC telechelic prepolymers, thereby altering the stoichiometry of the reagents and ultimately leading to side-products. Cleavage of the prepolymer backbone at the ester linkages by substitution with amino groups of EDR-148 cannot be ruled out either (*vide infra*).

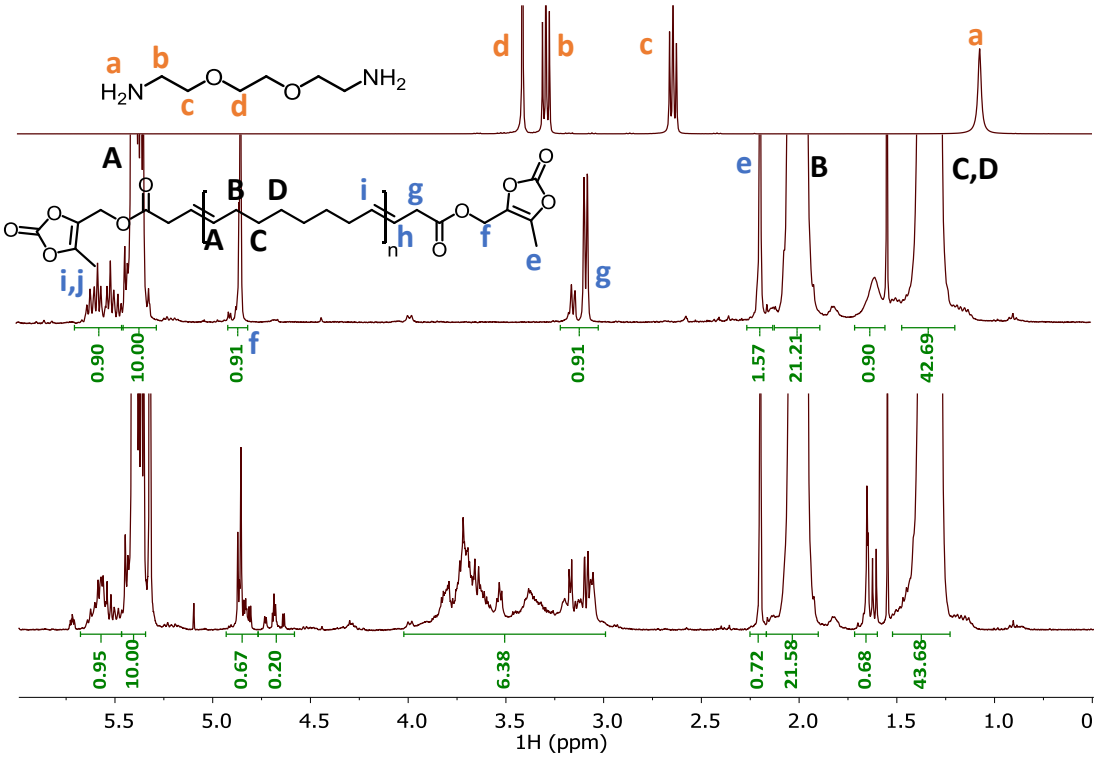

Figure 5. ^{1}H NMR spectra (400 MHz, $CDCl_3$, 25 °C) of EDR-148 (top), di(**VC3**)-PCOE (middle); and the product recovered from their stoichiometric reaction (Scheme 8).

In an attempt to get a better understanding of the reaction, the reaction of di(**VC3**)-PCOE with isopropylamine – used in excess (10 equiv) to promote the complete conversion of **VC3** moieties –, was investigated (40 °C, CH_2Cl_2, 2 h, argon atmosphere; Scheme 8). The ^{1}H NMR spectrum of the crude product showed the presence of the VC chain-end groups ($H^{a–h}$), with many other unassigned signals, thus suggesting different species than the ones expected (Figure S54). COSY, J-MOD, HSQC and HMBC NMR and ESI-MS analyses similarly remained inconclusive.

In a final effort to understand the reactivity of VC moieties in prepolymers toward primary amines, the simplest model reaction of **VC3** with isopropylamine was studied (Scheme 6). The ^{1}H NMR spectrum of the recovered product, reminiscent of the one recorded from the reaction of di(**VC3**)-PCOE and isopropylamine, remained also hardly informative,

besides showing large amount of exo-vinylene moieties (H^h, Figure S55). ESI-MS analyses carried out under several operating conditions evidenced the presence of four major compounds among others. The formation of these four products (**A–D**) is rationalized from the (hydroxymethyl)methyl dioxolone side-product, as depicted in Scheme 9, as inspired by the reactivity of DMDO with nucleophiles (Scheme 4) and by side-products identified in the reaction of five-membered cyclic carbonates with amines (Figure S56).[8,19,74]

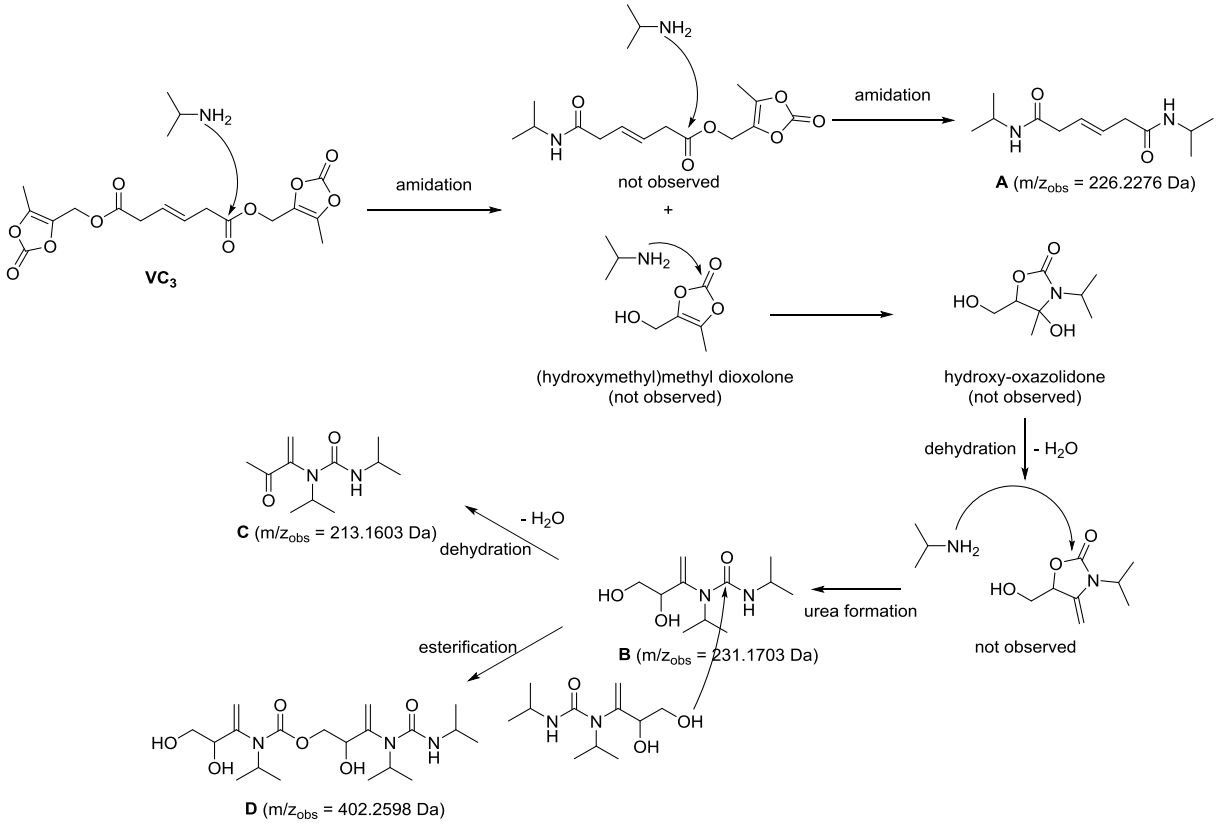

Scheme 9. Suggested mechanism for the formation of side-products observed by ESI-MS analysis during the reaction of **VC3** with isopropylamine.[75]

The reaction of **VC3**, and consequently of di(**VC3**)-PCOE, with (di)amines may involve competing side-reactions leading to (at least) partial amidation of the ester moieties; this would account for the observed absence of increasing molar mass values after the reaction.

Conclusion

The reactivity of DMDO, a model VC compound, toward nucleophiles, has been investigated. While hydroxy-oxazolidone compounds **1** and **2** (along with dehydration and urea side-products **1a–1c**) were obtained from the reaction with primary amines, and the oxo-urethane **3** was isolated from a secondary amine. These findings are in agreement with the reactivity previously reported for related α-alkylidene cyclic carbonates or cyclocarbonates.[19,28,43]

Three VC CTAs have been successfully synthesized from commercially available DMDO-OH and subsequently used in the ROMP/CM of COE catalyzed by **G2**. The acrylate CTA **VC1** revealed active in ROMP/CM but gave, besides VC-difunctional di(**VC3**)-PCOE, mono(**VC3**)-PCOE which would hamper the subsequent targeted polyaddition due to its monofunctional nature. The fumarate CTA **VC2** turned out to be poisonous to **G2** catalyst, then inhibited the ROMP/CM. On the other hand, the bifunctional symmetric hex-3-ene-1,6-dioate CTA **VC3** proved most effective in the ROMP/CM of COE and NB/CDT, selectively affording well-defined α,ω-di(vinylene carbonate) telechelic polyolefins, di(**VC3**)-PCOE and di(**VC3**)-P(NB-*co*-CDT), respectively.

The subsequent stoichiometric reaction of di(**VC3**)-PCOE with EDR-148 diamine did not provide the anticipated polyaddition PHOPO NIPUs, as suggested by detailed spectroscopic and SEC analyses. This is in sharp contrast with the reactivity of DMDO and of α-alkylidene cyclic carbonates.[43] Indeed, the reaction of di(**VC3**)-PCOE with isopropylamine, and the model reaction of **VC3** with isopropylamine, both suggested the deleterious contribution of competing side-reactions like amidation of main chain ester linkages, dehydration and/or formation of urea species from the releazed (hydroxymethyl)methyl dioxolone. The elaboration of a synthetic route avoiding such side-reactions and involving a

chemically related VC CTA free of ester function, may enable to obtain the targeted PHOPO NIPUs suitable for adhesive applications.

Acknowledgements

Financial support of this research by Bostik (Ph.D. grant to C.C.) is gratefully acknowledged. P. Jéhan (CRMPO - UMS Scanmat) and T. Roisnel (CDFIX - ISCR) are gratefully acknowledged for MS and X-ray diffraction analyses, respectively.

Supporting Information

The Supporting Information includes complementary (macro)molecular and characterization data, including ^{1}H, $^{13}C\{^{1}H\}$and 2D NMR, FTIR and MS spectra, X-ray molecular structure of organic compounds and polymers.

SUPPORTING INFORMATION

α,ω-Di(vinylene carbonate) telechelic polyolefins : Synthesis by metathesis reactions and studies as potential precursors toward hydroxy-oxazolidone-based polyolefin NIPUs

Cyril Chauveau,[a] Stéphane Fouquay,[b] Guillaume Michaud,[c] Frédéric Simon,[c] Jean-François Carpentier (ORCID: 0000-0002-9160-7662),[a,*] and Sophie M. Guillaume (ORCID: 0000-0003-2917-8657) [a,*]

[a] Univ Rennes, CNRS, ISCR (Institut des Sciences Chimiques de Rennes) – UMR 6226, F-35000 Rennes, France

[b] BOSTIK S.A., 420 rue d'Estienne d'Orves, F-92705 Colombes Cedex, France

[c] BOSTIK, ZAC du Bois de Plaisance, 101, Rue du Champ Cailloux, F-60280 Venette, France

* Corresponding authors: jean-francois.carpentier@univ-rennes1; sophie.guillaume@univ-rennes1.fr

Table, Schemes and Figures captions

Table S1. X-ray crystallographic data and data collection parameters of compound **1** isolated from the aminolysis of DMDO with isopropylamine.

Table S2. X-ray crystallographic data and data collection parameters for **VC2**.

Table S3. ROMP/CM of COE catalyzed by **G2** in the presence of CTAs **VC1** and benzoquinone (BZQ) in CH_2Cl_2 at 40 °C for 3 h (Scheme 6).

Table S4. ROMP/CM of COE catalyzed by **G2** in the presence of **VC2** and/or (*Z*)-**GA$_2$** CTAs in CH_2Cl_2 at 40 °C for 3 h (Scheme 6).

Scheme S1. Synthesis and dehydration of an oxazolidone from an α-alkylidene cyclocarbonate.[58]

Scheme S2. Reaction between VC3 and isopropylamine depicting the expected structure based on the reactivity of DMDO (Scheme 4) and α-alkylidene cyclocarbonates (Scheme 2).[25]

Figure S1. ^{1}H and J-MOD NMR spectra (400 and 100 MHz, $CDCl_3$, 25 °C) of compound **1** isolated from the aminolysis of DMDO with isopropylamine (Scheme 4a).

Figure S2. COSY NMR spectrum (400 MHz, $CDCl_3$, 25 °C) of compound **1**.

Figure S3. HSQC NMR spectrum (400 & 100 MHz, $CDCl_3$, 25 °C) of compound **1**.

Figure S4. HMBC NMR spectrum (400 & 100 MHz, $CDCl_3$, 25 °C) of compound **1**.

Figure S5. FTIR spectrum of compound **1**.

Figure S6. X-ray molecular structure of compound **1** (ellipsoids drawn at the 50% probability level) (Table S1).

Figure S7. ESI-MS analysis (NaI) of the main product isolated from the reaction of DMDO and isopropylamine, and suggested routes for the formation of side-products **1a**, **1b** and **1c**, respectively (Scheme 4a).

Figure S8. ^{1}H and J-MOD NMR spectra (400 and 100 MHz, $CDCl_3$, 25 °C) of compound **2** isolated from the aminolysis of DMDO with EDR-148 (Scheme 4b).

Figure S9. COSY NMR spectrum (400 MHz, $CDCl_3$, 25 °C) of compound **2**.

Figure S10. HSQC NMR spectrum (400 and 100 MHz, $CDCl_3$, 25 °C) of compound **2**.

Figure S11. HMBC spectrum (400 and 100 MHz, $CDCl_3$, 25 °C) of compound **2**.

Figure S12. FTIR spectrum of compound **2**.

Figure S13. ESI-MS analysis (NaI) of compound **2** and suggested routes for the formation of side-products **2'**, **2a**, and **2b**.

and simulation of linear nonfunctional (LNF) PCOE for n = 6; bottom right: zoomed spectrum and simulation of cyclic nonfunctional (CNF) PCOE for n = 7.

Figure S36. ^{1}H NMR spectrum (400 MHz, $CDCl_3$, 25 °C) of di(**VC2**)-PCOE (Table S4, entry 1).

Figure S37. COSY NMR spectrum (400 MHz, $CDCl_3$, 25 °C) of di(**VC3**)-PCOE (Scheme 6, Table 1, entry 3).

Figure S38. HSQC NMR spectrum (400 and 100 MHz, $CDCl_3$, 25 °C) of di(**VC3**)-PCOE (Scheme 6, Table 1, entry 3).

Figure S39. HMBC NMR spectrum (400 and 100 MHz, $CDCl_3$, 25 °C) of di(**VC3**)-PCOE (Scheme 6, Table 1, entry 3).

Figure S40. FTIR spectrum of di(**VC3**)-PCOE (Scheme 6, Table 1, entry 3).

Figure S41. COSY NMR spectrum (400 MHz, $CDCl_3$, 25 °C) of di(**VC3**)-P(NB-*co*-CDT) (Scheme 7).

Figure S42. HSQC NMR spectrum (400 and 100 MHz, $CDCl_3$, 25 °C) of di(**VC3**)-P(NB-*co*-CDT) (Scheme 7).

Figure S43. HMBC NMR spectrum (400 and 100 MHz, $CDCl_3$, 25 °C) of di(**VC3**)-P(NB-*co*-CDT) (Scheme 7).

Figure S44. FTIR spectrum of di(**VC3**)-P(NB-*co*-CDT) (Scheme 7).

Figure S45. ^{1}H NMR spectrum (400 MHz, $CDCl_3$, 25 °C) of a di(**VC3**)-PCOE (19.2 mg) mixed with 4-bromobenzonitrile (2.6 mg).

Figure 46. J-MOD NMR spectrum (100 MHz, $CDCl_3$, 25 °C) of the product from the stoichiometric reaction of di(**VC3**)-PCOE and EDR-148 (Scheme 8).

Figure S47. COSY NMR spectrum (400 MHz, $CDCl_3$, 25 °C) of the product from the stoichiometric reaction of di(**VC3**)-PCOE and EDR-148 (Scheme 8).

Figure S48. HSQC NMR spectrum (400 and 100 MHz, $CDCl_3$, 25 °C) of the product from the stoichiometric reaction of di(**VC3**)-PCOE and EDR-148 (Scheme 8).

Figure S49. HMBC NMR spectrum (400 and 100 MHz, $CDCl_3$, 25 °C) of the product from the stoichiometric reaction of di(**VC3**)-PCOE and EDR-148 (Scheme 8).

Figure S50. ^{1}H NMR spectrum (400 MHz, $CDCl_3$, 25 °C) of the product from the stoichiometric reaction of di(**VC3**)-P(NB-*co*-CDT) and EDR-148.

Figure S51. J-MOD NMR spectrum (100 MHz, $CDCl_3$, 25 °C) of the product from the stoichiometric reaction of di(**VC3**)-P(NB-*co*-CDT) and EDR-148.

Figure S52. HSQC NMR spectrum (400 and100 MHz, $CDCl_3$, 25 °C) of the product from the stoichiometric reaction of di(**VC3**)-P(NB-*co*-CDT) and EDR-148.

Figure S53. HMBC NMR spectrum (400 and100 MHz, $CDCl_3$, 25 °C) of the product from the stoichiometric reaction of di(**VC3**)-P(NB-*co*-CDT) and EDR-148.

Figure S54. ^{1}H NMR spectrum (400 MHz, $CDCl_3$, 25 °C) of the product from the reaction of di(**VC3**)-PCOE and isopropylamine (Scheme 8).

Figure S55. ^{1}H NMR spectrum (400 MHz, $CDCl_3$, 25 °C) of the product obtained from the reaction of **VC3** and isopropylamine (Scheme 6).

Figure S56. ESI-mass spectrum (DCTB matrix, NaI ionizing salt) of a sample issued from the reaction of **VC3** with isopropylamine, showing the four major compounds **A**–**D** among other side-products (Scheme 9).

Table S1. X-ray crystallographic data and data collection parameters of compound **1** isolated from the aminolysis of DMDO with isopropylamine.

Empirical formula	$C_8H_{15}NO_3$
Formula weight	173.21
Crystal system	orthorhombic
Space group	P 2_1 2_1 2_1
a (Å)	8.0077(12)
b (Å)	9.6919(13)
c (Å)	12.1153(16)
α(°)	90
β (°)	90
V (Å^3)	90
Z	4
D_{calcd} (g.cm^{-3})	1.224
Absorp coeff (mm^{-1})	0.093
Crystal color	Colorless
Crystal size (mm)	0.480 × 0.320 × 0.150
h, *k*, l_{max}	10, 12, 15
T_{min}, T_{max}	0.986, 0.677
Reflns collected	5314
R [I > 2σ(I)])	0.0567
wR^2 (all data)	0.1549
GOF on F^2	1.050

Table S2. X-ray crystallographic data and data collection parameters for **VC2**.

Empirical formula	$C_{14}H_{12}O_{10}$
Formula weight	340.24
Crystal system	monoclinic
Space group	P 1 $2_1/a$ 1
a (Å)	6.7084(8)
b (Å)	7.9387(12)
c (Å)	14.173(2)
α(°)	90
β (°)	103.610(5)
V (Å^3)	90
Z	2
D_{calcd} (g.cm^{-3})	1.540
Absorp coeff (mm^{-1})	0.135
Crystal color	Colorless
Crystal size (mm)	0.230 × 0.130 × 0.060
h, k, l_{max}	8, 10, 18
T_{min}, T_{max}	0.992, 0.906
Reflns collected	14371
R [I > 2σ(I)])	0.0412
wR^2 (all data)	0.0948
GOF on F^2	1.071

Table S3. ROMP/CM of COE catalyzed by **G2** in the presence of CTAs **VC1** and benzoquinone (BZQ) in CH_2Cl_2 at 40 °C for 3 h (Scheme 6).[a]

Entry	$[COE]_0/[$ **VC1**$]_0/[$**G2**$]_0$ [a]	**VC1** Conv.[b] (%)	$M_{n,theo}$[c] ($g.mol^{-1}$)	$M_{n,NMR}$[d] ($g.mol^{-1}$)	$M_{n,SEC}$[e] ($g.mol^{-1}$)	$Đ_M$ [e]
1	2000:20:1	100	11 200	14 000	19 500	1.7
2	2000:50:1	96	4800	4300	10 000	2.0
3	2000:100:1	93	2500	3200	7800	2.0
4	10000:250:1	93	4700	6400	29 000	1.6
5	50 000:1250:1	55	8200	7900	33 000	1.5
6	50 000:1250:1	34	13 100	15 000	30 000	1.7

[a] General operating conditions: Catalyst = 11.7 µmol, $[COE]_0$ = 1.5 $mol.L^{-1}$; COE and NB conversion = 100% as determined by ^{1}H NMR analysis (refer to the Experimental Section). [b] Conversion in CTA as determined by ^{1}H NMR analysis (refer to the Experimental Section). [c] Theoretical molar mass value calculated from $M_{n,theo} = \{M_{COE} \times ([COE]_0 \times Conv._{COE}) / ([\mathbf{VC1}]_0 \times Conv._{VC1})\} + M_{VC1}$, with M_{COE}= 110 $g.mol^{-1}$, $M_{\mathbf{VC1}}$ = 184 $g.mol^{-1}$, on the basis of the formation of only DF (i.e. without taking into account any CNF PCOEs). [d] Experimental molar mass value determined by ^{1}H NMR analysis (by comparing the integration of H^c and H^k chain-ends signals to that of H^A from the repeating unit (Figure S29). [e] Number-average molar mass ($M_{n,SEC}$) and dispersity ($Đ_M = M_w/M_n$) values determined by SEC vs polystyrene standards (uncorrected M_n values) in THF at 30 °C.

Different monomer-to-**VC1** and monomer-to-catalyst ratios were used. As expected, under similar operating conditions, the higher the initial ratio in **VC1**, the lower the molar mass values obtained as determined by ^{1}H NMR ($M_{n,NMR}$) and SEC ($M_{n,SEC}$) analyses (entries 1–3). The initial catalyst loading was varied to compare the efficiency of ROMP and CM steps. A similar conversion in CTA was observed upon going from $[COE]_0/[\mathbf{VC1}]_0/[\mathbf{G2}]_0$ = 2000:20:1 to 2000:250:1 (entries 1–3). Upon decreasing the catalyst loading to $[COE]_0/[\mathbf{VC1}]_0/[\mathbf{G2}]_0$ = 50000:1250:1, the **VC1** conversion significantly dropped from 93–100% to 34–55% (entries 5 and 6), suggesting the deactivation of **G2** by correspondingly increasing amount of impurities within higher monomer loadings. Moreover, at high monomer and CTA loadings, reactions turned out less reproducible (entries 5 and 6), probably

due to the catalyst sensitivity toward impurities in the reaction medium. Of note, DF, MF, LNF and CNF chains could not be separated, and their respective amount could not be determined by spectrometry analyses.

Table S4. ROMP/CM of COE catalyzed by **G2** in the presence of **VC2** and/or (*Z*)-**GA_2** CTAs in CH_2Cl_2 at 40 °C for 3 h.

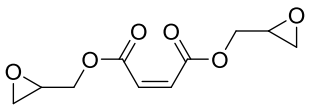

(Z)-GA_2

Entry	Loading [a] (equiv.)				Conversion [b] (%)		
	COE	**VC2**	(*Z*)-**GA_2**	**G2**	COE	**VC2**	(*Z*)-**GA_2**
1	2000	20	-	1	100	< 5	-
2	2000	20	-	1	100	< 5	-
3	2000	-	20	1	100	-	78
4	2000	20	20	1	100	< 5	30

[a] $[COE]_0$ = 1.5 mol.L^{-1}. [b] Determined by ^1H NMR.

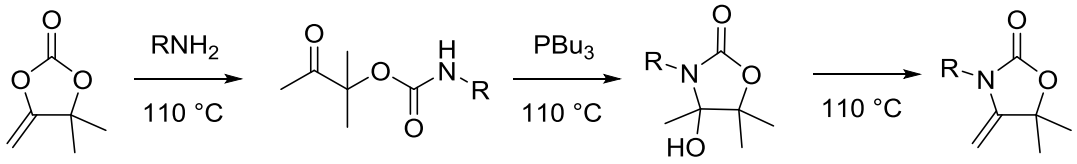

Scheme S1. Synthesis and dehydration of an oxazolidone from an α-alkylidene cyclocarbonate.[58]

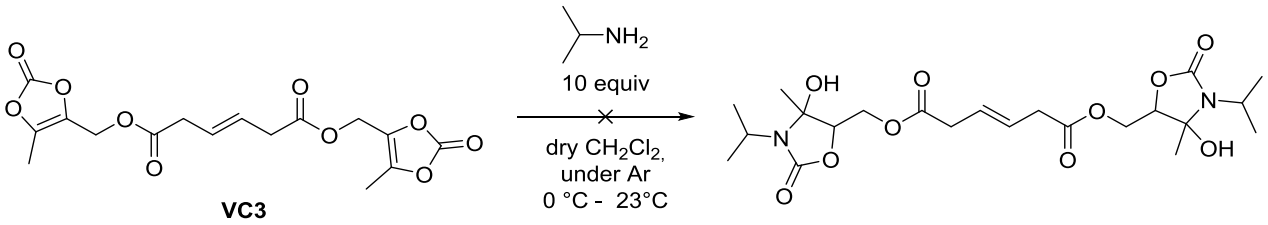

Scheme S2. Reaction between **VC3** and isopropylamine depicting the expected structure based on the reactivity of DMDO (Scheme 4) and α-alkylidene cyclocarbonates (Scheme 2).[25] An excess of isopropylamine (5 equiv vs. **VC3**) was used and the reaction was first carried out at 0 °C to avoid uncontrolled exothermicity; the reaction was then pursued at room temperature.

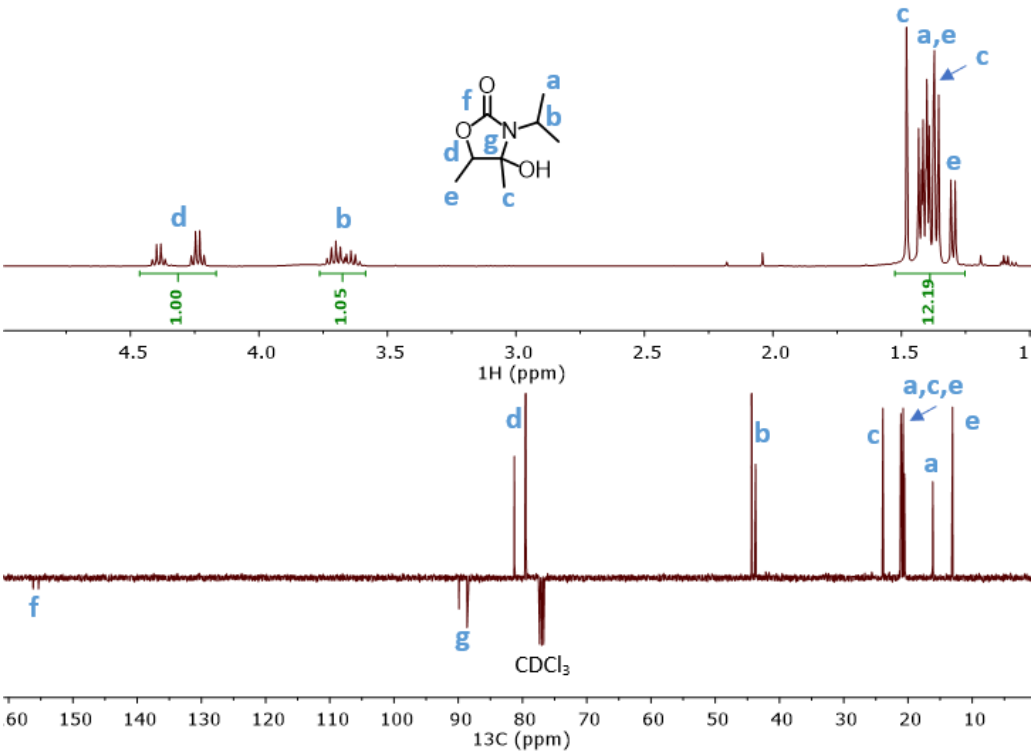

Figure S1. ^{1}H and J-MOD NMR spectra (400 and 100 MHz, $CDCl_3$, 25 °C) of compound **1** isolated from the aminolysis of DMDO with isopropylamine (Scheme 4a).

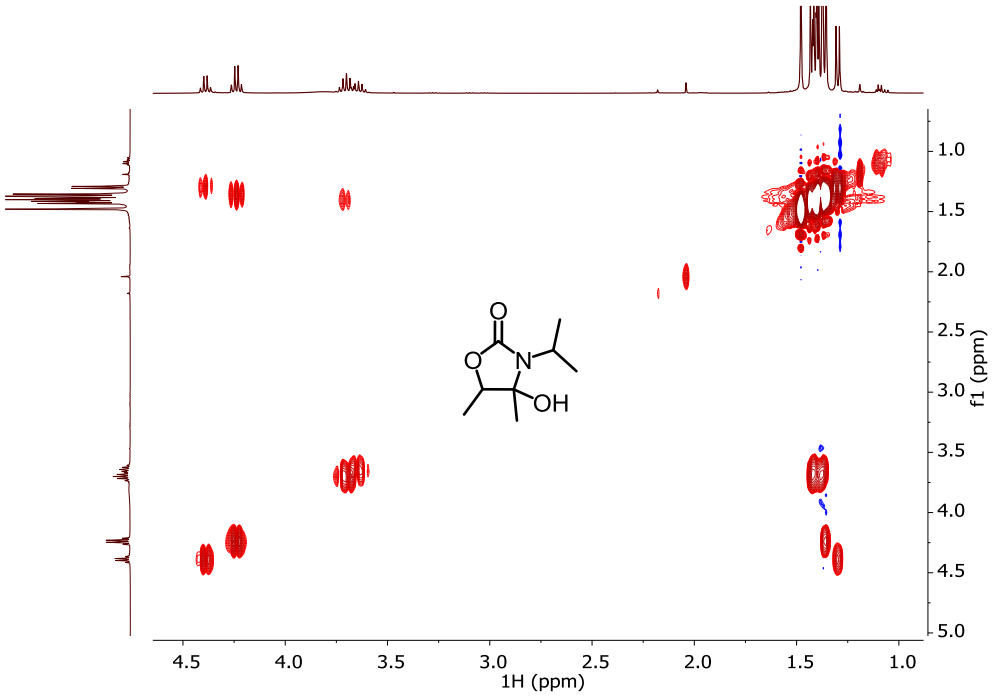

Figure S2. COSY NMR spectrum (400 MHz, $CDCl_3$, 25 °C) of compound **1**.

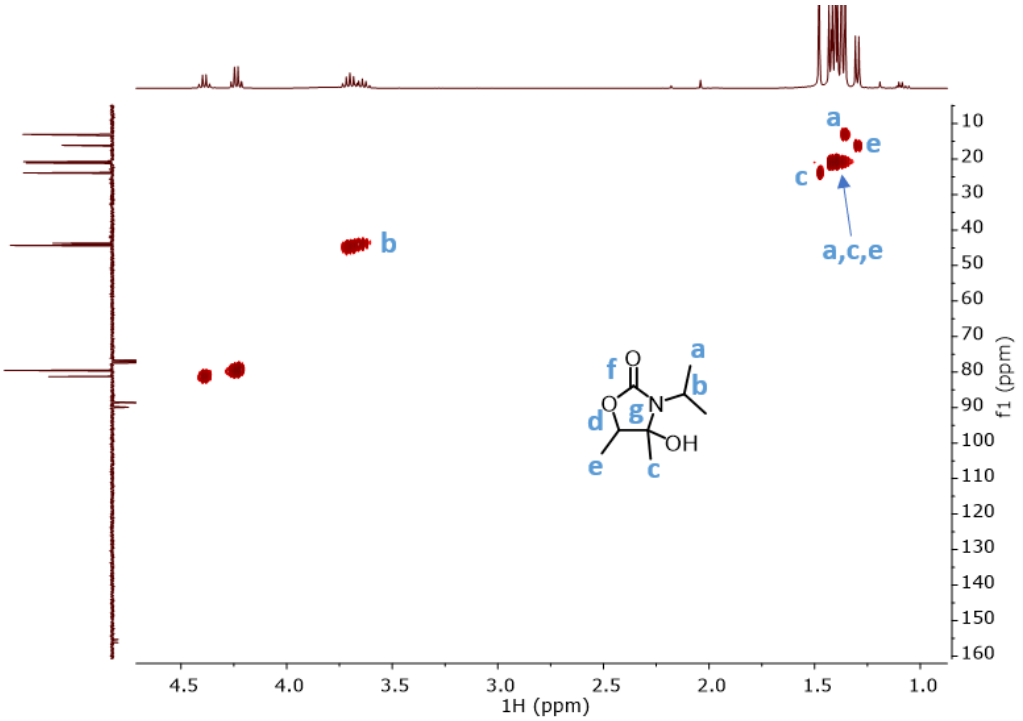

Figure S3. HSQC NMR spectrum (400 & 100 MHz, $CDCl_3$, 25 °C) of compound **1**.

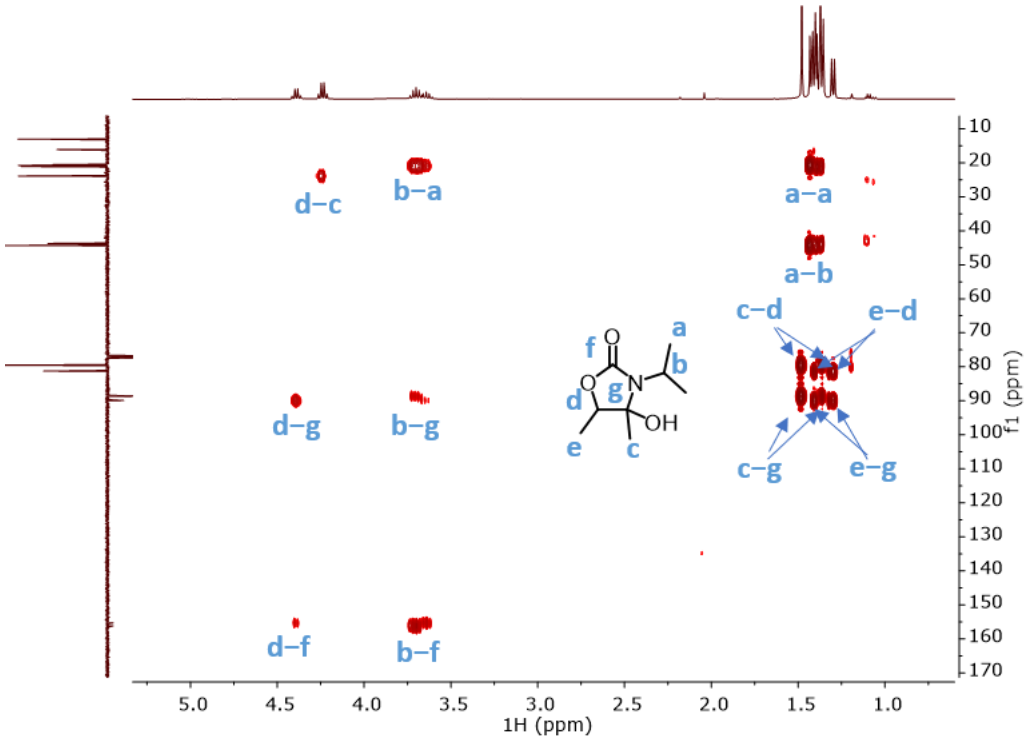

Figure S4. HMBC NMR spectrum (400 & 100 MHz, $CDCl_3$, 25 °C) of compound **1**.

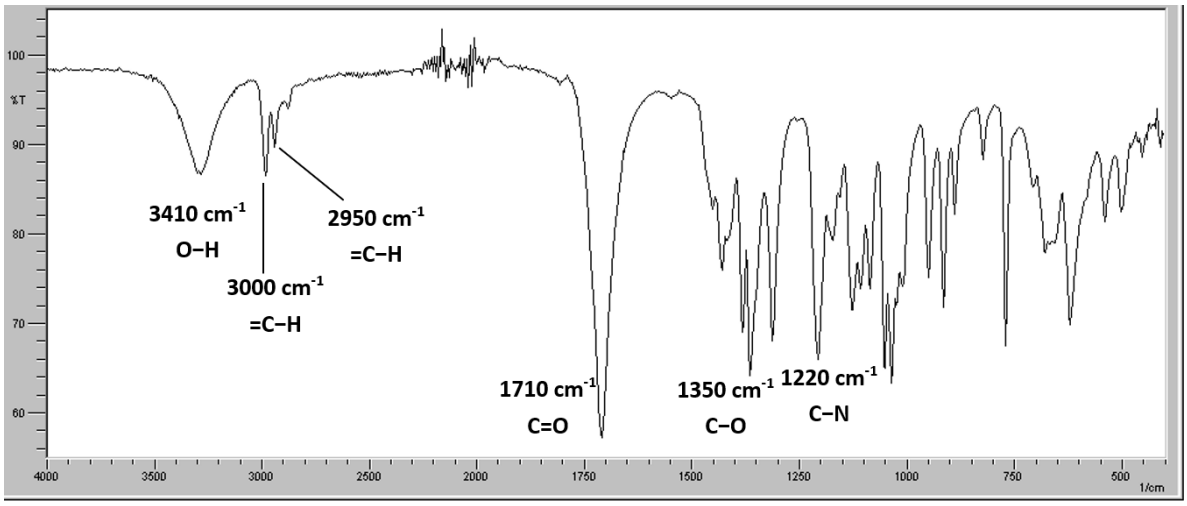

Figure S5. FTIR spectrum of compound **1**.

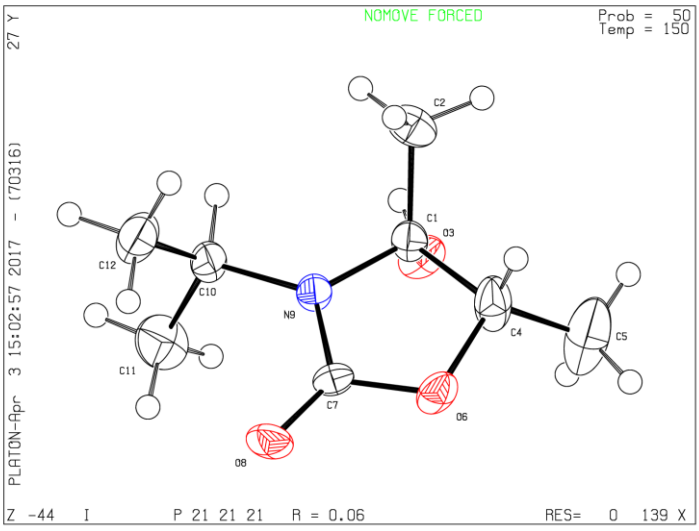

Figure S6. X-ray molecular structure of compound **1** (ellipsoids drawn at the 50% probability level) (Table S1).

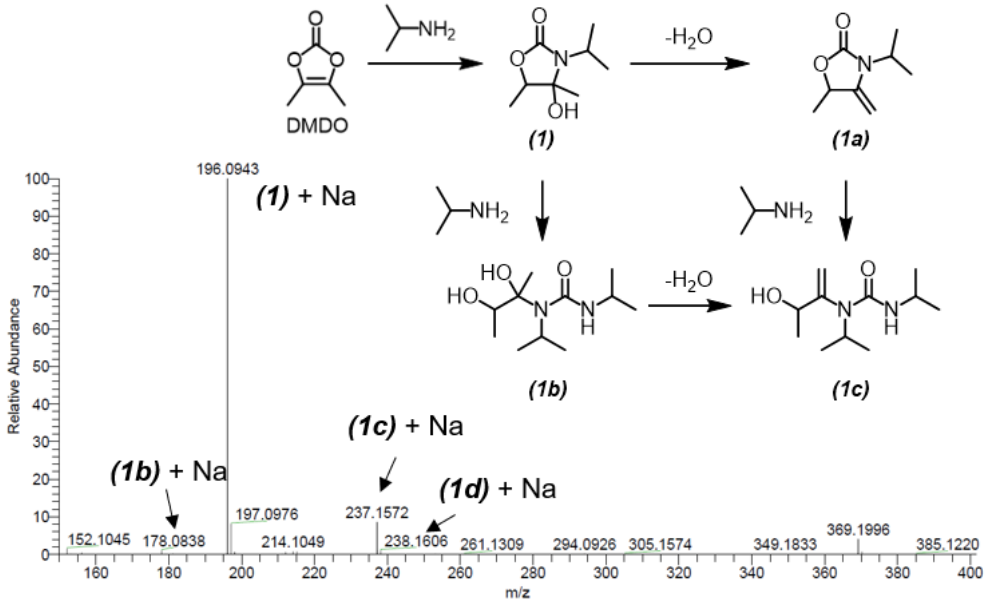

Figure S7. ESI-MS analysis (NaI) of the main product isolated from the reaction of DMDO and isopropylamine, and suggested routes for the formation of side-products **1a**, **1b** and **1c**, respectively (Scheme 4a).

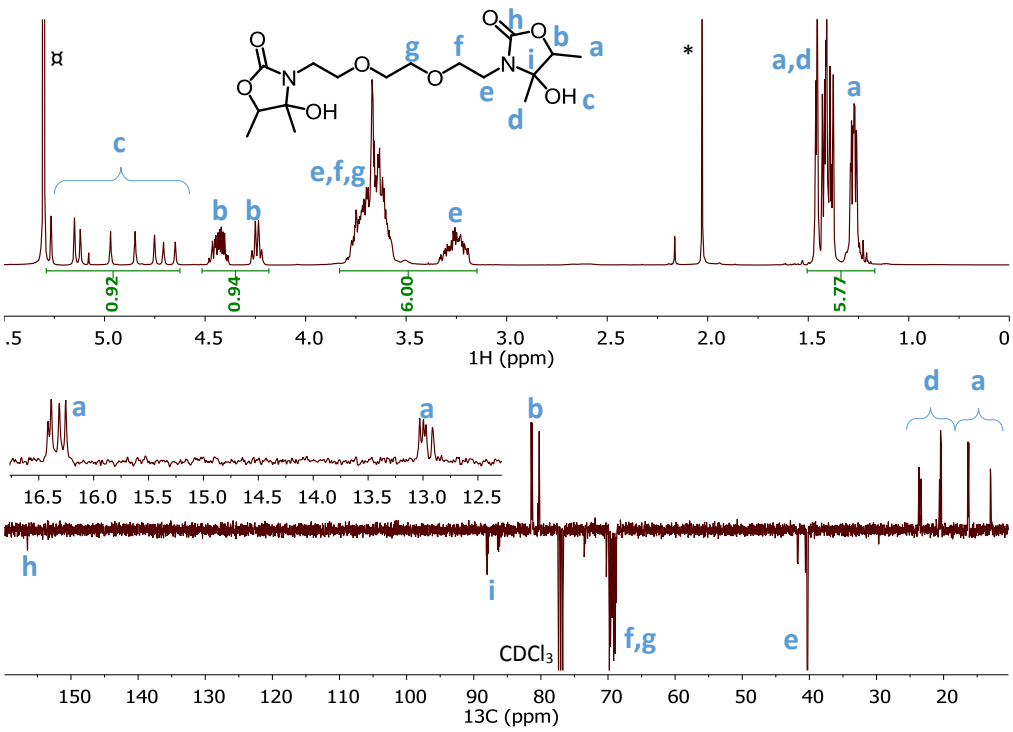

Figure S8. ^{1}H and J-MOD NMR spectra (400 and 100 MHz, $CDCl_3$, 25 °C) of compound **2** isolated from the aminolysis of DMDO with EDR-148 (Scheme 4b). * : residual acetone; ¤ : residual CH_2Cl_2.

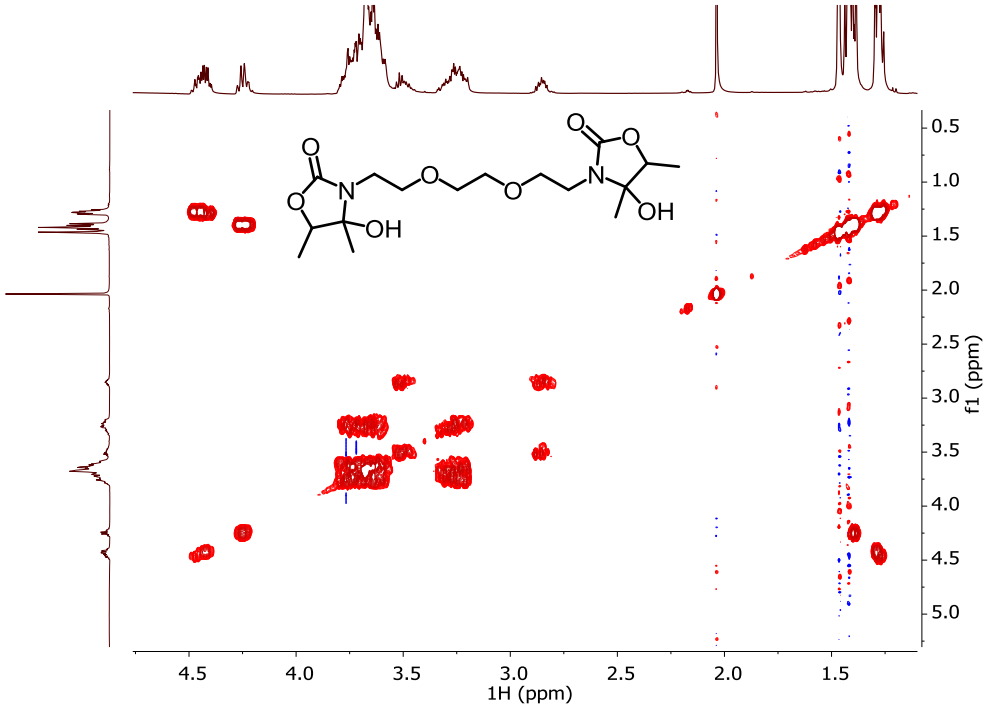

Figure S9. COSY NMR spectrum (400 MHz, $CDCl_3$, 25 °C) of compound **2**.

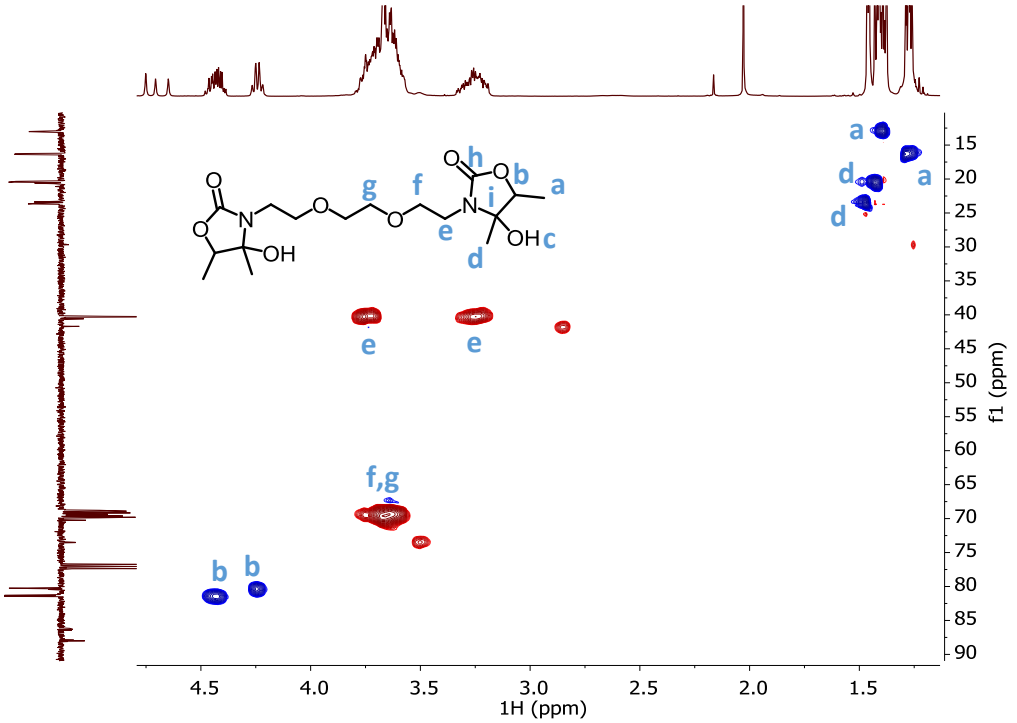

Figure S10. HSQC NMR spectrum (400 and 100 MHz, $CDCl_3$, 25 °C) of compound **2**.

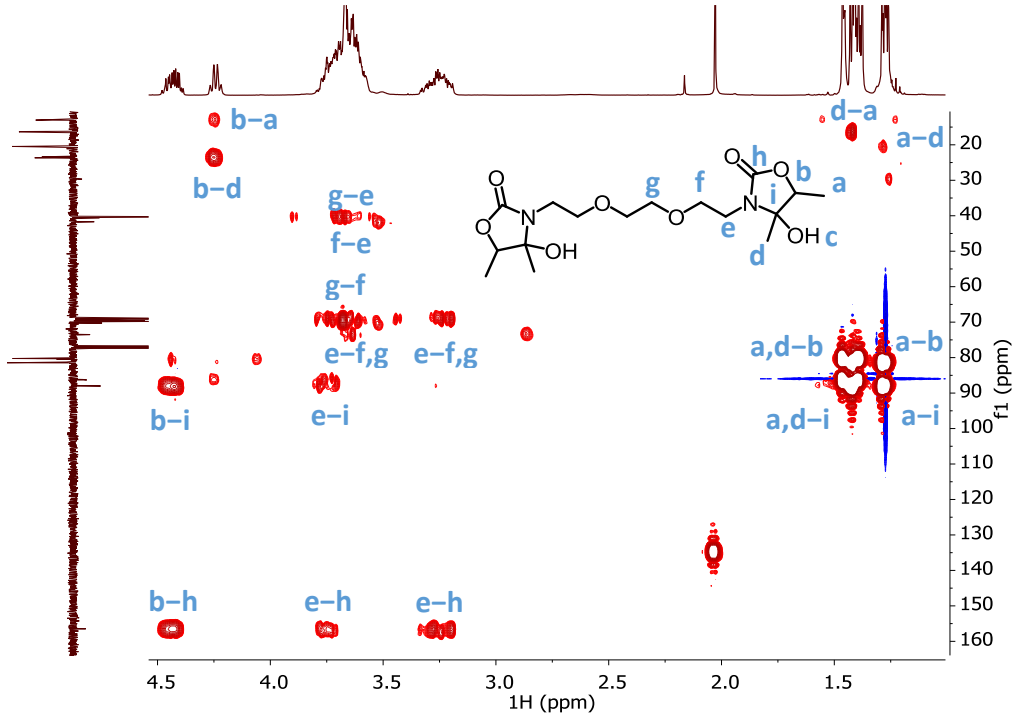

Figure S11. HMBC spectrum (400 and 100 MHz, $CDCl_3$, 25 °C) of compound **2**.

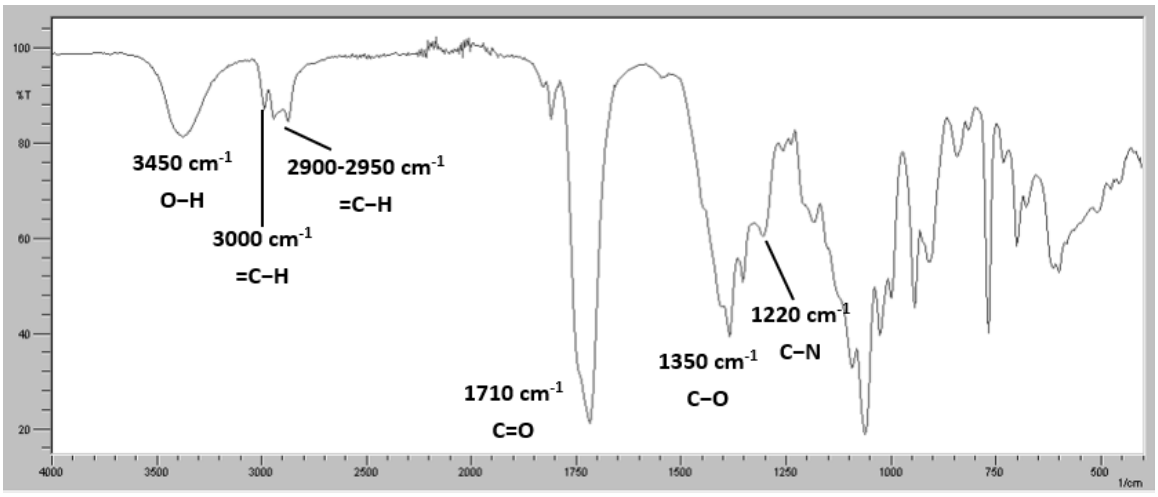

Figure S12. FTIR spectrum of compound **2**.

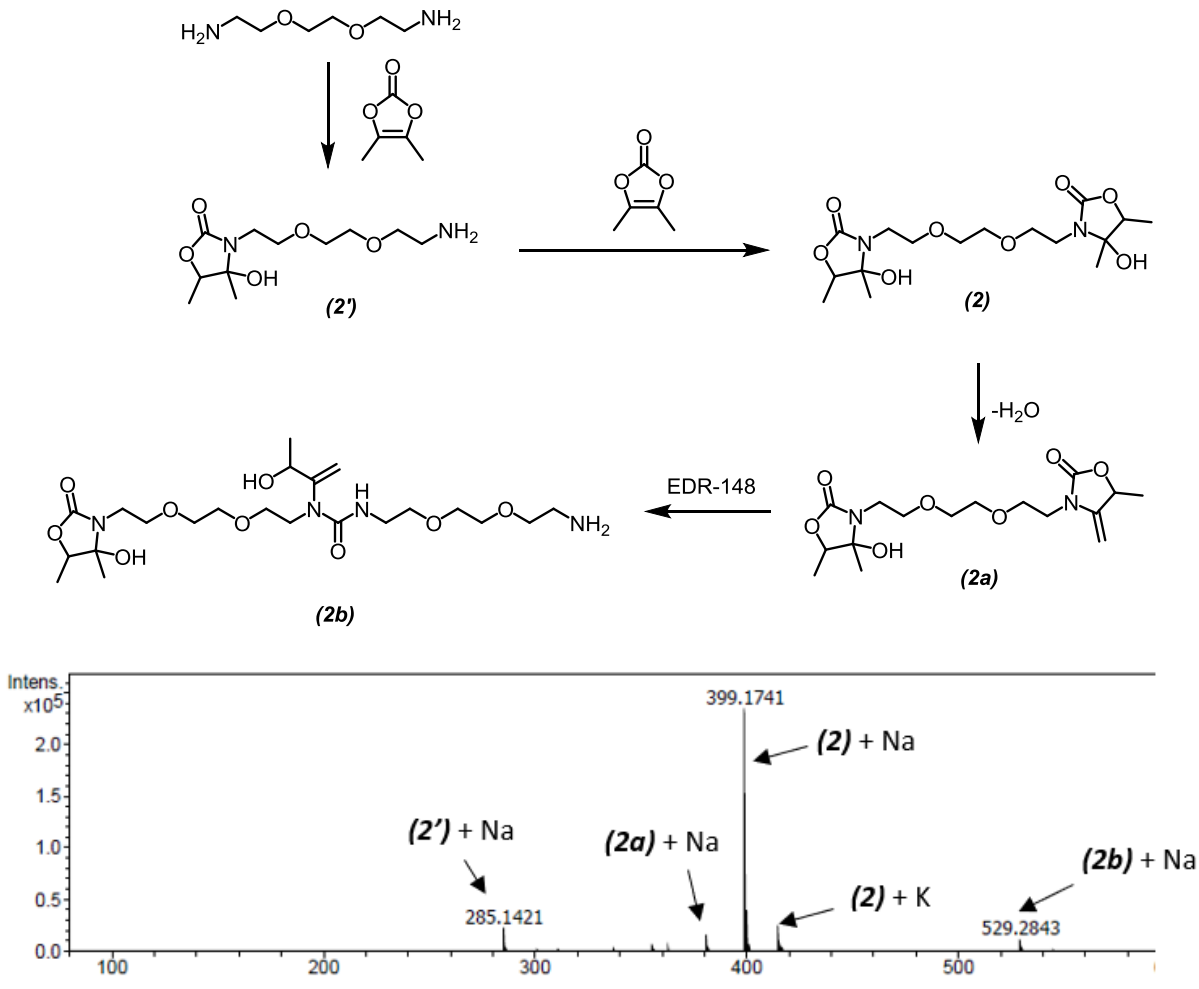

Figure S13. ESI-MS analysis (NaI) of compound **2** and suggested routes for the formation of side-products **2'**, **2a**, and **2b**.

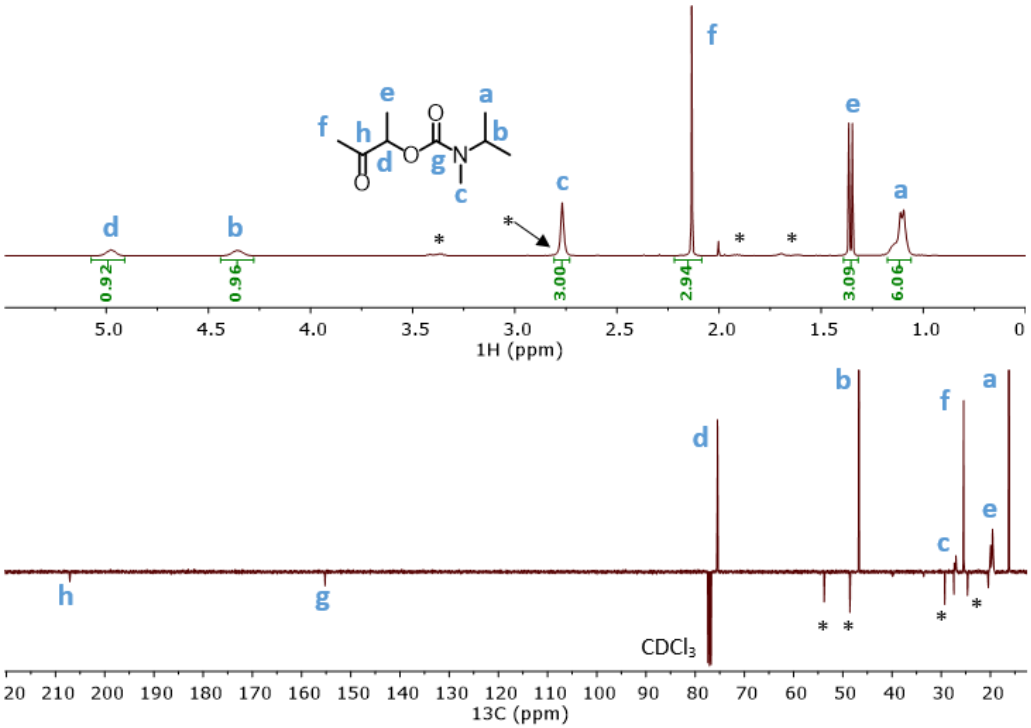

Figure S14. ^{1}H and J-MOD NMR spectra (400 and 100 MHz, $CDCl_3$, 25 °C) of compound **3** isolated from the aminolysis of DMDO with *N*-isopropylmethylamine EDR-148 (Scheme 4c). * : residual DBU.

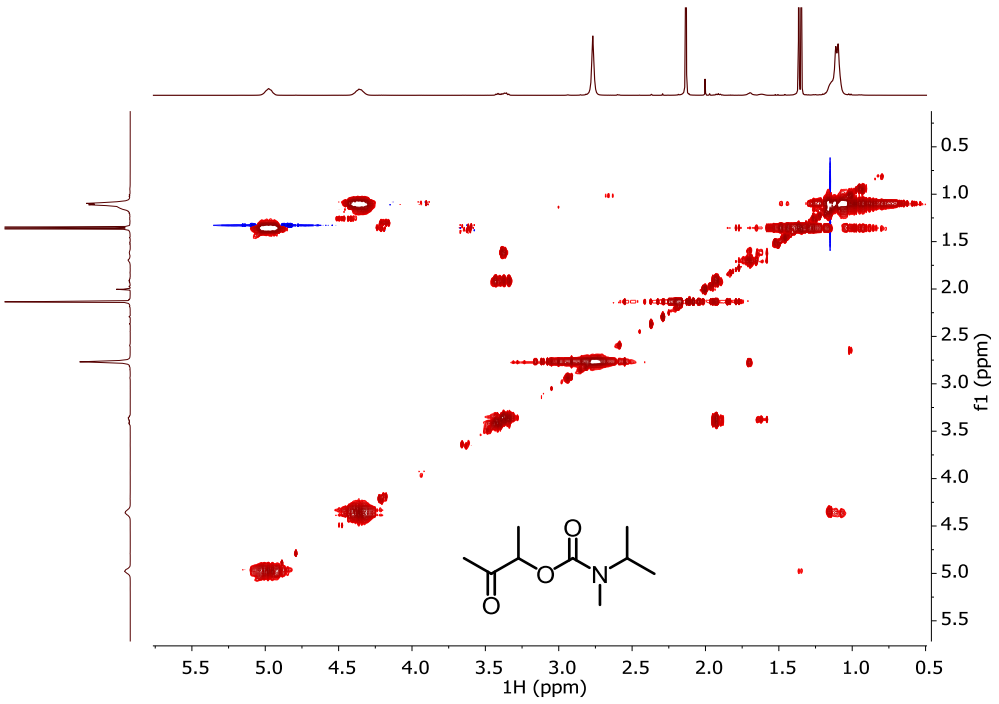

Figure S15. COSY NMR spectrum (400 MHz, $CDCl_3$, 25 °C) of compound **3**.

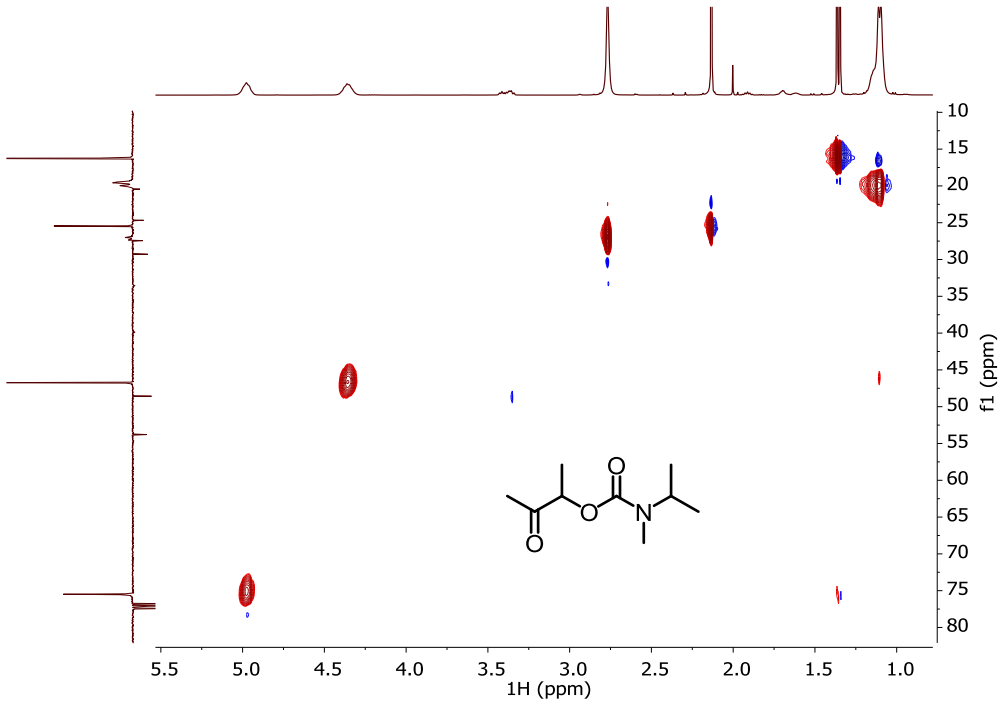

Figure S16. HSQC NMR spectrum (400 and 100 MHz, $CDCl_3$, 25 °C) of compound **3**.

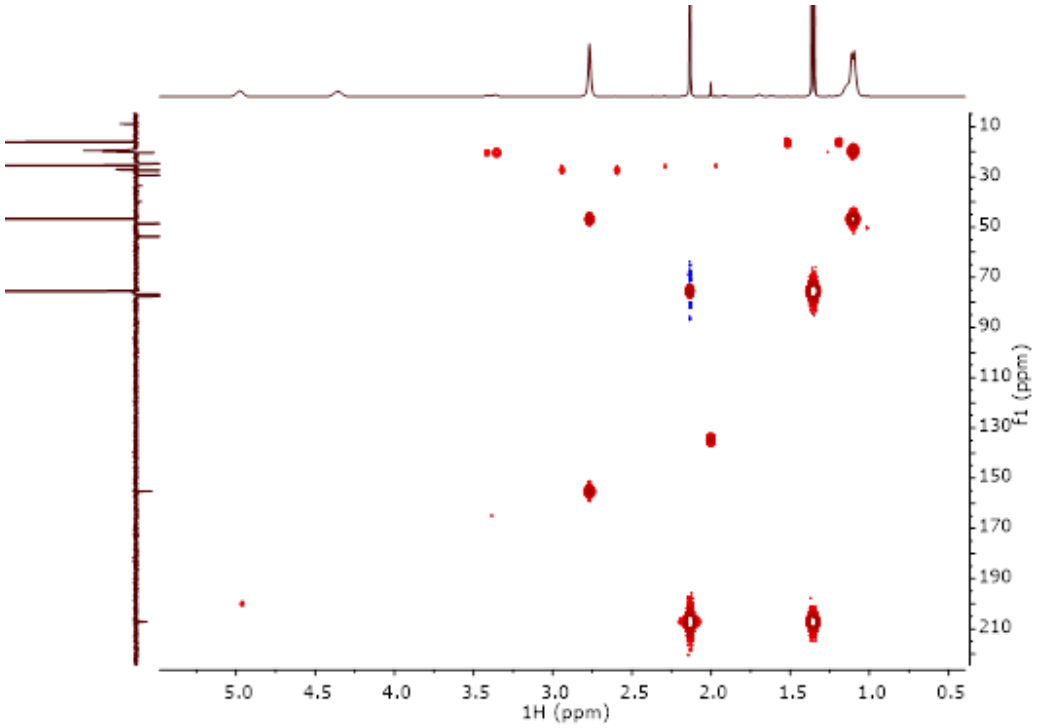

Figure S17. HMBC NMR spectrum (400 and 100 MHz, $CDCl_3$, 25 °C) of compound **3**.

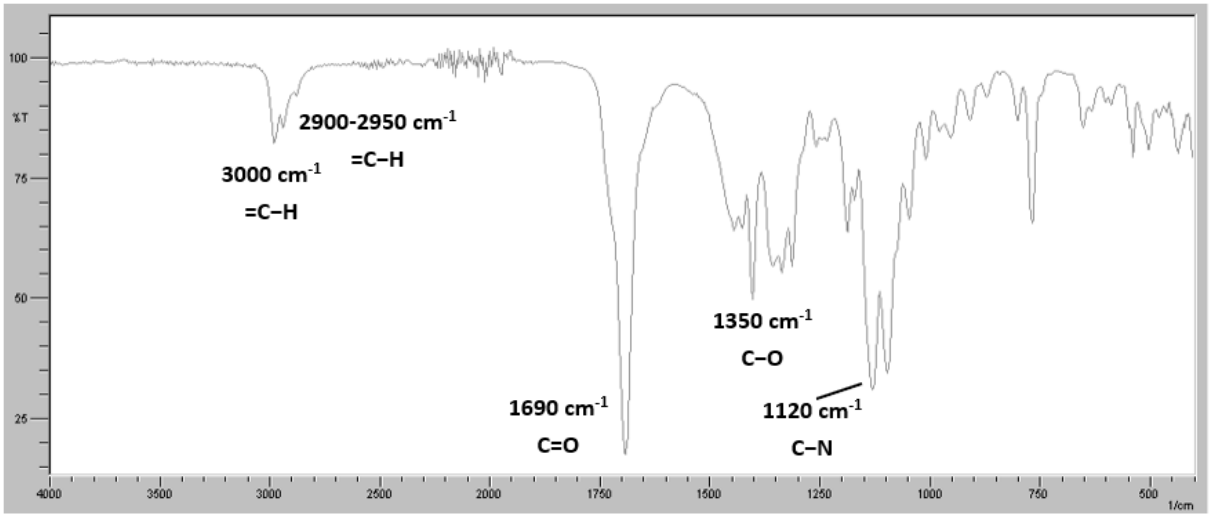

Figure S18. FTIR spectrum of compound **3**.

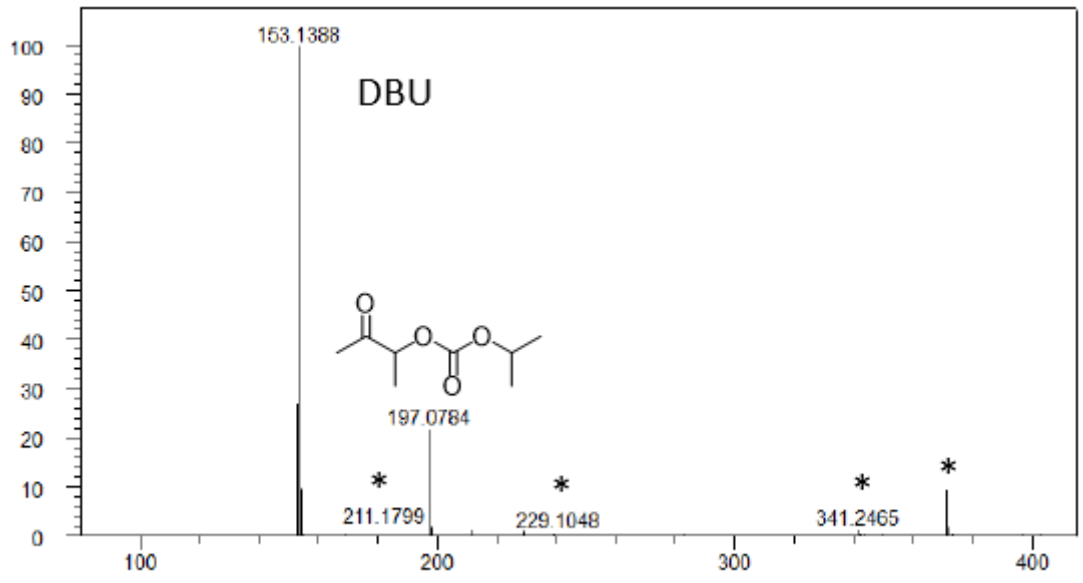

Figure S19. ESI-MS analysis (NaI) of compound **3**. *: minor DBU and other impurities.

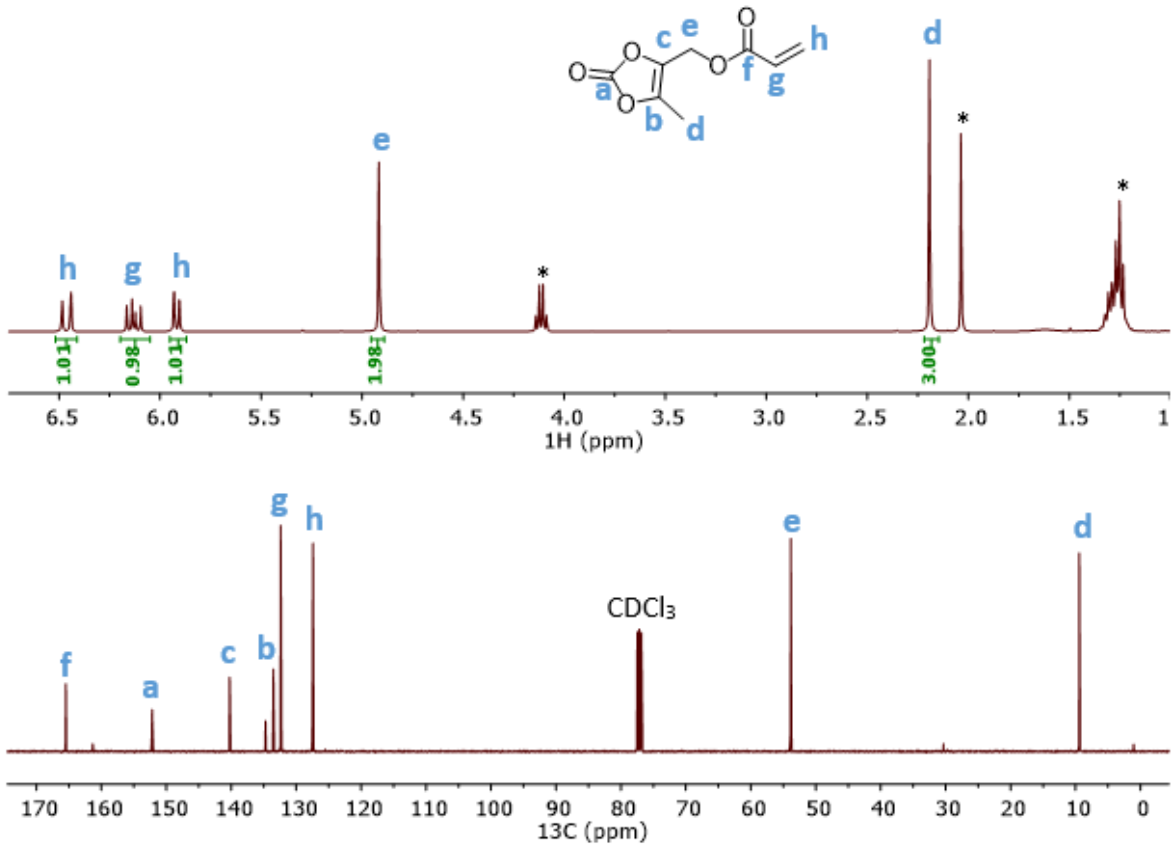

Figure S20. ^{1}H and ^{13}C NMR spectra (400 and 100 MHz, $CDCl_3$, 25 °C) of **VC1**. *: residual EtOAc.

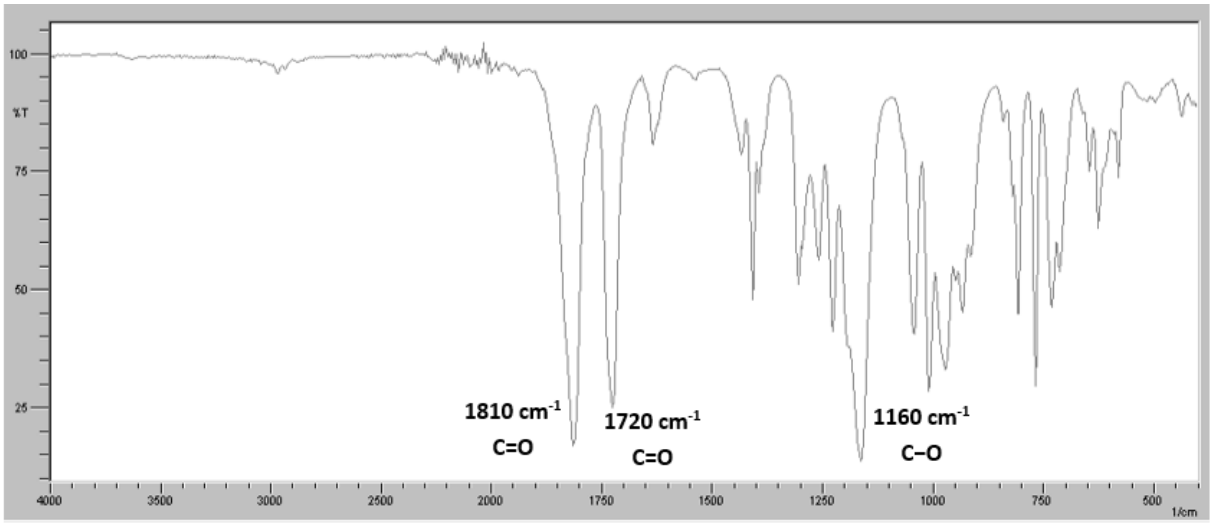

Figure S21. FTIR spectrum of **VC1**.

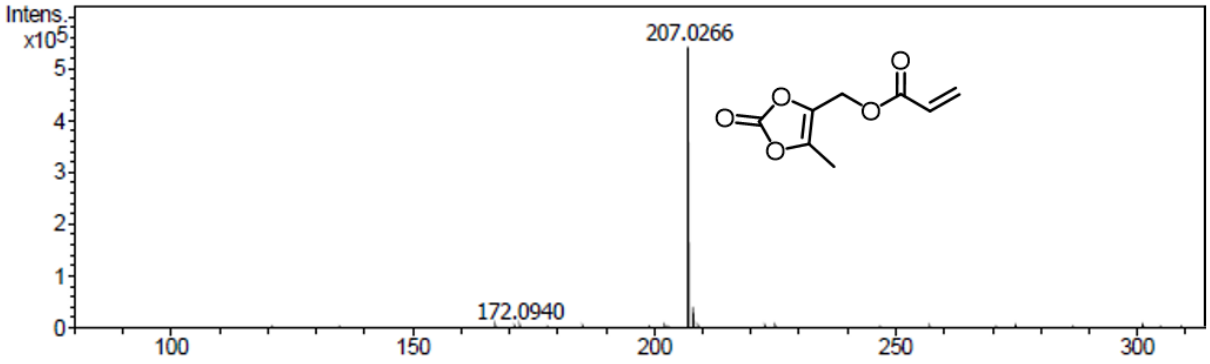

Figure S22. ESI-MS analysis (NaI) of CTA **VC1**.

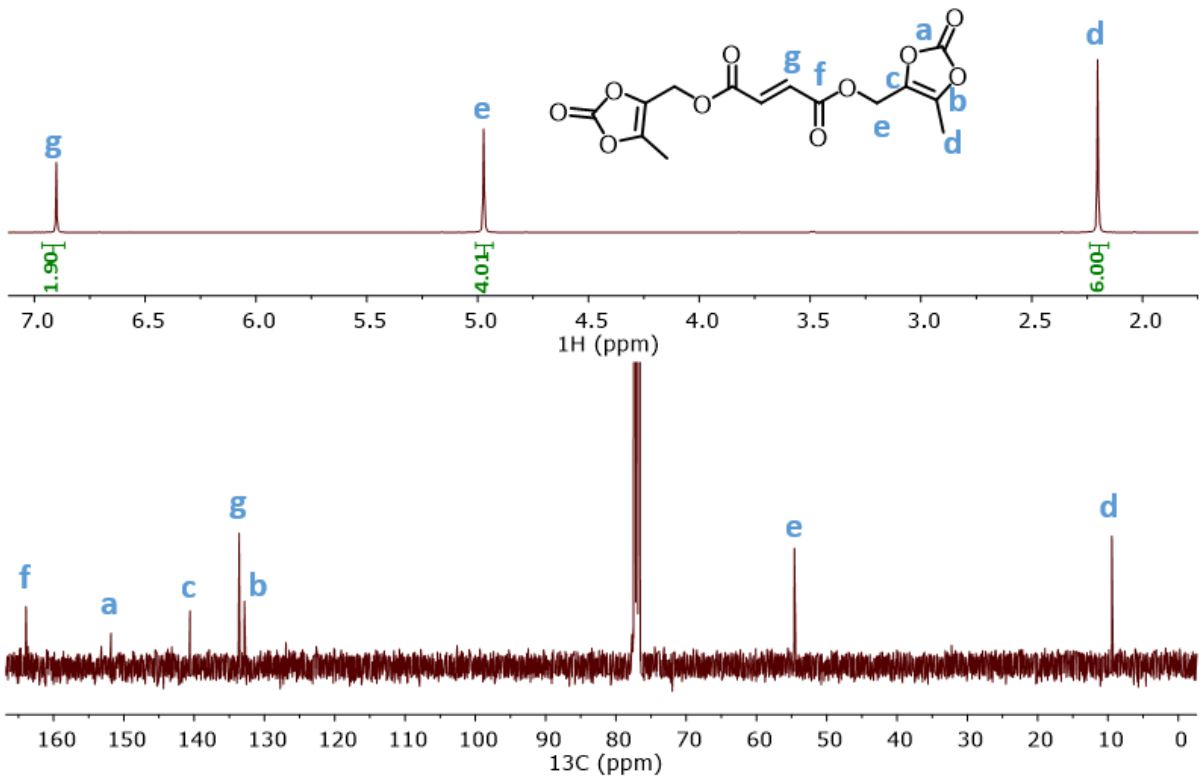

Figure S23. ^{1}H and ^{13}C NMR spectra (400 and 100 MHz, $CDCl_3$, 25 °C) of **VC2**.

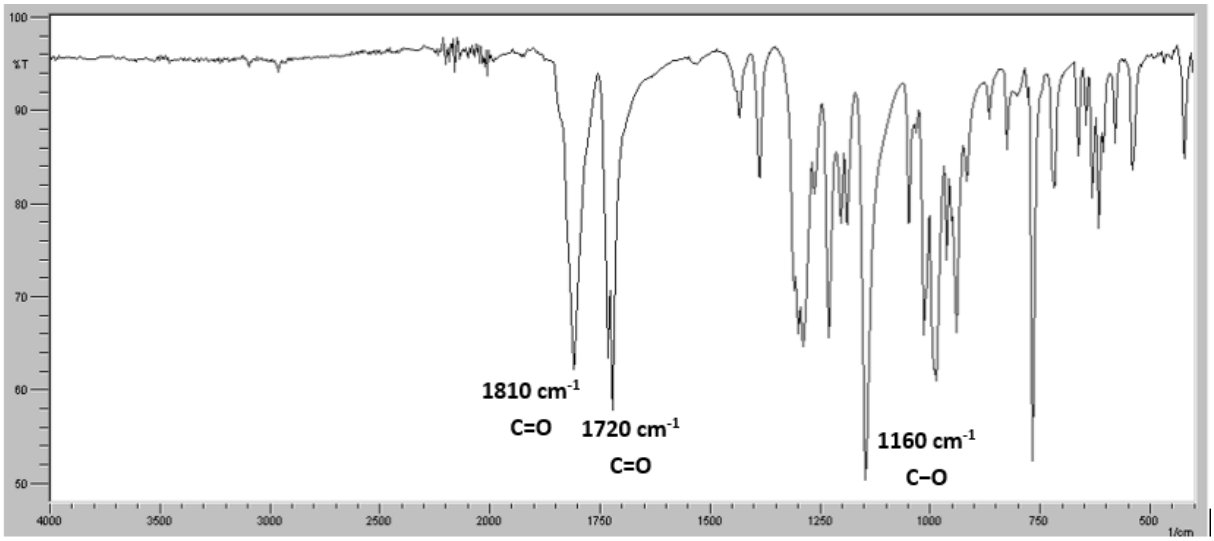

Figure S24. FTIR spectrum of **VC2**.

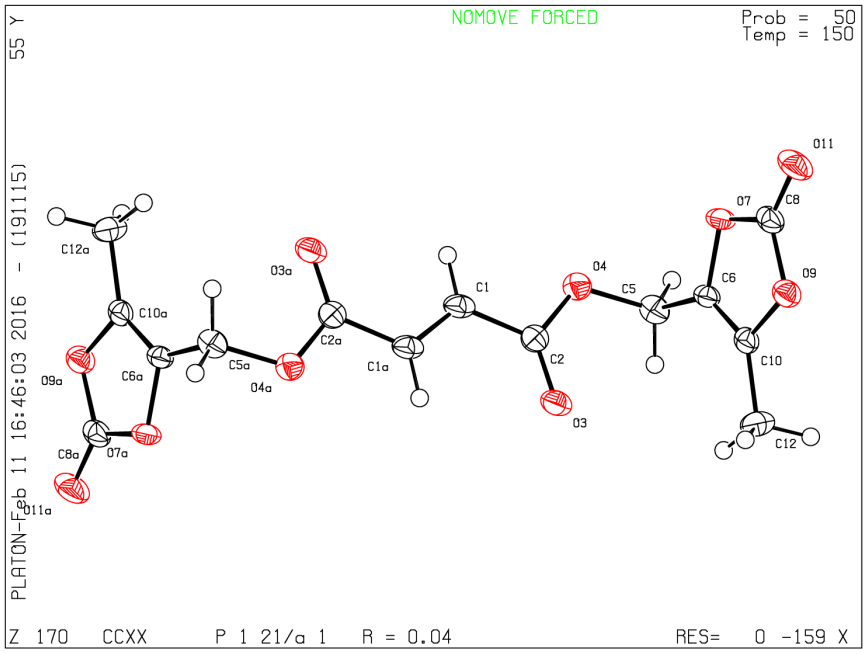

Figure S25. X-ray molecular structure of **VC2** (ellipsoids drawn at the 50% probability level) (Table S2).

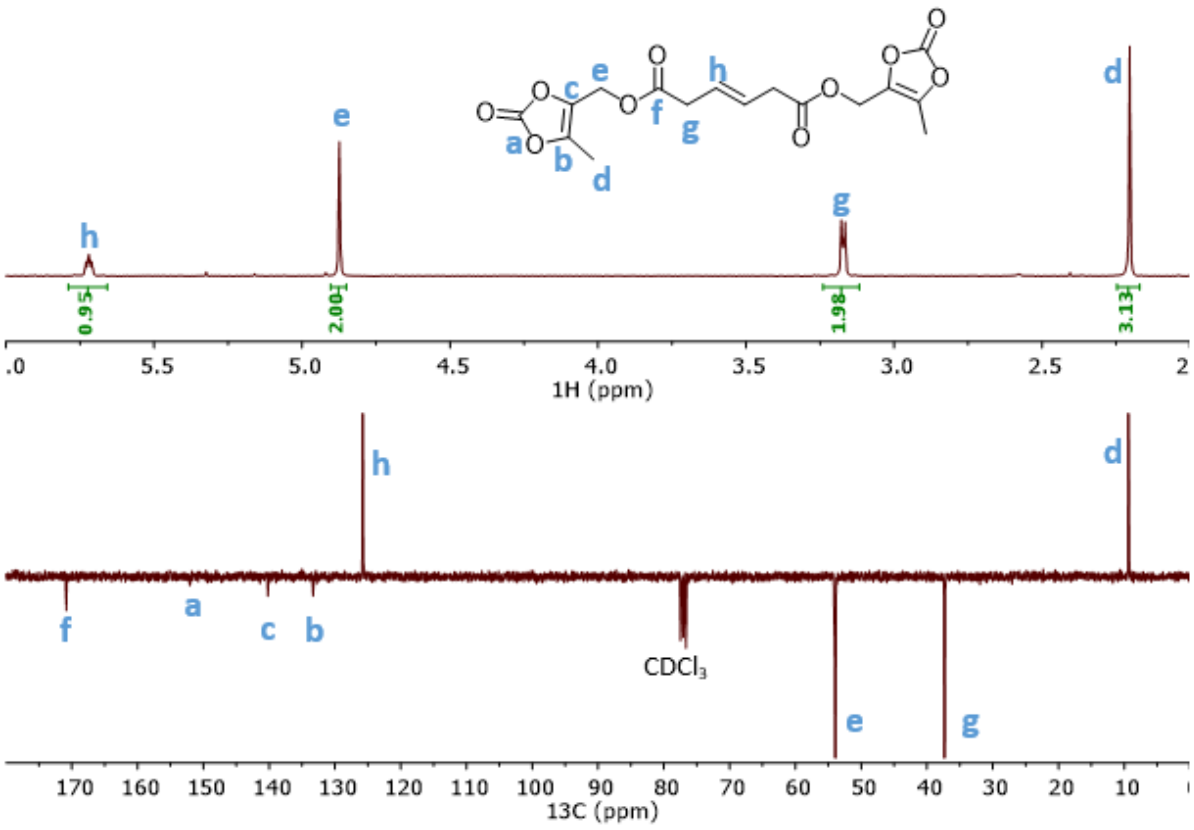

Figure S26. ^{1}H and J-MOD spectra (400 and 100 MHz, $CDCl_3$, 25 °C) of **VC3**.

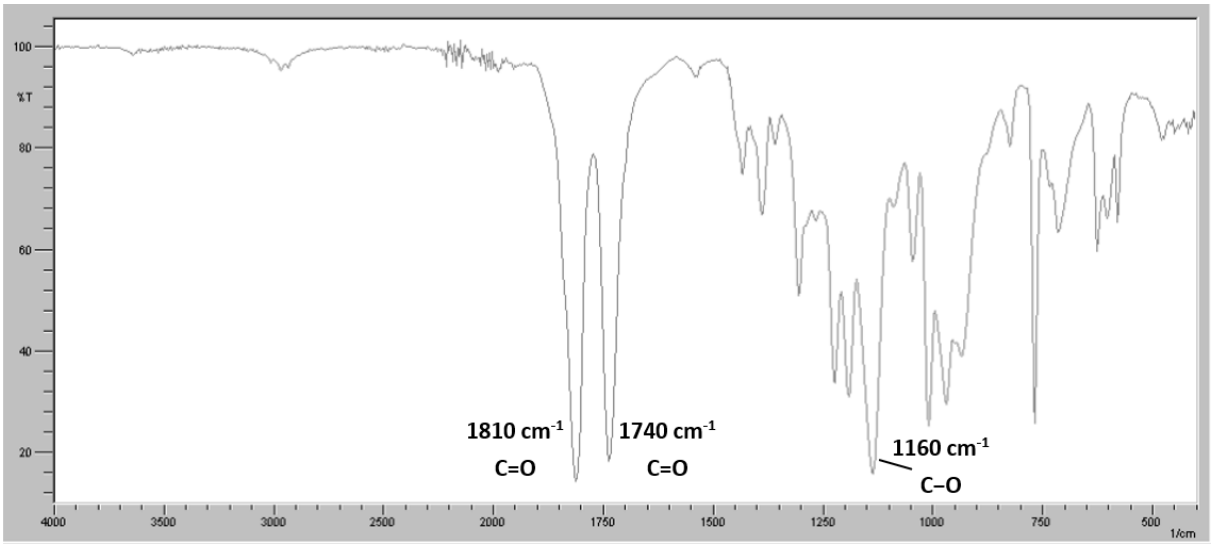

Figure S27. FTIR spectrum of **VC3**.

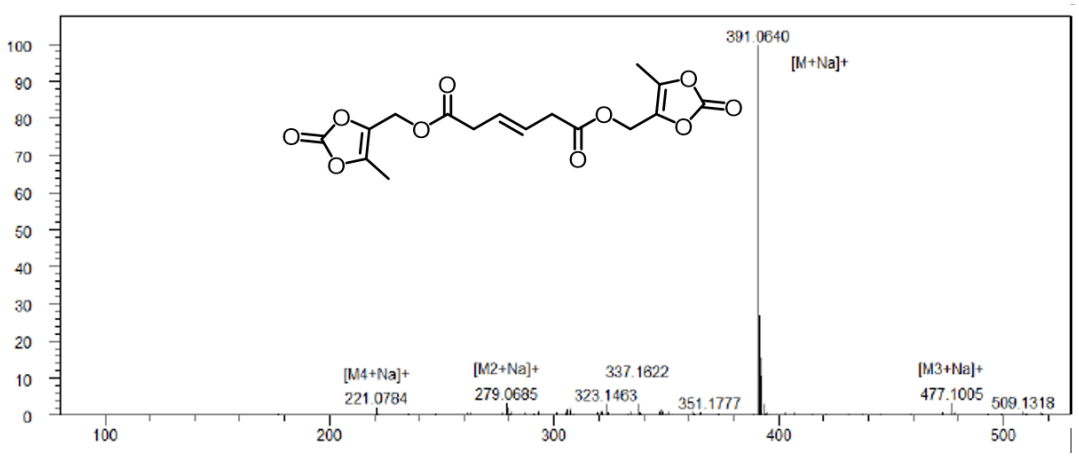

Figure S28. ESI-MS analysis (NaI) of **VC3**.

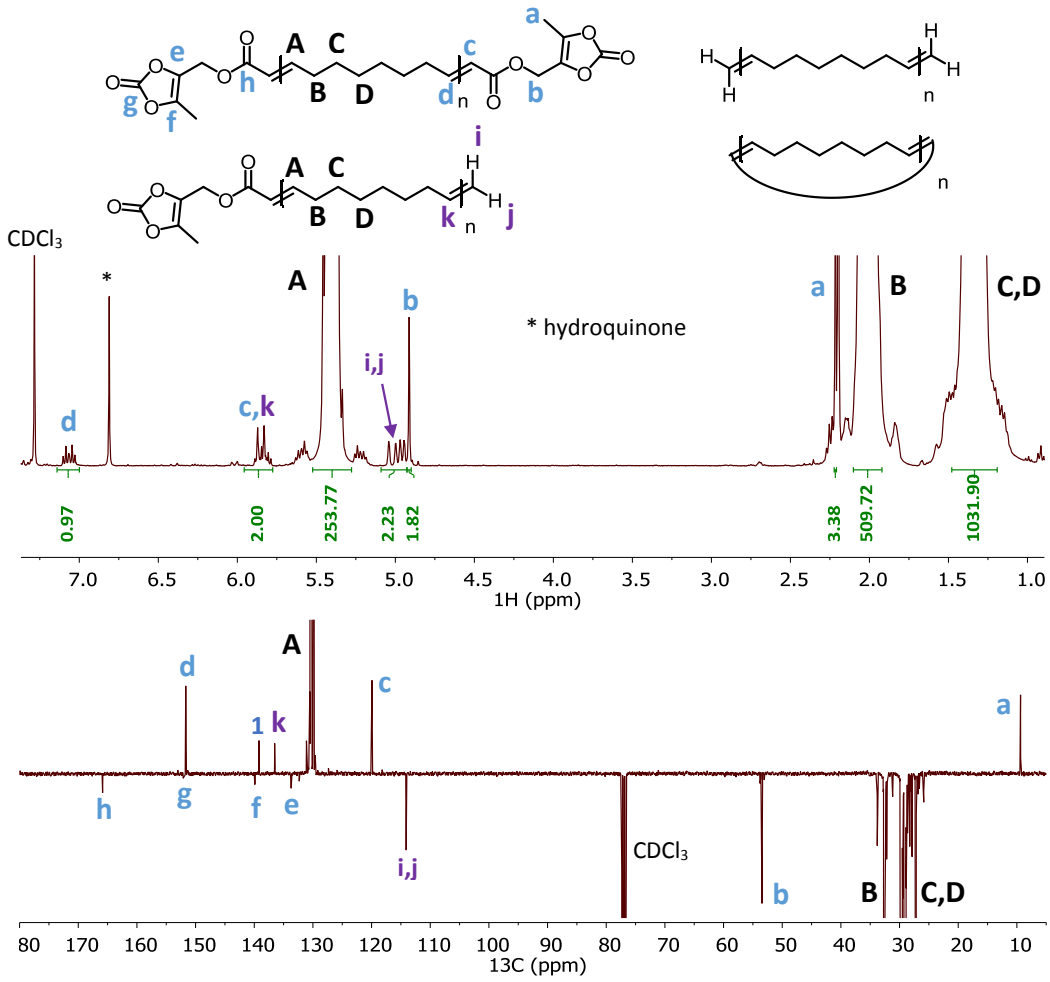

Figure S29. ^{1}H and J-MOD NMR spectra (400 and 100 MHz, $CDCl_3$, 25 °C) of a mixture of mono and di(**VC1**)-PCOE (Scheme **6**, Table S3, entry 1).

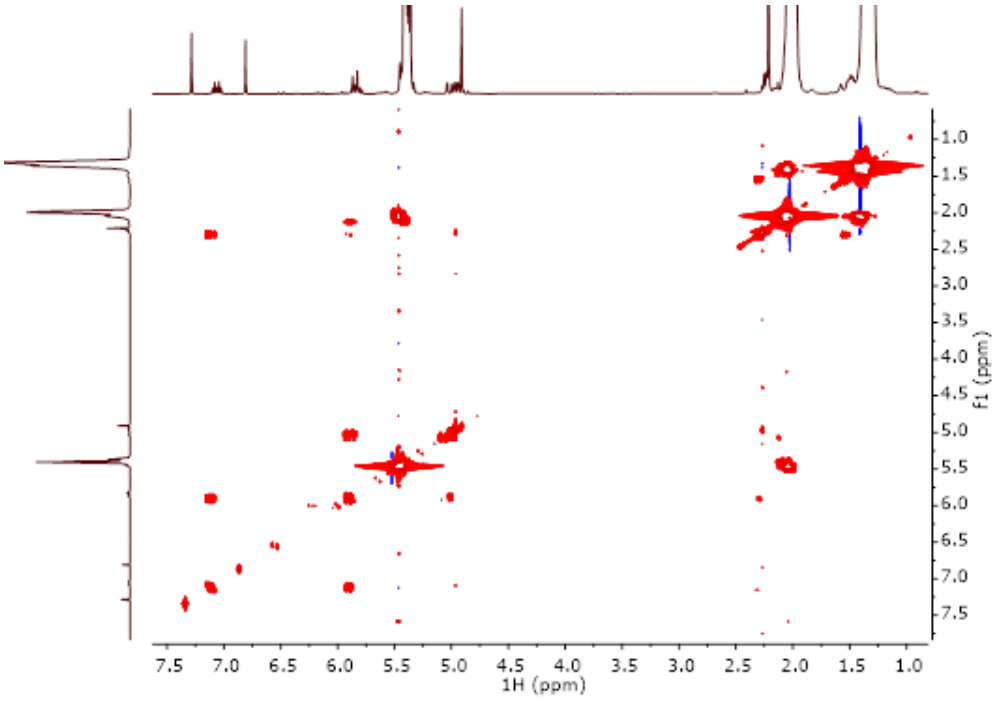

Figure S30. COSY NMR spectrum (400 MHz, $CDCl_3$, 25 °C) of a mixture of mono and di(**VC1**)-PCOE (Scheme 6, Table S3, entry 1).

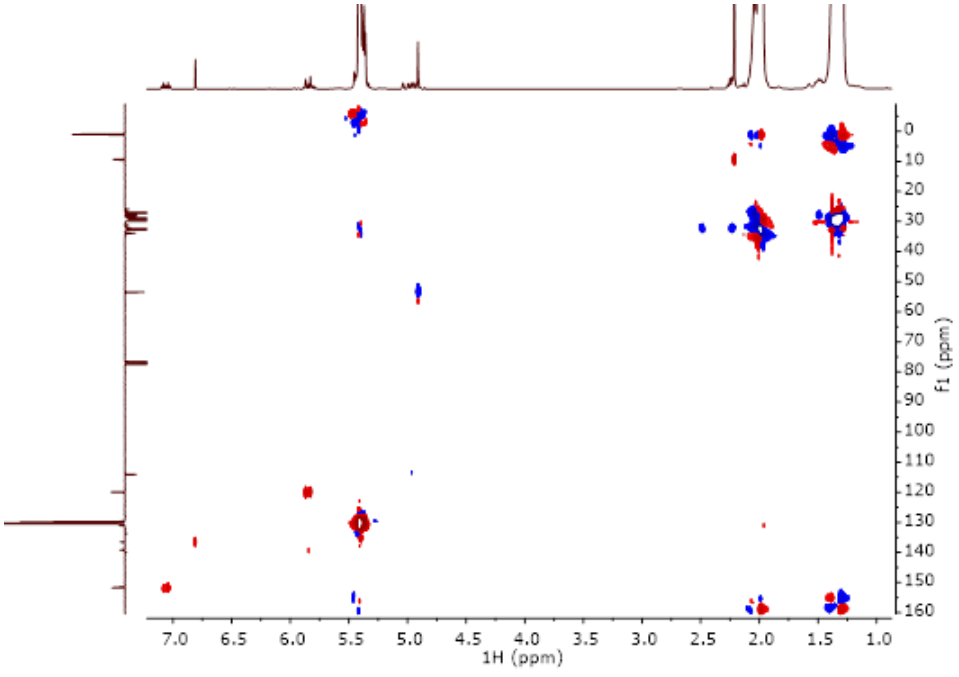

Figure S31. HSQC NMR spectrum (400 and 100 MHz, $CDCl_3$, 25 °C) of a mixture of mono and di(**VC1**)-PCOE (Scheme 6, Table S3, entry 1).

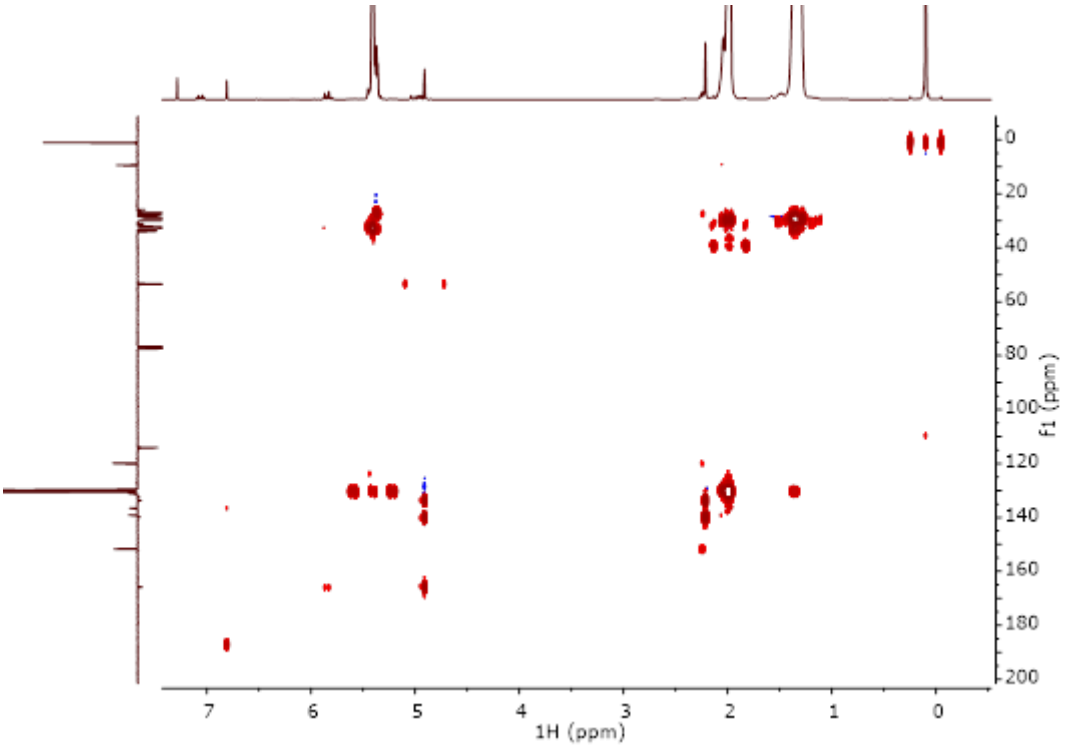

Figure S32. HMBC NMR spectrum (400 and 100 MHz, $CDCl_3$, 25 °C) of a mixture of mono- and di(**VC1**)-PCOE (Scheme 6, Table S3, entry 1).

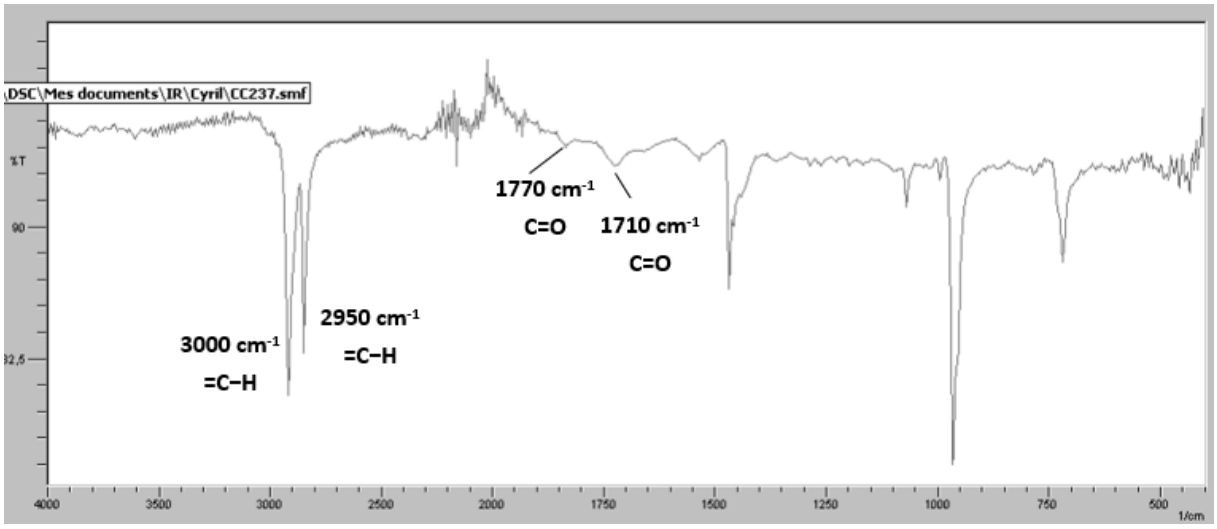

Figure S33. FTIR spectrum of a mixture of mono and di(**VC1**)-PCOE (Scheme **6**, Table S3, entry 1).

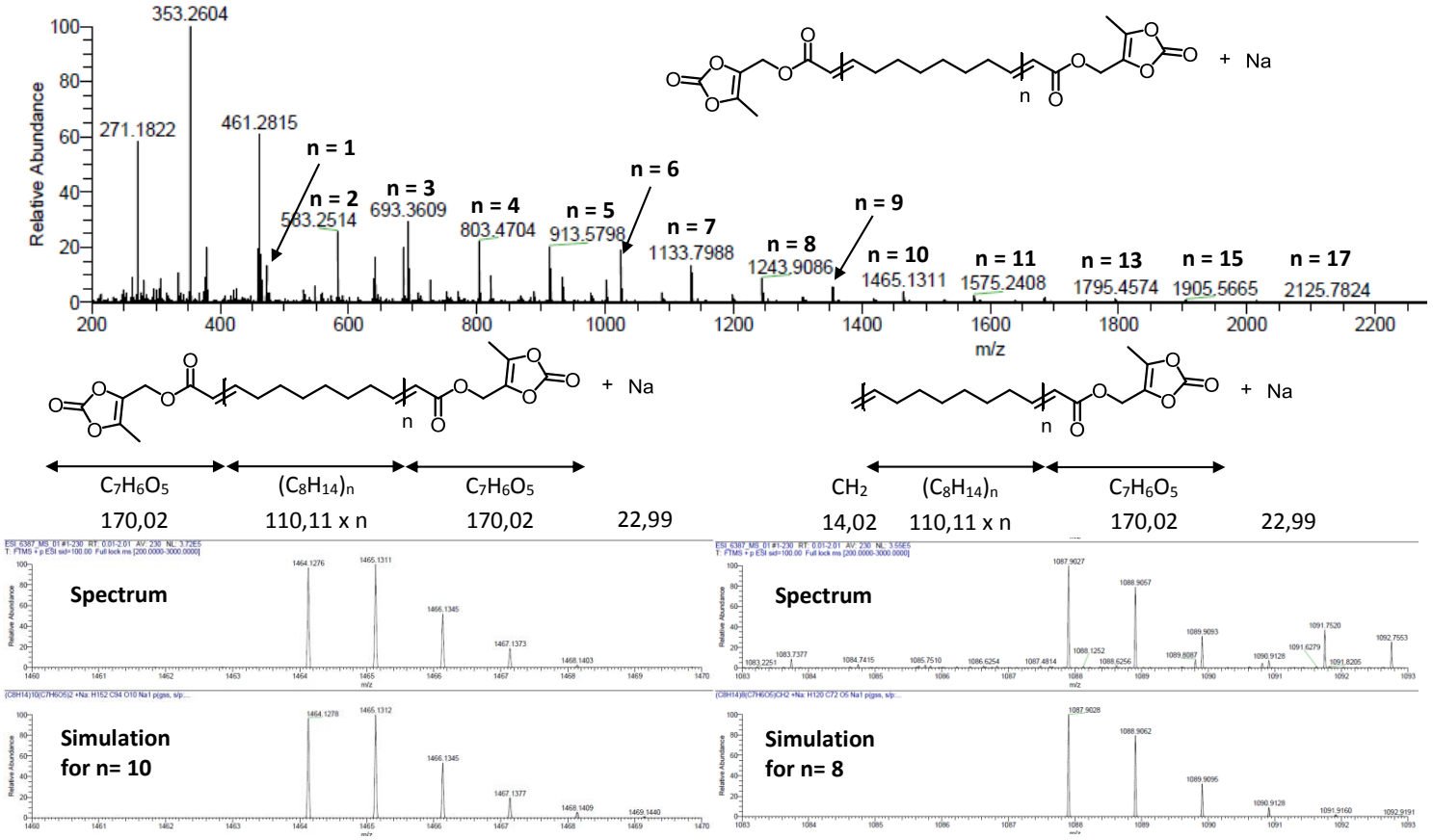

Figure S34. Top: ESI-MS mass spectrum (DCTB matrix, NaI ionizing salt) of a mixture of mono- and di(**VC1**)-PCOE (Scheme 6, Table S3, entry 1); bottom left: zoomed spectrum and simulation of difunctional (DF) PCOE for *n* = 10; bottom right: zoomed spectrum and simulation of monofunctional (MF) PCOE for *n* = 8.

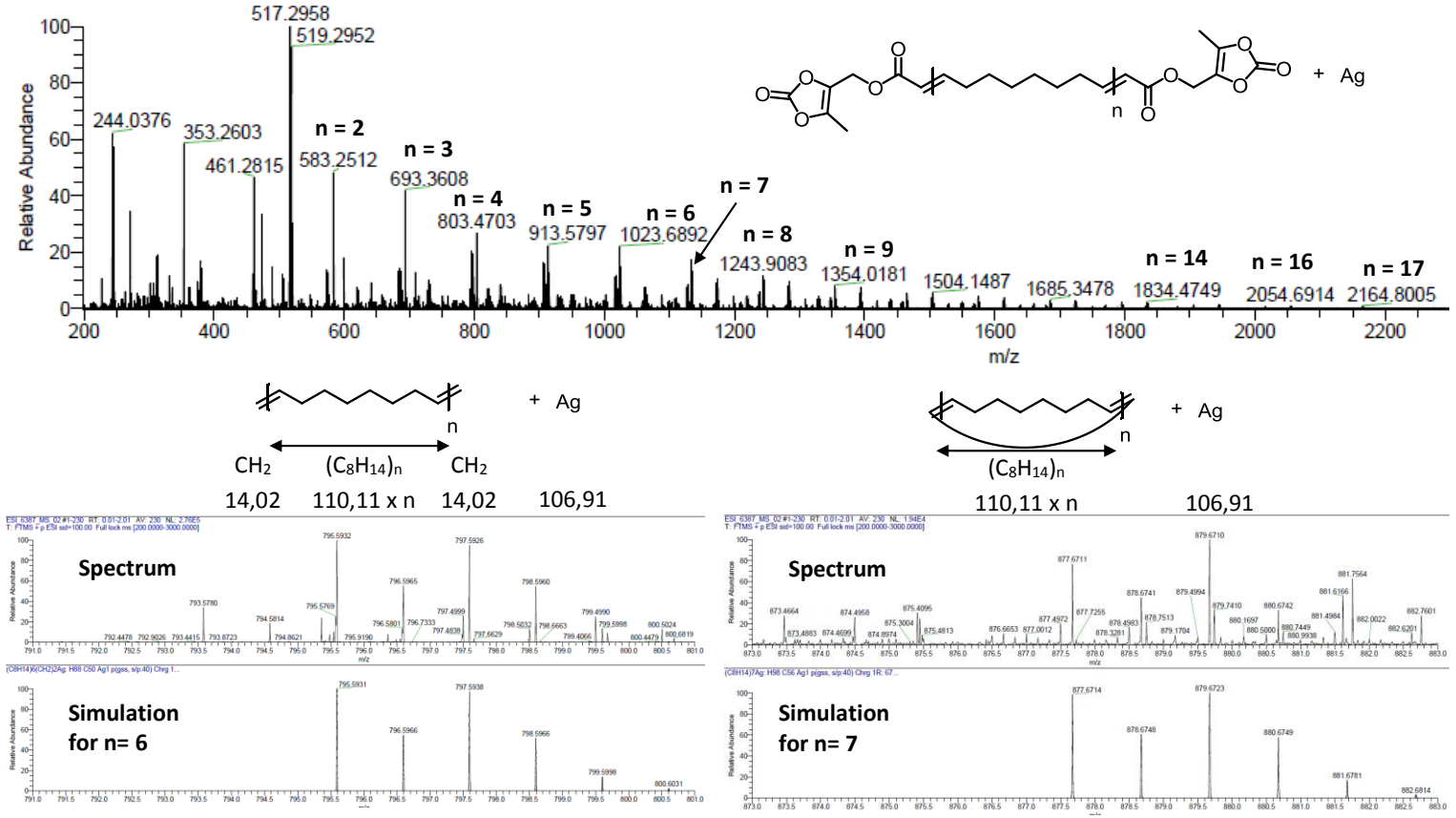

Figure S35. Top: ESI-MS mass spectrum (DCTB matrix, AgTFA ionizing salt) of a mixture of mono- and di(**VC1**)-PCOE (Scheme 6, Table S3, entry 1); bottom left: zoomed spectrum and simulation of linear nonfunctional (LNF) PCOE for *n* = 6; bottom right: zoomed spectrum and simulation of cyclic nonfunctional (CNF) PCOE for *n* = 7.

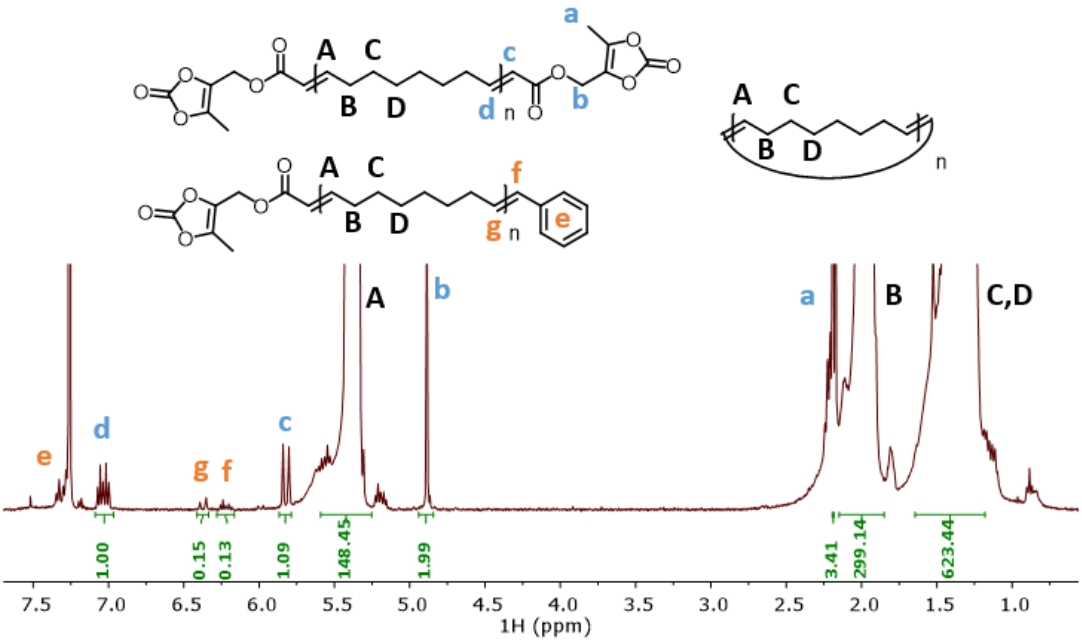

Figure S36. ^{1}H NMR spectrum (400 MHz, $CDCl_3$, 25 °C) of di(**VC2**)-PCOE (Table S4, entry 1).

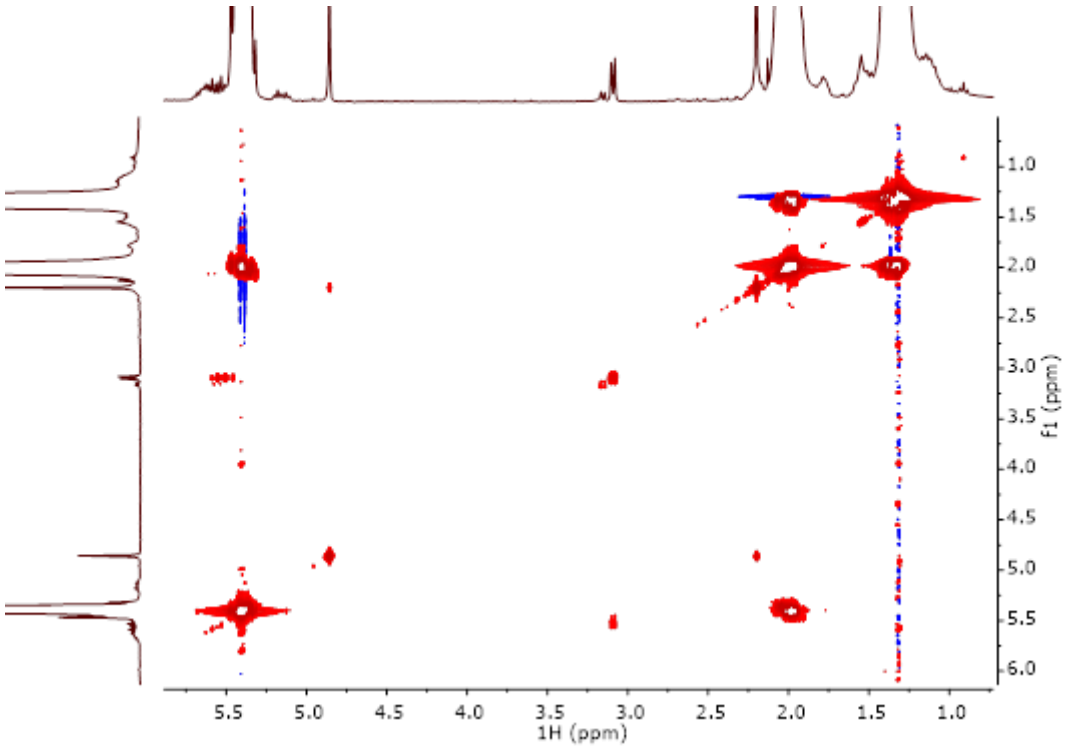

Figure S37. COSY NMR spectrum (400 MHz, $CDCl_3$, 25 °C) of di(**VC3**)-PCOE (Scheme 6, Table 1, entry 3).

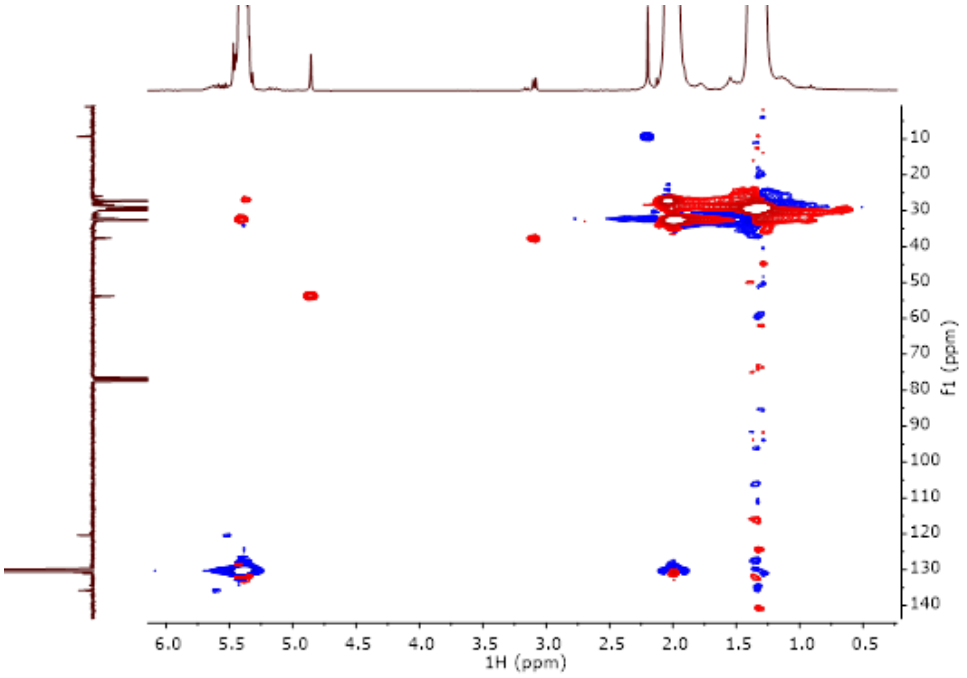

Figure S38. HSQC NMR spectrum (400 and 100 MHz, $CDCl_3$, 25 °C) of di(**VC3**)-PCOE (Scheme 6, Table 1, entry 3).

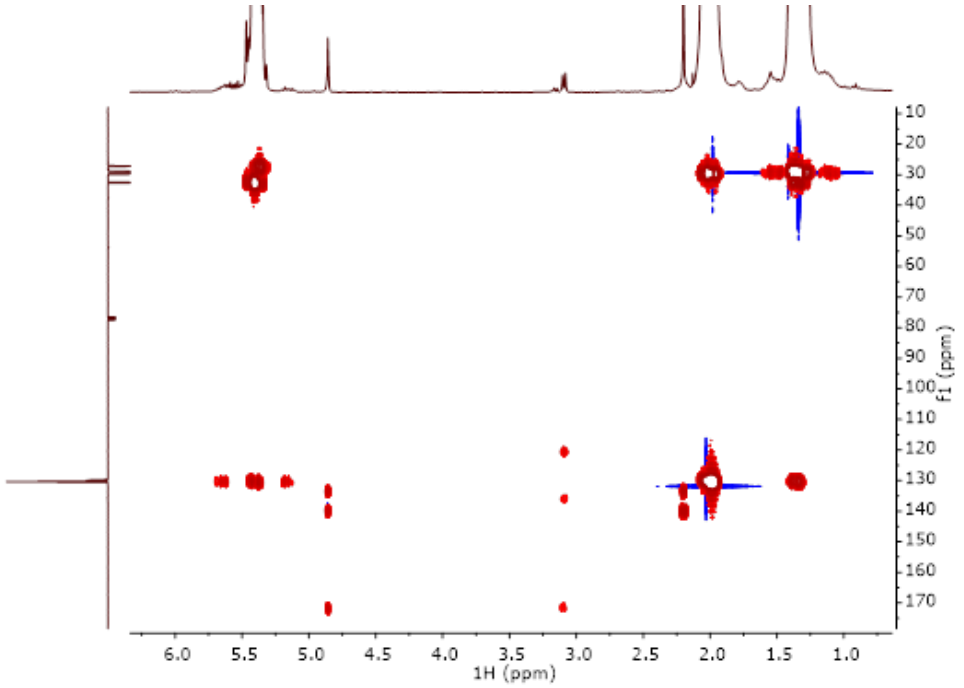

Figure S39. HMBC NMR spectrum (400 and 100 MHz, $CDCl_3$, 25 °C) of di(**VC3**)-PCOE (Scheme 6, Table 1, entry 3).

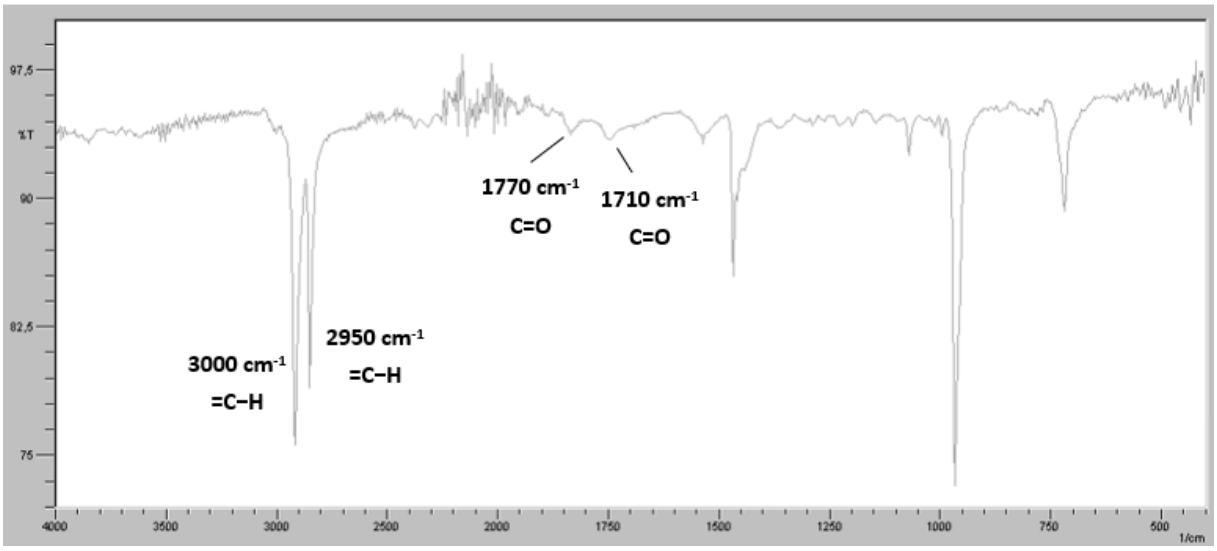

Figure S40. FTIR spectrum of di(**VC3**)-PCOE (Scheme 6, Table 1, entry 3).

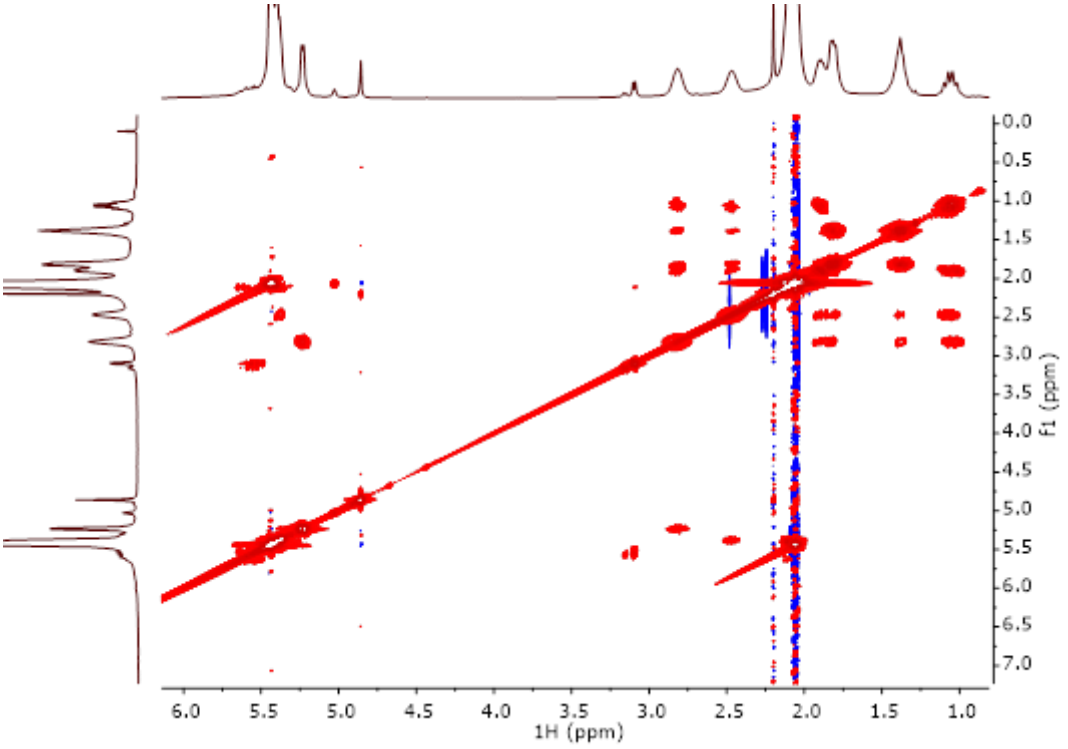

Figure S41. COSY NMR spectrum (400 MHz, $CDCl_3$, 25 °C) of di(**VC3**)-P(NB-*co*-CDT) (Scheme 7).

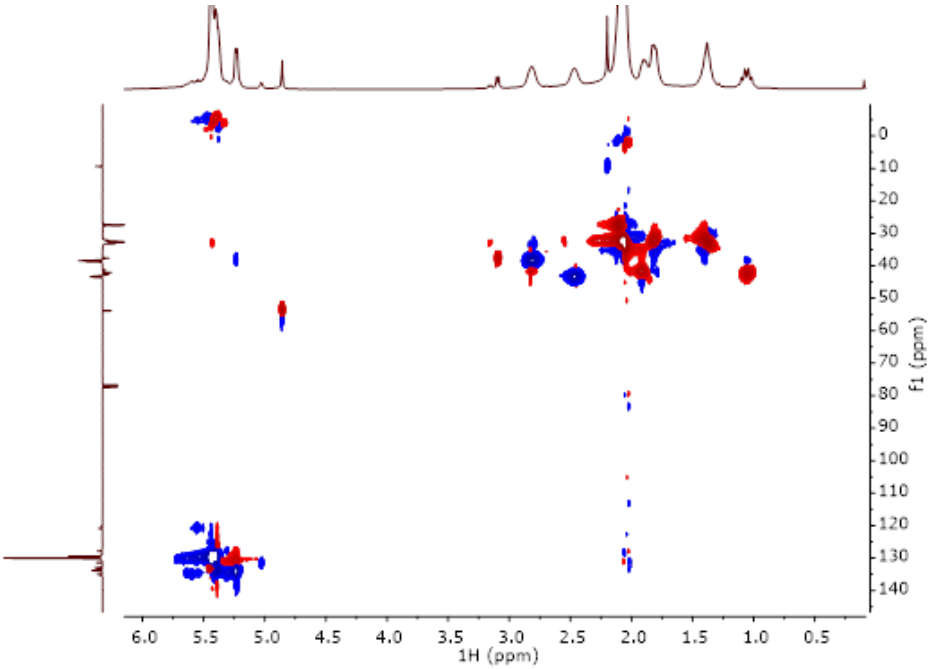

Figure S42. HSQC NMR spectrum (400 and 100 MHz, $CDCl_3$, 25 °C) of di(**VC3**)-P(NB-*co*-CDT) (Scheme 7).

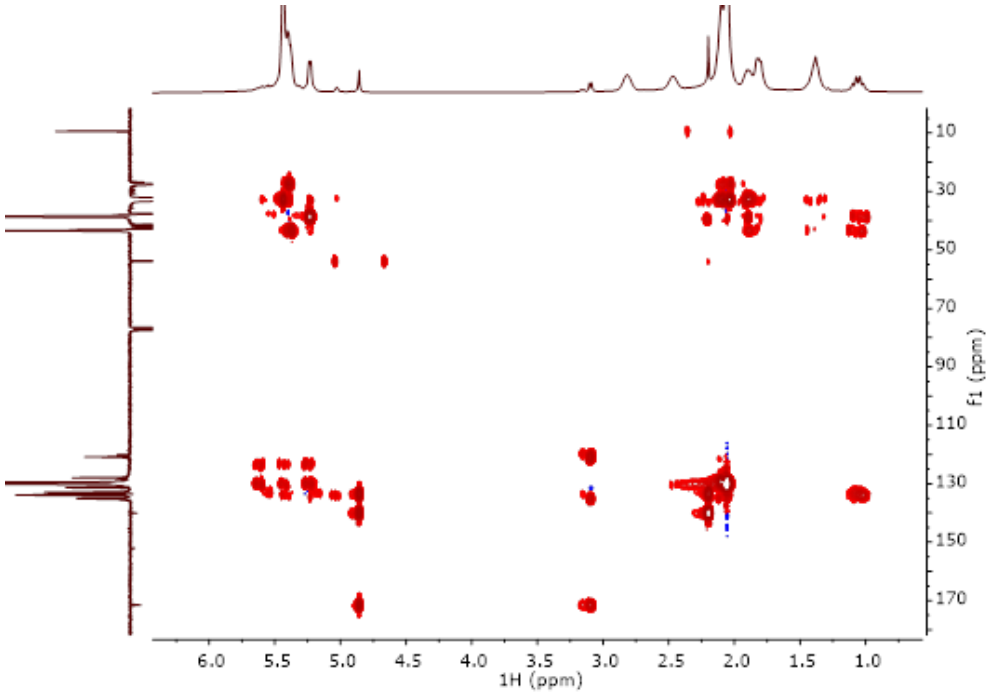

Figure S43. HMBC NMR spectrum (400 and 100 MHz, $CDCl_3$, 25 °C) of di(**VC3**)-P(NB-*co*-CDT) (Scheme 7).

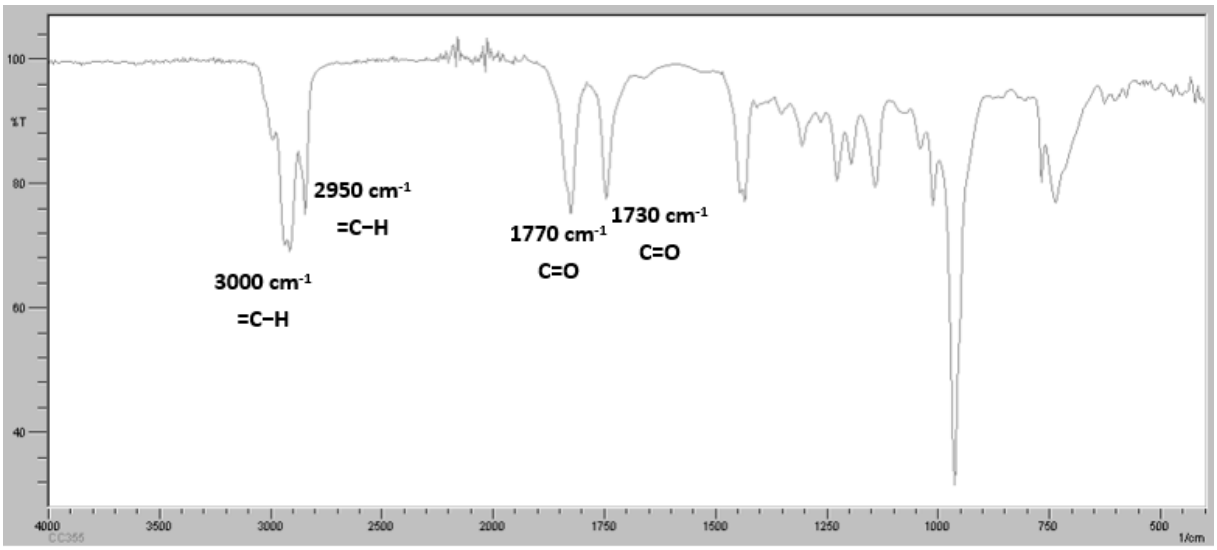

Figure S44. FTIR spectrum of di(**VC3**)-P(NB-*co*-CDT) (Scheme 7).

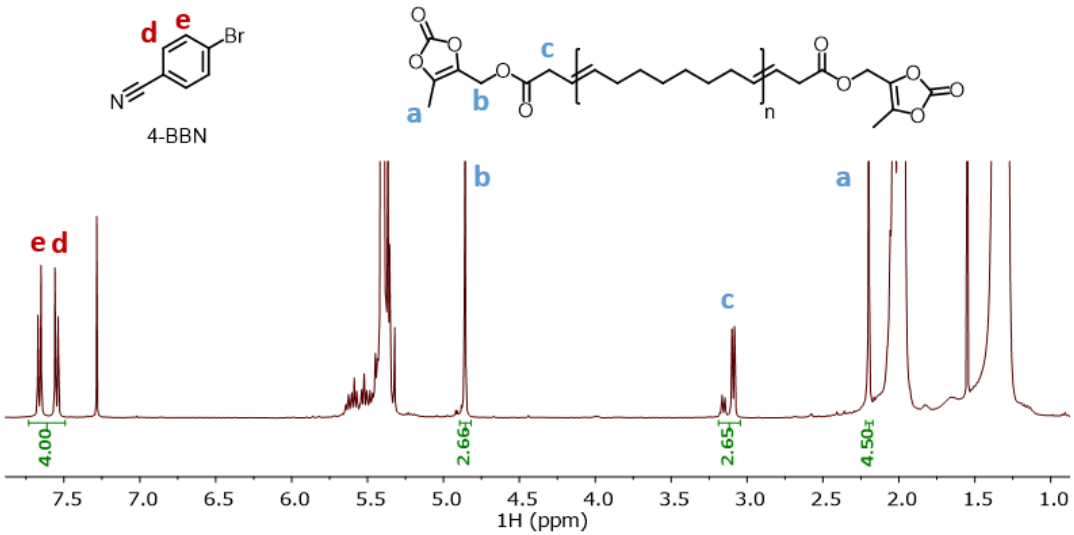

Figure S45. ^{1}H NMR spectrum (400 MHz, $CDCl_3$, 25 °C) of a di(**VC3**)-PCOE (19.2 mg) mixed with 4-bromobenzonitrile (2.6 mg). The concentration of **VC3** functions in the polymer thus determined is C_{VC3} = 0.98 mmol.g^{-1}.

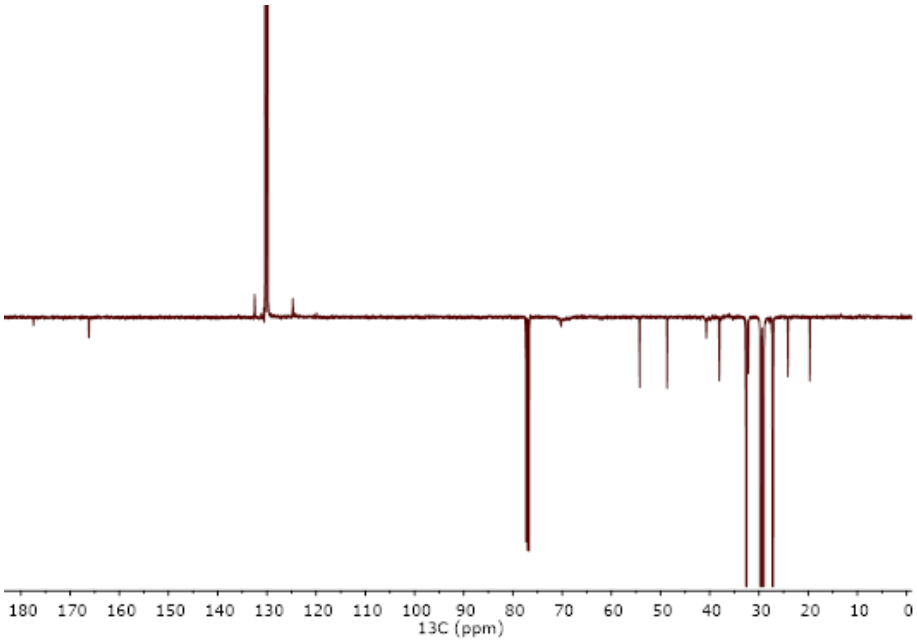

Figure 46. J-MOD NMR spectrum (100 MHz, $CDCl_3$, 25 °C) of the product from the stoichiometric reaction of di(**VC3**)-PCOE and EDR-148 (Scheme 8). The J-MOD signal of the tertiary asymmetric carbone atom –*C*(OH)(CH_3)– of the expected hydroxy-oxazolidone moiety (δ ca. 80 ppm) was not observed.

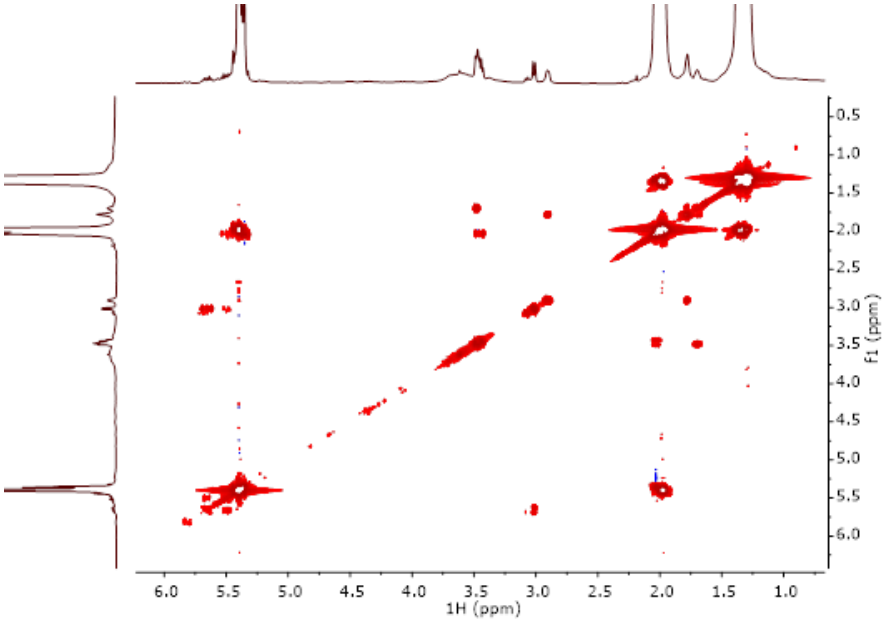

Figure S47. COSY NMR spectrum (400 MHz, $CDCl_3$, 25 °C) of the product from the stoichiometric reaction of di(**VC3**)-PCOE and EDR-148 (Scheme 8).

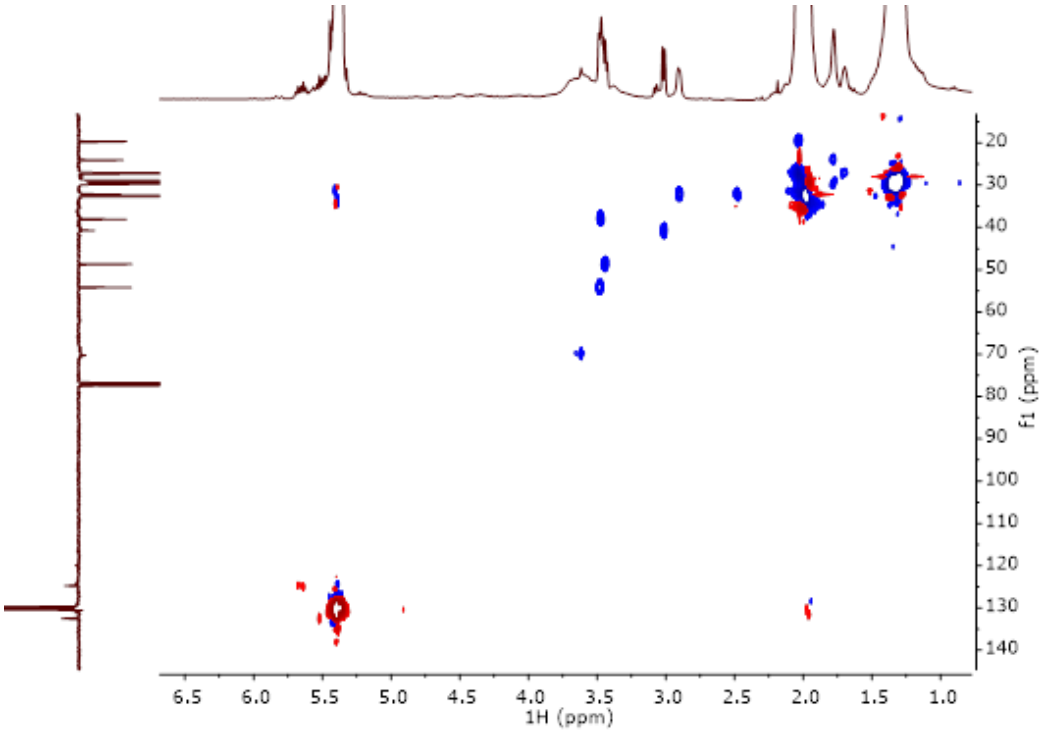

Figure S48. HSQC NMR spectrum (400 and 100 MHz, $CDCl_3$, 25 °C) of the product from the stoichiometric reaction of di(**VC3**)-PCOE and EDR-148 (Scheme 8).

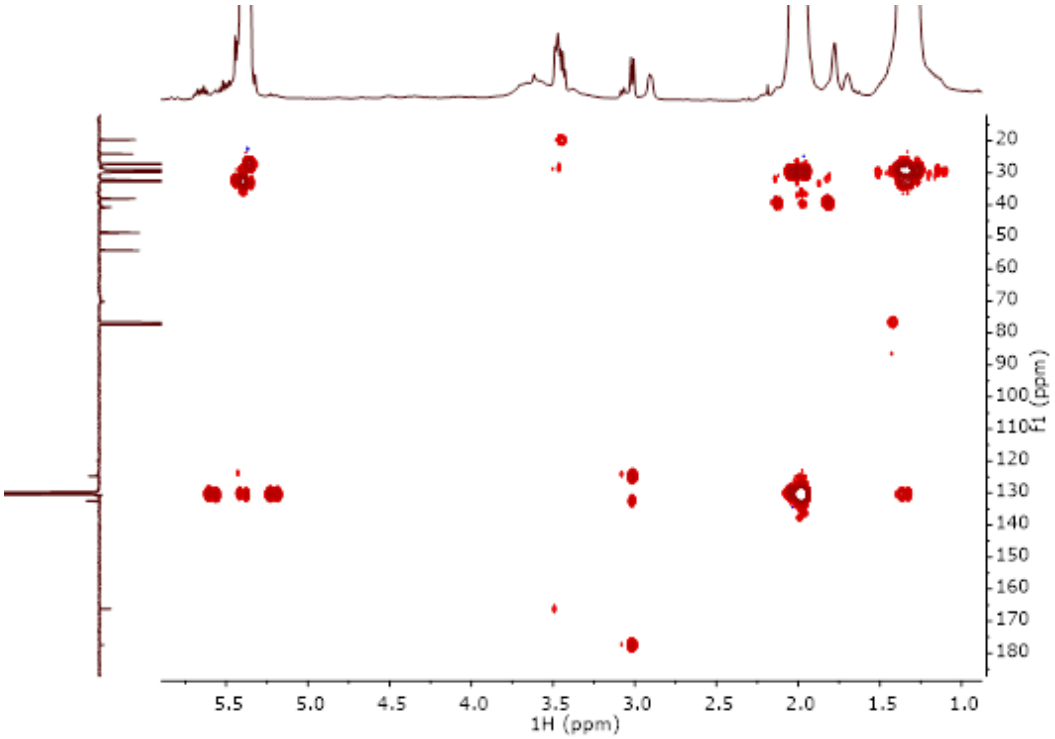

Figure S49. HMBC NMR spectrum (400 and 100 MHz, $CDCl_3$, 25 °C) of the product from the stoichiometric reaction of di(**VC3**)-PCOE and EDR-148 (Scheme 8). The correlation in the HMBC spectrum between the carbon bearing the ester function (O*C*=O) and methylene hydrogens on the other side of oxygen (C(=O)OC^f*H*$_2$C, δ ca. 3.07 ppm) was not observed, suggesting a cleavage of the ester moiety (note that the ester function (O*C*=OC^f*H*$_2$C) was observed in the initial polymer at δ 3.07 ppm, Figure S45).

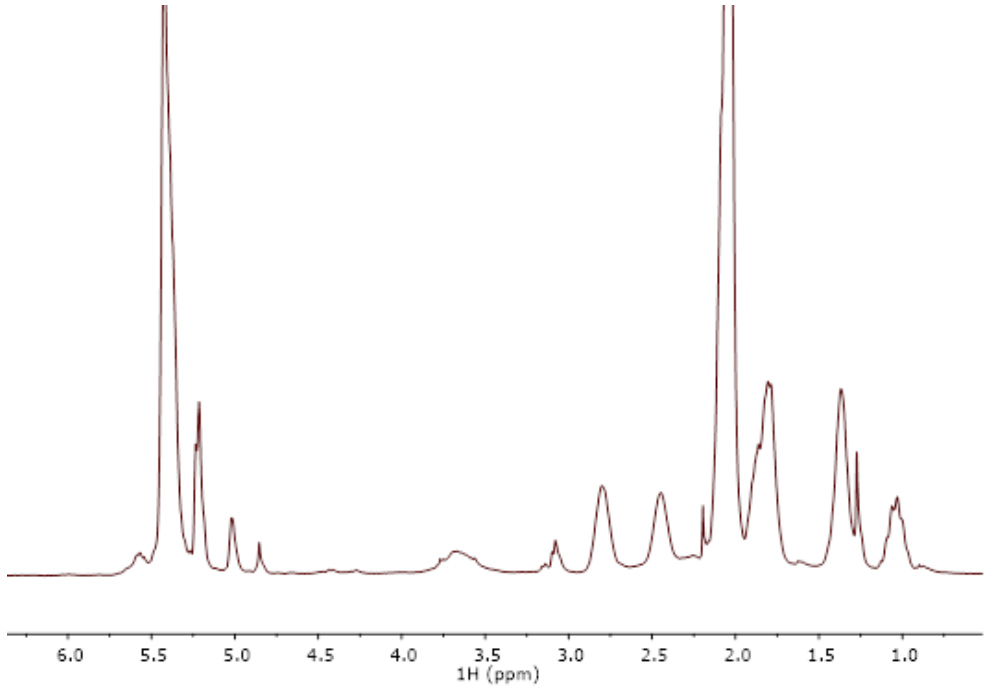

Figure S50. ^{1}H NMR spectrum (400 MHz, $CDCl_3$, 25 °C) of the product from the stoichiometric reaction of di(**VC3**)-P(NB-*co*-CDT) and EDR-148.

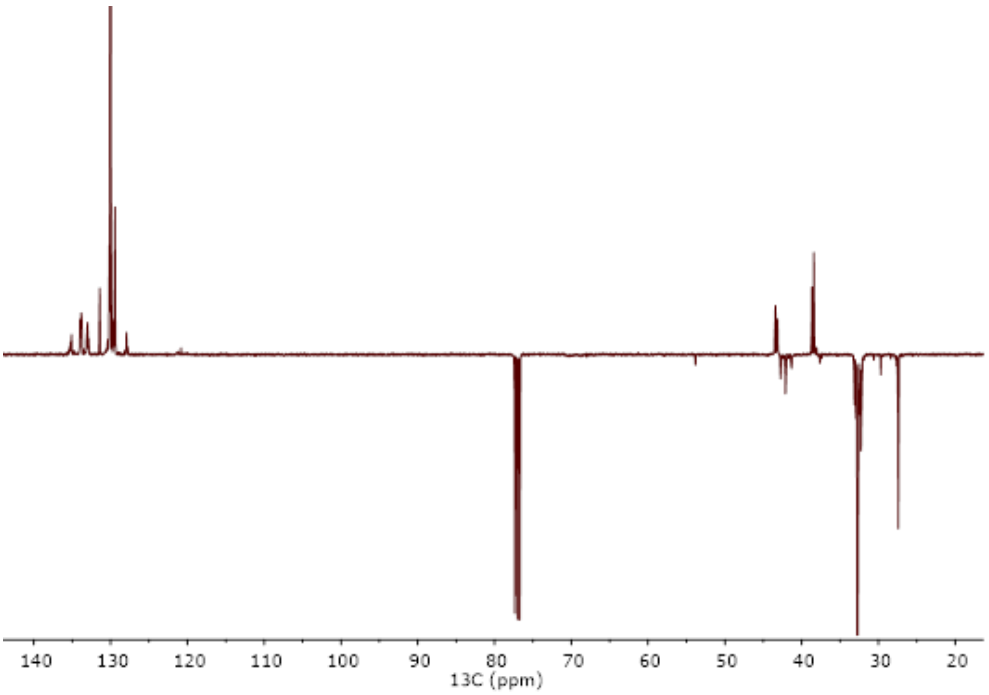

Figure S51. J-MOD NMR spectrum (100 MHz, $CDCl_3$, 25 °C) of the product from the stoichiometric reaction of di(**VC3**)-P(NB-*co*-CDT) and EDR-148.

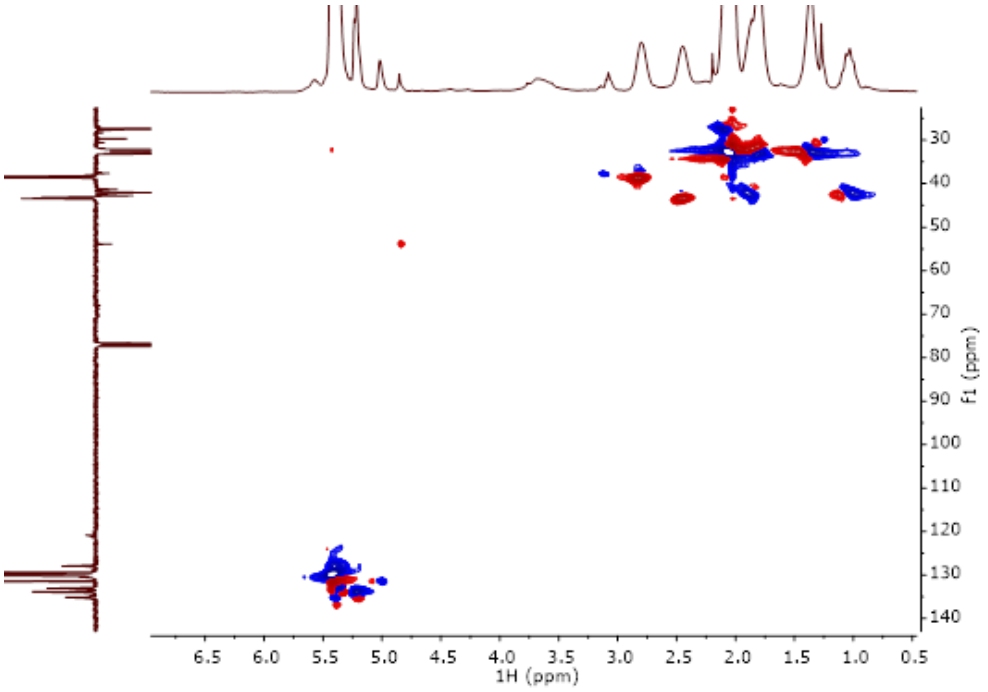

Figure S52. HSQC NMR spectrum (400 and100 MHz, $CDCl_3$, 25 °C) of the product from the stoichiometric reaction of di(**VC3**)-P(NB-*co*-CDT) and EDR-148.

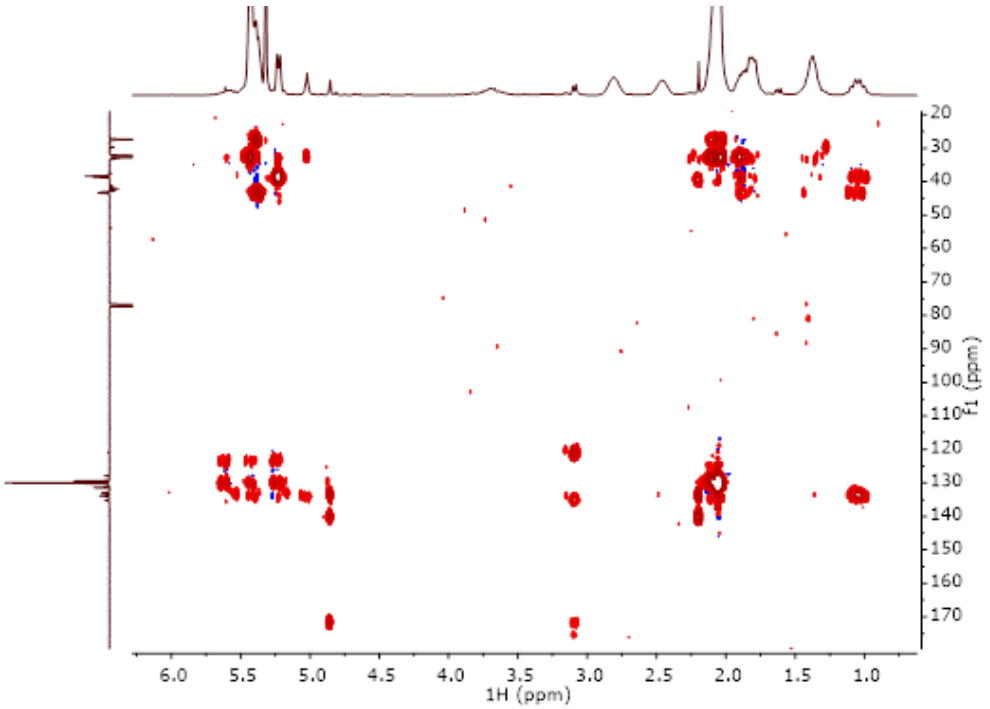

Figure S53. HMBC NMR spectrum (400 and100 MHz, $CDCl_3$, 25 °C) of the product from the stoichiometric reaction of di(**VC3**)-P(NB-*co*-CDT) and EDR-148.

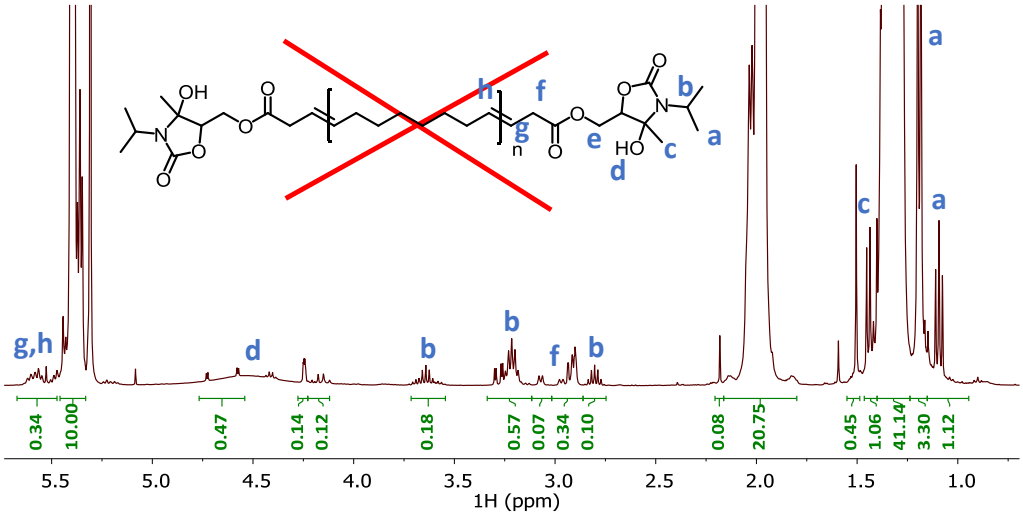

Figure S54. ^{1}H NMR spectrum (400 MHz, $CDCl_3$, 25 °C) of the product from the reaction of di(**VC3**)-PCOE and isopropylamine (Scheme 8).

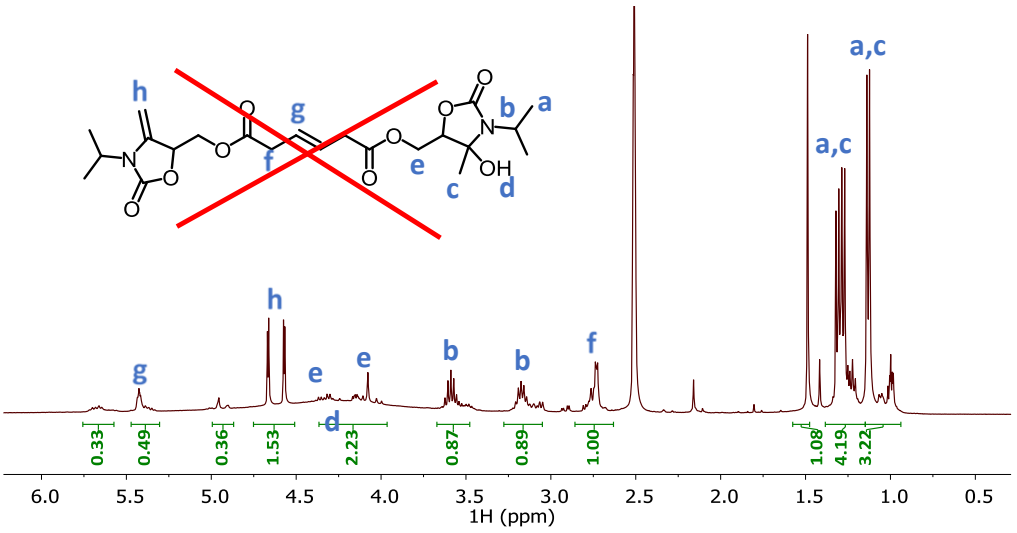

Figure S55. ^{1}H NMR spectrum (400 MHz, $CDCl_3$, 25 °C) of the product obtained from the reaction of **VC3** and isopropylamine (Scheme 6).

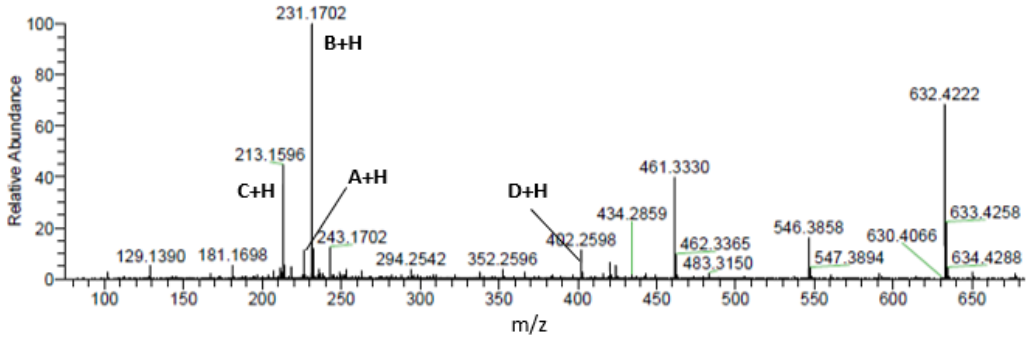

Figure S56. ESI-mass spectrum (DCTB matrix, NaI ionizing salt) of a sample issued from the reaction of **VC3** with isopropylamine, showing the four major compounds **A**–**D** among other side-products (Scheme 9). H stands for hydrogen.

References and Notes

[1] M. F. Sonnenschein, Polyurethanes: Science, Technology, Markets, and Trends, John Wiley & Sons, Inc, Hoboken, NJ, 2014.

[2] A. Prociak, G. Rokicki, J. Ryszkowska. Polyurethane Materials, PWN Press, Warsaw, Poland, 2014.

[3] H.-W. Engels, H.-G. Pirkl, R. Albers, R. W. Albach, J. Krause, A. Hoffmann, H. Casselmann, J. Dormish. Polyurethanes: versatile materials and sustainable problem solvers for today's challenges. *Angew. Chem., Int. Ed.* **2013**, *52*, 9422–9441.

[4] P. Furtwengler, L. Averous. Renewable polyols for advanced polyurethane foams from diverse biomass resources. *Polym. Chem.*, **2018**, *9*, 4258–4287.

[5] J. Datta, M. Wloch. Progress in non-isocyanate polyurethanes synthesized from cyclic carbonate intermediates and di- or polyamines in the context of structure–properties relationship and from an environmental point of view. *Polym. Bull.*, **2016**, *73*, 1459–1497.

[6] G. Rokicki, P. G. Parzuchowski, M. Masurek. *Polym.* Non-isocyanate polyurethanes: synthesis, properties, and applications. *Adv. Technol.* **2015**, *26*, 707–761.

[7] L. Maisonneuve, O. Lamarzelle, E. Rix, E. Grau, H. Cramail. Isocyanate-Free Routes to Polyurethanes and Poly(hydroxy Urethane)s. *Chem. Rev.* **2015**, *115*, 12407−12439.

[8] V. Besse, F. Camara, F. Méchin, E. Fleury, S. Caillol, J.-P. Pascault, B. Boutevin. How to explain low molar masses in PolyHydroxyUrethanes (PHUs). *Eur. Polym. J.* **2015**, *71*, 1–11.

[9] H. Blattmann, M. Fleischer, M. Bähr, R. Mülhaupt. Isocyanate- and Phosgene-Free Routes to Polyfunctional Cyclic Carbonates and Green Polyurethanes by Fixation of Carbon Dioxide. *Macromol. Rapid Commun.* **2014**, *35*, 1238–1254.

[10] B. Nohra, L. Candy, J.-F. Blanco, C. Guerin, Y. Raoul, Z. Mouloungui. From Petrochemical Polyurethanes to Biobased Polyhydroxyurethanes. *Macromolecules* **2013**, *46*, 3771−3792.

[11] O. Kreye, H. Mutlu, M. A. R. Meier. Sustainable routes to polyurethane precursors. *Green Chem.* **2013**, *15*, 1431−1455.

[12] M. Helou, J.-F. Carpentier, S. M. Guillaume. Poly(carbonate-urethane): an isocyanate-free procedure from α,ω-di(cyclic carbonate) telechelic poly(trimethylene carbonate)s. *Green Chem.* **2011**, *13*, 266–271.

[13] N. Kihara, T. Endo. Synthesis and properties of poly(hydroxyurethane)s. *J. Polym. Sci. Part A* **1993**, *31*, 2765–2773.

[14] M. S. Kathalewar, P. B. Joshi, A. S. Sabnis, V. C. Malshe. Non-isocyanate polyurethanes: from chemistry to applications. *RSC Adv* **2013**, *3*, 4110.

[15] O. Figovsky, L. Shapovalov, A. Leykin, O. Birukova, R. Potashnikova. Advances in the field of non-isocyanate polyurethanes based on cyclic carbonates. *Chem. Chem. Technol.* **2013**, *7*, 79-87.

[16] H. Tomita, F. Sanda, T. Endo. Structural analysis of polyhydroxyurethane obtained by polyaddition of bifunctional five-membered cyclic carbonate and diamine based on the model reaction. *J. Polym. Sci. Part A* **2001**, *39*, 851–859.

[17] H. Tomita, F. Sanda, T. Endo. Model reaction for the synthesis of polyhydroxyurethanes from cyclic carbonates with amines: Substituent effect on the reactivity and selectivity of ring-opening direction in the reaction of five-membered cyclic carbonates with amine. *J. Polym. Sci. Part A* **2001**, *39*, 3678–3685.

[18] A. Steblyanko, W. Choi, F. Sanda, T. Endo. Addition of five-membered cyclic carbonate with amine and its application to polymer synthesis. *J. Polym. Sci. Part A* **2000**, *38*, 2375–2380.

[19] A. Cornille, M. Blain, R. Auvergne, B. Andrioletti, B. Boutevin, S. Caillol. A study of cyclic carbonate aminolysis at room temperature: effect of cyclic carbonate structures and solvents on polyhydroxyurethane synthesis. *Polym. Chem.* **2017**, *8*, 592–604.

[20] B. Ochiai, S. Inoue, T. Endo. Salt effect on polyaddition of bifunctional cyclic carbonate and diamine. *J. Polym. Sci. Part A* **2005**, *43*, 6282–6286.

[21] H. Tomita, F. Sanda, T. Endo. Polyaddition behavior of bis(five- and six-membered cyclic carbonate)s with diamine. *J. Polym. Sci., Part A: Polym. Chem.* **2001**, *39*, 860–867.

[22] H. Tomita, F. Sanda, T. Endo. Polyaddition of bis(seven-membered cyclic carbonate) with diamines: a novel and efficient synthetic method for polyhydroxyurethanes. *J. Polym. Sci., Part A: Polym. Chem.* **2001**, *39*, 4091–4100.

[23] D. J. Fortman, J. P. Brutman, M. A. Hillmyer, W. R. Dichtel. Structural effects on the reprocessability and stress relaxation of crosslinked polyhydroxyurethanes. *J Appl Polym Sci* **2017**, *134*, 44984.

[24] H. Matsukizono, T. Endo. Reworkable Polyhydroxyurethane Films with Reversible Acetal Networks Obtained from Multifunctional Six-Membered Cyclic Carbonates. *J. Am. Chem. Soc.* **2018**, *140*, 884–887.

[25] H. Matsukizono, T. Endo. Synthesis and hydrolytic properties of water-soluble poly(carbonate–hydroxyurethane)s from trimethylolpropane. *Polym. Chem.* **2016**, *7*, 958–969.

[26] B. Nohra, L. Candy, J.-F. Blanco, Y. Raoul, Z. Mouloungui. Synthesis of five and six-membered cyclic glycerilic carbonates bearing exocyclic urethane functions. *Eur. J. Lipid. Sci. Tech.* **2013**, *115*, 111–122.

[27] H. Tomita, F. Sanda, T. Endo. Reactivity comparison of five- and six-membered cyclic carbonates with amines: basic evaluation for synthesis of poly(hydroxyurethane). *J. Polym. Sci., Part A: Polym. Chem.* **2001**, *39*, 162–168.

[28] L. Maisonneuve, A.-L. Wirotius, C. Alfos, E. Grau, H. Cramail. Fatty acid-based (bis) 6-membered cyclic carbonates as efficient isocyanate free poly(hydroxyurethane) precursors. *Polym. Chem.* **2014**, *5*, 6142–6147.

[29] A. Yuen, A. Bossion, E. Gomez-Bengoa, F. Ruipérez, M. Isik, J. L. Hedrick, D. Mecerreyes, Y. Y. Yang, H. Sardon. Room temperature synthesis of non-isocyanate polyurethanes (NIPUs) using highly reactive *N*-substituted 8-membered cyclic carbonates. *Polym. Chem.*, **2016**, *7*, 2105–2111.

[30] G. Fiorani, W. Guo, A. W. Kleij. Sustainable conversion of carbon dioxide: the advent of organocatalysis. *Green Chem.*, **2015**, *17*, 1375–1389.

[31] M. Alves, B. Grignard, R. Mereau, C. Jerome, T. Tassaing, C. Detrembleur. Organocatalyzed coupling of carbon dioxide with epoxides for the synthesis of cyclic carbonates: catalyst design and mechanistic studies. ***Catal. Sci. Technol.***, 2017,**7**, 2651–2684.

[32] E. Vanbiervliet, S. Fouquay. G. Michaud, F. Simon, J.-F. Carpentier, S. M. Guillaume, From Epoxide to Cyclodithiocarbonate Telechelic Polycyclooctene through Chain-Transfer Ring-Opening Metathesis Polymerization (ROMP): Precursors to Non-Isocyanate Polyurethanes (NIPUs), *Macromolecules* **2017**, *50*, 69-82.

[33] Y. Zhang, A. Sudo, T. Endo. Syntheses of bisphenol-type oligomers having five-membered dithiocarbonate groups at the terminals and their application as accelerators to epoxy-amine curing system. *J. Polym. Sci. A: Polym. Chem.* **2008**, *46*, 1907–1912.

[34] M. Horikiri, A. Sudo, T. Endo. Acceleration effect of five-membered cyclic dithiocarbonate on an epoxy-amine curing system. *J. Polym. Sci.: Part A: Polym. Chem.* **2007**, *45*, 4606–4611.

[35] A. Suzuki, D. Nagai, B. Ochiai, T. Endo. Facile synthesis and crosslinking reaction of trifunctional five-membered cyclic carbonate and dithiocarbonate. *J. Polym. Sci. Part A* **2004**, *42*, 5983–5989.

[36] H. Tomita, F. Sanda, T. Endo. Polyaddition of Bis(cyclic thiocarbonate) with Diamines. Novel Efficient Synthetic Method of Polyhydroxythiourethanes. *Macromolecules*, **2001**, *34*, 727−733.

[37] T. Moriguchi, T. Endo. Polyaddition of Bifunctional Dithiocarbonates Derived from Epoxides and Carbon Disulfide. Synthesis of Novel Poly(thiourethanes). *Macromolecules* **1995**, *28*, 5386–5387.

[38] D. J. Darensbourg, S. J. Wilson, A. D. Yeung. Oxygen/Sulfur Scrambling During the Copolymerization of Cyclopentene Oxide and Carbon Disulfide: Selectivity for Copolymer vs Cyclic [Thio]carbonates. *Macromolecules* **2013**, *46*, 8102–8110.

[39] M. P. Garcia, M. Weis, A. Lanver, M. Blanchot, A. Flores-Figueroa, R. Klopsch, C. Haaf, O. Kutzki. Polymerizable Alkylidene-1, 3-Dioxolane-2-One and Use Thereof, US Patent Application 20130331532, **2013** (to BASF).

[40] V. Mormul, R. Klopsch, M. Yu, G. Scherr, D. Ghislieri. Cyclic carbonates, EP 15164849.0, **2015** (to BASF).

[41] U. Licht, K.-H. Schumacher, R. Klopsch, D. Ghislieri. Copolymer made from cyclic exo-vinyl carbonate acrylates, EP 15172703.9, **2015** (to BASF).

[42] U. Licht, V ; Leonhardt, V. Mormul, K.-H. Schumacher, G. Boerzsoenyl, R. Klopsch, D. Ghislieri. Compounds comprising two or more exovinylene cyclic-carbonate units, EP 15172703.9, **2015** (to BASF).

[43] S. Gennen, B. Grignard, T. Tassaing, C. Jérôme, C. Detrembleur. CO2-Sourced α-Alkylidene Cyclic Carbonates: A Step Forward in the Quest for Functional Regioregular Poly(urethane)s and Poly(carbonate)s. *Angew. Chem. Int. Edit.* **2017**, *56*, 10394–10398.

[44] Formation of oxazolidone from an α-alkylidene cyclocarbonate at room temperature was also described; see: N. B. Chernysheva, A. A. Bogolyubov, V. V. Semenov. Reactions of 5-methylene-1,3-dioxolan-2-ones with amines. Synthesis of 2-oxazolidinones. *Chem. Heterocyc. Compd.* **1999**, *35*, 216–224.

[45] T. Watai, M. Takase, T. Sagae, S. Mori, N. Kawahara. Process for Producing (Dioxolenon-4-Yl)Methyl Ester Derivative, **2004**, US Pat. Appl. 2004133016.

[46] M. Ionescu, Chemistry and Technology of Polyols for Polyurethane, 2007. Rapra Technology, Shrewsbury, UK

[47] Functional Liquid Polymers - Poly bd™, Poly ip™, EPOL™ (IDEMITSU) ; http://www.idemitsu.com/products/petrochemicals/flp/index.html.

[48] L. Annunziata, A. K. Diallo, S. Fouquay, G. Michaud, F. Simon, J.-M. Brusson, J.-F. Carpentier, S. M. Guillaume. α,ω-Di(glycerol carbonate) telechelic polyesters and polyolefins as precursors to polyhydroxyurethanes: an isocyanate-free approach. *Green Chem.* **2014**, *16*, 1947–1956.

[49] A. K. Diallo, L. Annunziata, S. Fouquay, G. Michaud, F. Simon, J.-M. Brusson, S. M. Guillaume, J.-F. Carpentier. Ring-opening metathesis polymerization of cyclooctene derivatives with chain transfer agents derived from glycerol carbonate. *Polym. Chem.* **2014**, *5*, 2583-2591.

[50] L. Annunziata, S. Fouquay, G. Michaud, F. Simon, S. M. Guillaume, J.-F. Carpentier. Mono- and di-cyclocarbonate telechelic polyolefins synthesized from ROMP using glycerol carbonate derivatives as chain-transfer agents. *Polym. Chem.* **2013**, *4*, 1313–1316.

[51] A. K. Diallo, X. Michel, S. Fouquay, G. Michaud, F. Simon, J.-M. Brusson, J.-F. Carpentier, S. M. Guillaume. α-Trialkoxysilyl Functionalized Polycyclooctenes Synthesized by Chain-Transfer Ring-Opening Metathesis Polymerization. *Macromolecules* **2015**, *48*, 7453–7465.

[52] Michel, S. Fouquay, G. Michaud, F. Simon, J.-M. Brusson, J.-F. Carpentier, S. M. Guillaume. α,ω-Bis(trialkoxysilyl) difunctionalized polycyclooctenes from ruthenium-catalyzed chain-transfer ring-opening metathesis polymerization. *Polym. Chem.* **2016**, *7*, 4810-4823.

[53] X. Michel, S. Fouquay, G. Michaud, F. Simon, J.-M. Brusson, P. Roquefort, T. Aubry, J.-F. Carpentier, S. M. Guillaume. Tuning the properties of α,ω-bis(trialkoxysilyl) telechelic copolyolefins from ruthenium-catalyzed chain-transfer ring-opening metathesis polymerization (ROMP). *Polym. Chem.* **2017**, *8*, 1177–1187.

[54] E. Vanbiervliet, S. Fouquay, G. Michaud, F. Simon, J.-F. Carpentier, S. M. Guillaume. α,ω-Epoxide, oxetane and dithiocarbonate telechelic copolyolefins: access by ring-

opening metathesis/cross-metathesis polymerization (ROMP/CM) of cycloolefins in the presence of functional symmetric chain-transfer agents. *Polymers*, **2018**, *10*, 1241-1260.

[55] X. Michel, S. Fouquay, G. Michaud, F. Simon, J.-M. Brusson, J.-F. Carpentier, S. M. Guillaume. Simple access to alkoxysilyl telechelic polyolefins from ruthenium-catalyzed cross-metathesis depolymerization of polydiene. *Eur. Polym. J.*, **2017**, *96*, 403-413.

[56] C. Chauveau, E. Vanbiervliet, S. Fouquay. G. Michaud, F. Simon, J.-F. Carpentier, S. M. Guillaume. Azlactone telechelic polyolefins as precursors to polyamides: a combination of metathesis polymerization and polyaddition reactions. *Macromolecules* **2018**, *51*, 8084-8099.

[57] (a) Sheldrick, G. M. SHELXS-97, Program for the Determination of Crystal Structures; University of Goettingen: Germany, 1997; (b) Sheldrick, G.M. SHELXL-97, Program for the Refinement of Crystal Structures; University of Goettingen: Germany, 1997.

[58] M. Shi, Y.-M. Shen, Y.-J. Chen. Reactions of 5,5-Dimethyl-4-methylene-1,3-dioxolan-2-one with Amines in the Presence of Palladium Catalyst. *Heterocycles* **2002**, *57*, 245.

[59] These side-reactions may be thermally promoted by the exothermic reaction between DMDO and primary amines.

[60] S. H. Hong, D. P. Sanders, C. W. Lee, R. H. Grubbs. Prevention of Undesirable Isomerization during Olefin Metathesis. *J. Am. Chem. Soc.* **2005**, *127*, 17160-17161.

[61] P. A. Fokou, M. A. R. Meier. Studying and Suppressing Olefin Isomerization Side Reactions During ADMET Polymerizations. *Macromol. Rapid Commun.* **2001**, *31*, 368-373.

[62] G. B. Djigoue, M. A. R. Meier. Improving the selectivity for the synthesis of two renewable platform chemicals via olefin metathesis. *Appl. Catal. A Gen.* **2009**, *368*, 158-162.

[63] S. Kanaoka, R. H. Grubbs. Synthesis of Block Copolymers of Silicon-Containing Norbornene Derivatives via Living Ring-Opening Metathesis Polymerization Catalyzed by a Ruthenium Carbene Complex. *Macromolecules* **1996**, *28*, 4707–4713.

[64] J. C. Lee, K. A. Parker, N. S. Sampson. Amino Acid-Bearing ROMP Polymers with a Stereoregular Backbone. *J. Am. Chem. Soc.* **2006**, *128*, 4578–4579.

[65] R. Singh, C. Czekelius, R. R. Schrock. Living Ring-Opening Metathesis Polymerization of Cyclopropenes. *Macromolecules* **2006**, *39*, 1316–1317.

[66] T. Morita, B. R. Maughon, C. W. Bielawski, R. H. Grubbs. A Ring-Opening Metathesis

Polymerization (ROMP) Approach to Carboxyl- and Amino-Terminated Telechelic Poly(butadiene)s. *Macromolecules* **2000**, *33*, 6621–6623.

[67] L. M. Pitet, M. Hillmyer. Carboxy-Telechelic Polyolefins by ROMP Using Maleic Acid as a Chain Transfer Agent. *Macromolecules* **2011**, *44*, 2378–2381.

[68] S. Kobayashi, H. Kim, C. W. Macosko, M. A. Hillmyer. Functionalized linear low-density polyethylene by ring-opening metathesis polymerization. *Polym. Chem.* **2013**, *4*, 1193–1198.

[69] M. Shetty, V. A. Kothapalli, C. E. Hobbs. Toward the (nearly) complete elimination of solvent waste in Ring Opening Metathesis Polymerization (ROMP) reactions. *Polymer* **2015**, *80*, 64–66.

[70] T. Hino, N. Inoue, T. Endo. Ring-opening metathesis copolymerization behaviors of cyclooctene and norbornene bearing a five- or six-membered ring cyclic carbonate. *J. Polym. Sci., Part A: Polym. Chem.,* **2005**, *43*, 6599–6604.

[71] M. L. Gringolts, Y. I. Denisova, G. A. Shandryuk, L. B. Krentsel, A. D. Litmanovich, E. S. Finkelshtein, Y. V. Kudryavtsev. Synthesis of norbornene–cyclooctene copolymers by the cross-metathesis of polynorbornene with polyoctenamer. *RSC Adv.,* **2015**, *5*, 316–331.

[72] M. Lichtenheldt, D. Wang, K. Vehlow, I. Reinhardt, C. Kuhnel, U. Decker, S. Blechert, M. R. Buchmeiser. Alternating Ring-Opening Metathesis Copolymerization by Grubbs- Type Initiators with Unsymmetrical *N*-Heterocyclic Carbenes. *Chem. Eur. J.*, **2009**, *15*, 9451–9457.

[73] Reproducing the reaction using amine/**VC3** ratios ranging from 0.5 to 2.0 did not provide further clues to the understanding of the lack of formation of the PHOPO.

[74] A. Cornille, R. Auvergne, O. Figovsky, B. Boutevin, S. Caillol, *Eur. Polym. J.* **2017**, *87*, 535–552.

[75] The double amidation of **VC3** may lead to the formation of **A**. The (hydroxymethyl)methyl dioxolone product released from this amidation could then be attacked by the isopropylamine, leading to the hydroxy-oxazolidone compound, yet not observed by ESI-MS. Dehydration could then occur, and the resulting exo-vinylene oxazolidone compound (not observed) could be opened by isopropylamine, leading to a urea compound **B**. Further dehydration of this compound could lead to **C**, whereas esterification by another molecule of **A** could lead to a urea-urethane compound **D.**